Greenhouse gas emissions from an intensively cropped field under various water and fertilizer management practices

By

Cynthia Crézé, agr.

Department of Bioresource Engineering
McGill University, Montreal
December 2015

A thesis submitted to McGill University in partial fulfillment of the requirements of the degree of Master of Science

Abstract:

Water table management has not only proven to have positive effects on crop yields but can also improve water quality by reducing nitrate (NO_3^--N) concentrations in the drainage water, and by regulating drain outflow volumes. However, a higher water table level may also lead to soil conditions favorable to denitrification and organic matter decomposition, resulting in increased soil emissions of greenhouse gases (GHG). The main objective of this study was to investigate the influence of two water management systems on GHG fluxes: conventional tile drainage (FD) and controlled tile drainage with sub-irrigation (CDSI). The second objective was to investigate the effects of five different doses of N-fertilizer application: 70 kg N/ha, 170 kg N/ha, 200 kg N/ha, 230 kg N/ha in one application and 230 kg N/ha in two applications with a one-week interval. This study particularly focused on the combined effects of water table management and the fertilizer amounts. The study was conducted on a 4.2-ha sandy loam field located in South-western Quebec, Canada. Within the four years of this study, the crop rotation was yellow beans followed by three years of grain-corn. GHG fluxes (CO_2, CH_4 and N_2O) were obtained using a vented non-steady state closed chamber method, with measurements taken at 15-minute intervals over a one-hour period, for 9 days throughout the growing season in 2012, for 14 days in 2013, for 21 days in 2014 and for 24 days in 2015. In addition, the following parameters were measured: daily rainfall amounts, daily air temperature, and both soil volumetric water content and soil temperature at the time of sampling. Agronomic management practices were recorded.

Increasing N-fertilizer amounts accelerated soil respiration, methane oxidation and the production of nitrous oxide. For fertilizer amounts of 200 kg N/ha and more, large punctual bursts of N_2O production ($\geq$ 0.5 mg $N\text{-}N_2O.m^{-2}.hr^{-1}$) were measured approximately 15-20 days following fertilizer application. Sub-dividing total N-fertilizer into two applications spaced one-week apart reduced the bursts of N_2O production. In 2013, N_2O production was present prior to harvest, which was attributed to microbial consumption of fixed nitrogen from the green manure and yellow bean residues of the previous year. The corn canopy created a microclimate within the field and regulated both soil temperatures and soil volumetric water contents in this study. Soil temperature was a stronger regulator of GHG fluxes compared to soil water content. Neither FD nor CDSI were found to have significant effects on any of the GHG fluxes.

Résumé:

La gestion de la nappe phréatique en agriculture permet non seulement d'augmenter les rendements mais peut également améliorer la qualité de l'eau en réduisant les concentrations en nitrates (NO_3^--N) de l'eau drainée d'un champ. Ce système de gestion présente également un moyen de contrôler le volume d'eau évacué par drainage sous-terrain. Cependant, une nappe phréatique plus élevée pourrait également créer des conditions de sol favorable à la dénitrification et à la décomposition organique, ce qui augmenterait les émissions de gaz à effet de serre (GES) provenant du sol. L'objectif principal de cette recherche est étudier l'influence de deux systèmes de gestion d'eau sur les flux d'émissions de gaz à effet de serre. Les deux systèmes étudiés seront le drainage sous-terrain libre conventionnel (FD) et le drainage contrôlé avec sous-irrigation (CDSI). Le deuxième objectif est d'analyser l'effet sur les flux de GES qu'auraient cinq différentes doses d'application d'engrais azotés: 70 kg N/ha, 170 kg N/ha, 200 kg N/ha, 230 kg N/ha en une application et 230 kg N/ha en deux applications à une semaine d'intervalle. L'étude se concentre particulièrement sur les effets combinés du contrôle de la nappe phréatique et de la quantité d'azote apportée par les engrais. Cette recherche a été réalisée sur un champ de 4.2 ha de limon sablonneux situé dans la région sud-ouest du Québec, Canada. Durant les quatre ans de cette recherche, la rotation des cultures alternait une année de haricot jaune suivi de trois ans de maïs-grain. Les flux d'émissions de gaz à effet de serre (CO_2, CH_4 and N_2O) ont été mesurés par la méthode de chambre fermée à état non-stable ventilée. Une prise d'échantillon était réalisée toutes les 15 minutes pendant une heure, pour 9 jours espacés tout au long de la saison en 2012, 14 jours en 2013, 21 jours en 2014 et 24 jours en 2015. Afin d'identifier quelques événements et paramètres clés dans la production de GES, cette étude présentera les registres des pratiques de gestion agronomiques, des variations climatiques, et des conditions de sols (température, teneur volumétrique en eau) de chaque saison.

L'augmentation des doses d'application d'engrais azotés a accéléré la production de CO_2 et de N_2O ainsi que l'oxydation du méthane. Pour des taux de 200 kg N/ha et plus, des importants pics de N_2O ($\geq$ 0.5 mg $N\text{-}N_2O.m^{-2}.hr^{-1}$) ont été mesurés environ 15-20 jours suivant l'application des engrais. La division des taux d'azote en deux applications espacées d'une semaine a réduit les pics de production de N_2O. En 2013, des flux de production de N_2O ont été mesurés avant le semis, ce qui a été associé à la consommation microbienne de l'azote fixé par les résidus d'engrais vert et par les haricots jaunes de l'année précédente. La canopée formée par

le maïs a créé un microclimat dans le champ et a régulé les températures du sol ainsi que la teneur volumétrique en eau. La température du sol a eu une plus grande influence sur les émissions de GES que la teneur volumétrique en eau. Ni le drainage libre ni le drainage contrôlé avec sous-irrigation ont eu d'effets significatifs sur les émissions de GES.

Acknowledgments:

First of all, I would like to thank Agriculture and Agri-Food Canada, who have made this research possible and provided funding for this project. I would like to thank McGill University and particularly, my supervisor and former Dean of the Faculty of Agricultural and Environmental Sciences, Dr. Chandra Madramootoo. I am very grateful to Mr. Guy Vincent and his family who allowed me to run my experiment on their farm. Our numerous discussions were enlightening. Thank you for showing your interest in the sustainable development of agriculture and thank you for sharing your experience and extensive knowledge in agriculture.

Thank you to Dr. Joann Whalen and Dr. Viacheslav Adamchuk, who shared their expertise and provided valuable advice. I would like to acknowledge the invaluable role of Mr. Hicham Benslim and Mr. Blake Bissonnette, who spent countless hours running and re-running my samples through the gas chromatographer. I would like to extend my gratitude to Ahmad Mat Su for his advice and support throughout my research. I would also like to recognize the help of Hélène Lalande, in the realization of laboratory soil chemical analysis. I am grateful to Eduardo Ganem Cuenca, who plays a key role in the AGGP program. I give thanks to the dynamic research assistants, who gave their time and energy for the collection of data and field work: notably, Kaitlin Lloyd, Pernilla Talec, Sukhjot Singh Mann, Gianni Montanaro, Paddy Enright, Liam Maclure, and Sophia Yee. Very special thanks to Kaitlin Lloyd. Your friendship and continuous support is precious.

Finally, I would like to thank my family and friends, who have always supported me. I send you all my love.

Table of Contents

List of Tables

List of Figures

List of Abbreviations and Symbols

CDSI	Controlled-drainage with sub-irrigation
CH_4	Methane
CHU	Corn heat unit
C_m	Concentration (mass/volume)
CO_2	Carbon dioxide
C_v	Concentration (volume/volume)
ECD	Electron capture detector
FD	Free drainage
FDH	Formate dehydrogenase
Fe^{2+}	Iron (II) oxide
FID	Flame ionization detector
ε	Apparent dielectric constant
GC	Gas chromatograph
GHG	Greenhouse gas
GWP	Global warming potential
H_2	Hydrogen gas
IPCC	Intergovernmental Panel on Climate Change
K_{sat}	Saturated hydraulic conductivity
LOI	Loss on ignition
MMO	Methane monooxygenase
N_2	Nitrogen gas
NAD^+	Aldehyde dehydrogenase
NH_2OH	Hydroxylamine
N_2O	Nitrous oxide
NH_4^+	Ammonium ion
NO	Nitric oxide
NO_2^-	Nitrite
NO_3^-	Nitrate

θ_A	Air-filled porosity
θ_v	Volumetric water content
P_B	Soil bulk density
ρ_s	particle density
ppb	parts per billion
ppm	parts per million
R	Universal gas constant
SOC	Soil organic matter
TCD	Thermal conductivity detector
τ	Tortuosity
WFPS	Water filled pore space
WTD	Water table depth

Chapter 1: Introduction

1.1 Problem definition

The atmospheric concentrations of carbon dioxide (CO_2), methane (CH_4) and nitrous oxide (N_2O) have increased since 1750 due to human activity. In 2011, concentrations of these greenhouse gases were 391 ppm, 1803 ppb, and 324 ppb, respectively, which represent increases of 40%, 150% and 20% from pre-industrial levels (IPCC, 2013). The rising concentration of atmospheric GHG has largely contributed to the disruption of balances within Earth systems including Earth's energy budget, the global water cycle, and carbon and other biogeochemical cycles, thus creating changes in overall climate systems (IPCC, 2013). Studies were undertaken to identify sources but also possible sinks of these GHGs. In Quebec, agriculture accounts for only a small portion of greenhouse gas (GHG) emissions with 7.8% of total anthropogenic GHG emissions (MDDELCC, 2014). However, of particular concern is the contribution of agriculture to global N_2O and CH_4 emissions, which are 60% and 50% of global emissions respectively (Linquist *et al.,* 2012). The global warming potential of N_2O and CH_4 are 310 and 21 times greater, respectively, than that of CO_2 (Reicosky *et al.,* 2000). The concept of global warming potential (GWP) was developed by the Intergovernmental Panel on Climate Change (IPCC) in order to compare the ability of GHGs to trap heat in the atmosphere relatively to carbon dioxide.

A number of factors will influence GHG emissions from agricultural soils including environmental conditions (temperature, precipitation), agronomic practices (tillage, fertilisation, irrigation and drainage), soil properties (pH, texture, bulk density, and organic matter) and the size of microbial communities in the soil. Agricultural soils can act as both sources and sinks of GHGs. Thus, adapted agronomic practices can work to mitigate the effects of climate change by both reducing the sources and enhancing the sinks of GHGs. However, the understanding of how anthropogenic activities will affect GHG fluxes from cultivated fields is limited.

Although controlled drainage with sub-irrigation is known to increase yields and reduce nitrate losses from soils, increased soil moisture may stimulate microbial activity favouring the production of GHGs. Moreover, N-fertilizer application will provide additional directly available substrate to these reactions. Therefore, the influence of water and fertilizer input on biogeochemical processes could substantially affect GHG emissions from agricultural soils. As such, this study compared two water management systems and different N-fertilizer applications to determine whether these practices considerably contribute to the production of GHGs.

1.2 Objectives

The objectives of this research were as followed:

1) The main objective of this study was to investigate the influence of two water management systems on GHG fluxes: conventional tile drainage (FD) and controlled tile drainage with sub-irrigation (CDSI).
2) The second objective was to investigate the effects of five different N-fertilizer application amounts: 70 kg N/ha, 170 kg N/ha, 200 kg N/ha, 230 kg N/ha in one application and 230 kg N/ha in two applications with a one-week interval.

This study focused on the combined effects of water table management and of nitrogen fertilizer amounts on GHG fluxes.

Chapter 2 : Literature Review

2.1 Grain-corn production

2.1.1 Grain-corn production in Quebec

Corn-grain is an increasingly prevalent crop in Quebec. Although, in recent years, there have been small decreases in grain-corn acreage (-6.4% between 2005 and 2008), there has been a considerable increase in grain-corn production since the 1990s (Morisset *et al*., 2006). In 2013, producers seeded one million acres of grain-corn, 13.4% more than the 882 200 acres seeded in 2011. Of the total acreage of cultivated land in Quebec, 21.4% is used for corn-grain. The Montérégie region accounts for 59% of this total Quebec acreage in corn-grain (Morisset *et al*., 2006).

We could expect further increases in corn-grain production. The choice of corn hybrids is based on Corn Heat Units (CHU) in Quebec. These temperature-based units allow growers to select hybrids that will mature before a killing frost in the fall. Cool temperatures delay the progress of the corn to maturity while warm temperatures hasten it. With climate change and particularly the process of global warming, there has been a general trend of increasing Corn Heat Units in Quebec over the last decade (Bootsma, 2013). Growing seasons are longer and warmer. Moreover, northern areas, which traditionally did not have sufficient heat units, now have the potential to support corn production. Producers can select corn hybrids with higher CHU requirements and higher yield potential. As of now, the range of corn heat units (CHU) in South-western Quebec is of 2300-3300 CHU (CRAAQ, 2002).

2.1.2 Corn agricultural management practices

2.1.2.1 Corn rooting system

Water and nutrient needs will vary greatly amongst agricultural crops. The rooting depth and overall rhizosphere volume, which are variable amongst plant-species, will determine the dimensions of soil water and nutrient supply available to a crop. It is estimated that a crop with a rooting depth of 100 cm will have around twice more available water than a crop with a rooting depth of 50 cm, and the water supply will last twice as long (Parent *et al*., 2010). Corn roots have a deep rooting system and can reach on average depths of 75-120 cm depending on soil conditions and agronomic practices (Parent *et al*., 2010). However, the corn rooting system consists primarily of tap roots, which may reach deeper soil nutrient pools but may not exploit

the full nutrient potential of accessed soil. Indeed, crops such as yellow bean and alfalfa will benefit from very fine roots, and from nodules in which rhizobia contribute to the nitrogen-fixing capacity of the crop. These crops will make more thorough use of their soil water and nutrient pools.

During its vegetative stage, corn roots will grow within the soil profile. At this time, it is not recommended to provide irrigation. By stressing the crop, corn roots will have to scavenge the soil for water, thus providing robust anchoring to the crop and providing a greater soil nutrient pool for later stages. After pollination, corn will shift its energy supply towards kernel filling. At this stage, corn will not grow additional roots. Irrigation will be necessary if crop evapotranspiration exceeds precipitation levels so as to ensure optimum yields. A previous study on sandy loam in South-western Quebec indicated that daily water uptake of corn from silking to the full dent stage will be of 3.55-5.93 mm/day (Singh, 2013). As grain-corn is a high-biomass yielding crop, it will also require substantial amounts of fertilizer during the growing season (Radford *et al*., 2001).

2.1.2.2 Application of fertilizer

Grain-corn is a high yielding crop, which requires considerably high inputs of N fertilizer. Corn accounts for 16% of total fertilizer use and 17% of the total world use of nitrogenous fertilizer (Singh, 2013). In Quebec, depending on climatic zone and soil texture, recommendations of nitrogen application for grain-corn are of 120 to 170 kg N/ha, of which 30 to 50 kg/ha should be band applied at seeding (Parent *et al*., 2010). These recommended applications were calculated to obtain best economic yields and not maximum yields. Grain-crop production systems including corn, wheat and rice have received particular attention in terms of N_2O emissions, as they consume an estimated 50% of all N fertilizer produced globally and the N use efficiency of these systems can still be substantially improved (Wolfe, 2013).

2.1.2.3 Benefits of free-drainage (FD)

The three modes of water table management discussed in this study are: free drainage (FD), controlled drainage (CD) and controlled drainage with subirrigation (CDSI), illustrated in **Figure 2.01**.

Prominent soil types in the Lower Great Lakes/St Lawrence River regions are clay, clay loams, and shallow sandy soils over a clay subsoil. As such, the region is characterized by soils of poor internal drainage. Shallow water tables occur not only due to the presence of an impermeable layer of clay but also due to flat topography. High soil moisture conditions will particularly be a problem in the spring, following spring-thaw. In order to have the longest growing period possible, producers must seed as early as possible and before the arrival of spring storms. Planting early also ensures that the corn will be mature earlier, which reduces the risks of damage from early fall frost or adverse weather at harvest. Farm operators must also start planting well before the optimum planting date to ensure that they have sufficient time to seed their entire corn acreage. Generally, the loss of potential yield associated with planting 2-3 weeks before the optimum date is less comparatively to planting 2-3 weeks after the optimum planting date (Brown *et al*., 2009). Thus, tile drainage would allow soils to dry and warm faster early in the spring creating favorable conditions for seeding and improving field trafficability. Indeed, subsurface or free drainage (FD) improves the free outflow of water from an agricultural field through installed, perforated tile drains. This system has been installed extensively in the Lower Great Lakes/St Lawrence River regions.

2.1.2.4 Benefits of controlled drainage and subirrigation (CDSI)

Water table management has two main components: controlled drainage (CD) and subirrigation (SI). In a controlled drainage system, farmers can close the tile drain outlets to retain water during the dry periods of the growing season. This will reduce the need of water from external sources for irrigation. Subirrigation is achieved by supplying water into the closed drainage system during dry periods to maintain an elevated water table depth in the field. By controlling the outflow of drainage water, water table management technology can reduce NO_3^--N water pollution problems by retaining water in the field, creating anaerobic conditions, favourable to denitrification (Elmi, 2002). The use of controlled drainage, as compared to conventional drainage, has shown to reduce NO_3^--N losses 46.5% in field runoff and to reduce its accumulation as much as 52% below the root zone in soil (Tait *et al.,* 1995). However, by promoting denitrification processes, the use of CDSI may have adverse environmental consequences due to increased production of N_2O through denitrification.

Figure 2.01 **Three modes of water table management (based on Bourke, 2011)**

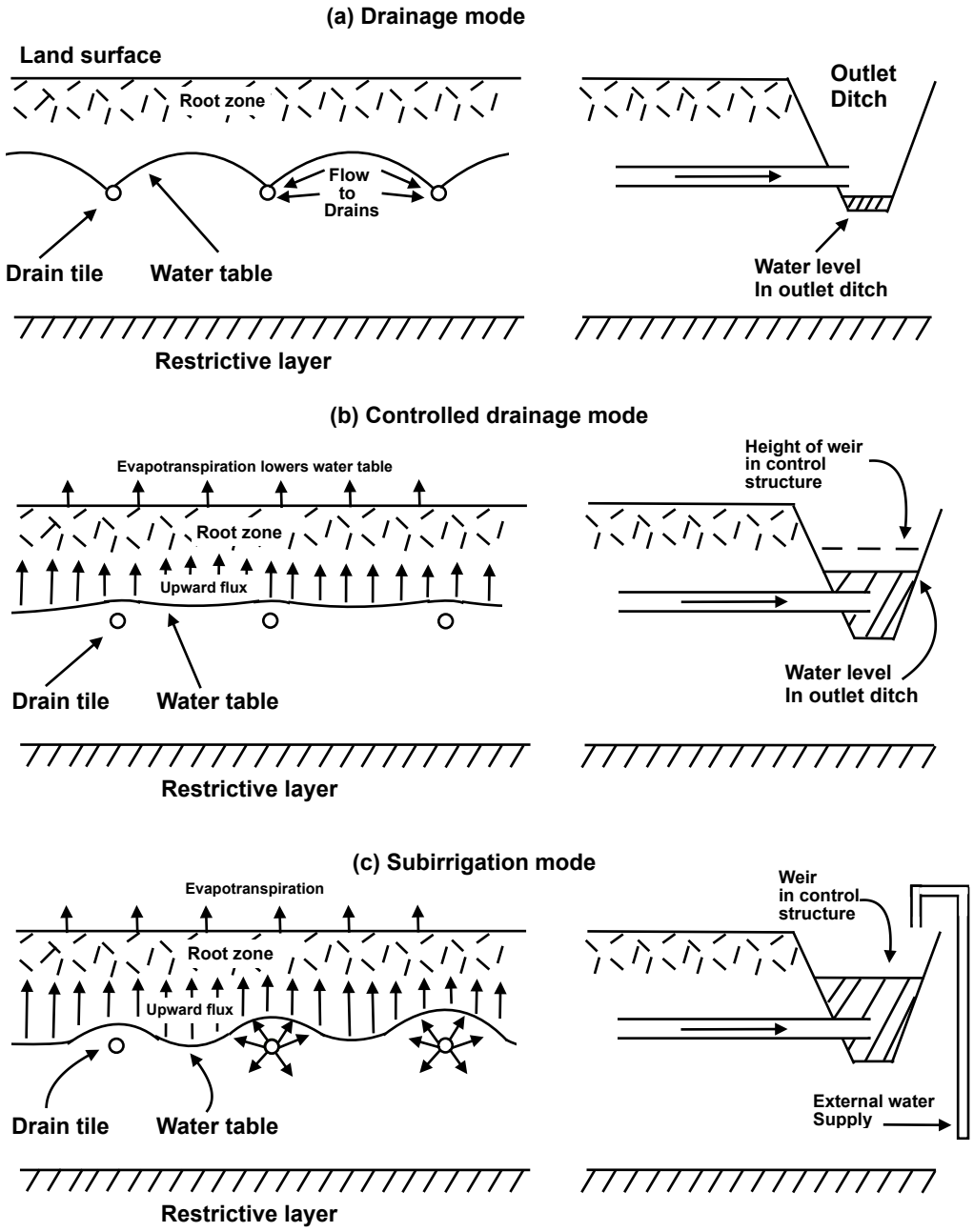

2.1.2.5 Irrigation scheduling for grain-corn through water table management

Successful management of soil water regimes during a growing season can optimize yields and reduce agricultural input costs. In the South-western region of Quebec, precipitation will be inferior to potential evapotranspiration rates during much of the growing season. The relative levels of precipitation and evapotranspiration on a 30-year average in Valleyfield, Quebec is presented in **Figure 2.02.** Depending on the distribution of rainfall events, this can cause frequent periods of water deficit for the crops (Parent *et al*., 2010). This water stress can be reduced through irrigation scheduling. Under a CDSI system, the water table depth (WTD) must be high enough to permit capillary rise into the root zone but low enough to ensure adequate soil aeration. Through a study of CDSI in a sandy-loam soil in South-western Quebec under grain-corn production, Dr. Ajay Singh found that the required sub-irrigation water supply was highest during the month of August and represented 34-36% of the total water supplied. Overall, throughout each growing season of the study, an average of 167.8 mm of irrigation water was provided to the field to maintain the desired WTD (Singh, 2013). To further improve the accuracy of an irrigation schedule, there exist a number of hydrological models. MIKE SHE (Refsgaard *et al*., 1996) and DRAINMOD (Skaggs, 2012) are both models that are fit to field-scales.

Figure 2.02 Evapotranspiration and normal precipitations (30 year average) in Valleyfield, Quebec, Canada (Parent *et al.,* 2010)

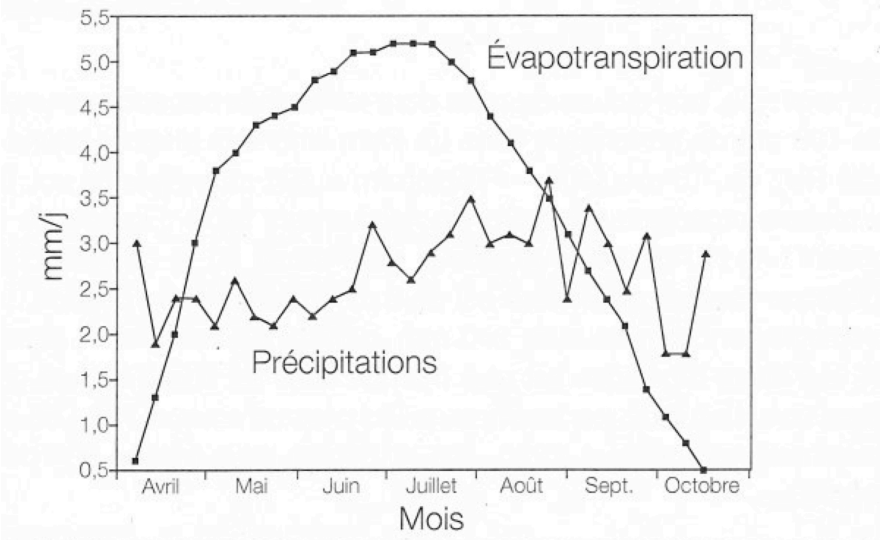

2.2 Biogeochemical reactions involved in GHG production

2.2.1 Carbon dioxide

2.2.1.1 Soil respiration

Carbon dioxide (CO_2) fluxes will be the result of both *aerobic* and *anaerobic soil respiration*, which will include the sum of all respiratory activity within the biologically active soil layers, including microbial and root respiration as the main sources of CO_2 emission. Soil respiration will be apart of the process of *decomposition,* through which organic material will be transformed into CO_2, inorganic nutrients and humus. The respiration of the soil fauna is considered to be a negligible source of CO_2 in soils. However, soil fauna will be important controllers of soil microbial communities. Indeed, it was found that soil CO_2 respiration was increased 1.9-fold by soil fauna in the bare soil, but to a lesser extent in soil litter (Whalen *et al.,* 2010). It is estimated that CO_2 fluxes emitted from the soil will be considerably greater than that from plants. Indeed, the soil organic matter pool in terrestrial ecosystems represents about four times (about 2 000 Pg. C with 1 Pg = 1015 g) the carbon stored in plant biomass (500 Pg. C) (Whalen *et al.,* 2010). This pool of soil organic matter (SOC) has largely been depleted since the 1850s, due to the shift from natural to agricultural land use: loss of carbon from terrestrial ecosystems has amounted to about 156 Pg C with losses in SOC due to mineralisation accounting for about one-third or 52 ± 8 Pg C (Butterbach-Bahl *et al.,* 2012).

2.2.1.2 Soil carbon sequestration

Within the Carbon cycle, SOC pools can also be replenished following decomposition through *stabilization* processes. Chemical stabilization of residues will result from the depletion of easily decomposable substances and the accumulation of more resistant materials (Whalen *et al.,* 2010). Organic carbon compounds may also become stabilized through biochemical and physical processes. Once stabilized, these residues and other by-products can persist in the soil for many decades and even centuries and can thus be stored in the soil before it is eventually released back to the atmosphere in the form of CO_2. This stabilized organic matter is referred to as humus. Yet, organic substrates of plant, animal and microbial origin can also be stabilized in the soil in the short term (weeks or months) and to medium term (years to decades). Although these substrates are not considered apart of humus, they contribute to 'soil carbon credits' as they are stabilized and not immediately returned to the atmosphere as CO_2 (Whalen *et al.,* 2010). Soil

carbon sequestration will occur when the rate of carbon stored in the soil is greater than the carbon emitted from the soil as CO_2. Thus, historical SOC losses could be reversed through the use of improved agricultural management practices, and could furthermore contribute to reducing atmospheric CO_2 concentrations.

Within grain-corn cropping systems, farmers will have control over organic matter input to the fields, through a number of agronomic practices. At harvest, they will determine the amount of organic residues that will be returned to agro-ecosystems by setting combines to cut at a particular crop height. Furthermore, at harvest, straw can either be left in the field or removed and used for animal bedding. The time of year at which residues are added or incorporated to fields will have a strong impact on its decomposition rate due to seasonally variable temperatures. Tillage practices in the spring or autumn, such as plowing, harrowing, disking, and roto-tilling, can fragment and mix residues, thus accelerating rates of decomposition (Whalen *et al.,* 2010). Decomposition can be limited due to lacking essential nutrients, such as nitrogen. As such, fertilization practices will support soil respiration and decomposition processes. Thus, nitrogen and carbon cycles will be interlinked.

2.2.1.3 Effect of soil moisture and temperature

Rates of soil organic matter decomposition will be first and foremost defined by litter quality (N, C:N, lignin (%), lignin:N and P, K, Ca, Mg) (Lorenz *et al.,* 2012). Indeed, microbes will require high energy and nutrient supply for fast matter decomposition. Thus, a high quality litter with high nutrient (N and P) concentrations, a high proportion of easily degradable C-compounds (sugars) and low concentrations of substances inhibiting microbial activity will more likely undergo a faster decomposition than low quality litter. However, controlling factors of microbial and their associated enzymatic activity will also play important roles in defining decomposition rates. In particular, adequate temperature, water content and soil aeration will be indispensable to ensure the proper diffusion of enzymes to organic substrates (Lorenz *et al.,* 2012).

In general, warmer and wetter temperatures will accelerate decomposition processes and corresponding CO_2 emission. However, optimum conditions for decomposition rates are still under debate. According to Linn and Doran, optimum microbial respiration would be at about 30°C and 55-60% WFPS (Linn and Doran, 1984). Schaufler however indicated maximum CO_2

emission levels from soils in the range of 20-60% WFPS (Schaufler *et al*., 2010). Scheer *et al*. indicated a diurnal pattern in CO_2 emissions similar to diurnal patterns found in other studies (Scheer *et al*., 2013; Parkin and Kaspar, 2003; Wang *et al*., 2010). This further confirmed results of previous studies, which found that soil temperature, soil moisture and substrate availability were main drivers of CO_2 emissions (Scheer *et al*., 2013 citing Almagro *et al*., 2009; Han *et al*., 2007). The relative contribution of soil moisture and temperature to CO_2 fluxes are still uncertain. In a field study on surface drip irrigated and subsurface drip irrigated tomato productions, Edwards found that the majority of CO_2 emissions were influenced by soil temperature, and to a much lesser extent by soil moisture (Edwards, 2014). Similarly, in a field study on cranberry fields under two different water table management systems, Grant found that 45% of the CO_2 fluxes were explained by temperature alone whilst soil moisture explained 14% of fluxes throughout the season (Grant, 2014). As such, both studies suggested that CO_2 might not be intrinsically linked to the specific irrigation practices, but will rather have temperature as a primary determinant factor.

2.2.2 Methane

2.2.2.1 Methanogenesis/Methane Oxidation

Methane fluxes from the soil are the difference between methane production in a process called *methanogenesis*, and methane consumption through the process of *methane oxidation*. The two processes can occur simultaneously within soils. If the difference of the two is positive, the soil will act as a methane sources, whereas if the difference is negative, the soil will act as a methane sink. There exist a number of possible substrates for methanogenesis including H_2+CO_2, acetate, formate, methylated compounds and primary and secondary alcohols. Corresponding reactions are detailed in **Table 2.01**. However, the main pathways of CH_4 production will be through acetotrophy and CO_2 reduction by H_2. Acetotrophy is generally considered responsible for about two-thirds of the CH_4 produced (Le Mer *et al*., 2001). Although some soil C can be lost by emission of CH_4, the majority of CH_4 produced will be consumed by methanotrophic bacteria before escaping back to the atmosphere (Lorenz *et al*., 2012). For substantial methanogenesis to take place, a low oxydo-reduction potential (Eh < -200 mV) is required (Le Mer *et al*., 2001). As such, methane production has been much more extensively studied in rice paddies and waterlogged upland soils. The majority of conventional agricultural soils in Eastern Canadian

soils will not have the necessary redox potential for methanogenesis (Edwards, 2014). These agricultural soils will act as CH_4 sinks rather than sources.

In the process of methane oxidation, the enzymatic complex MMO will initiate the oxidation of CH_4 to form methanol, which is further oxidized to formaldehyde by methanol dehydrogenase. The oxidation of formaldehyde to formate and then to CO_2 will provide most of the reducing power necessary for the initial oxygenation of CH_4. In a final step, formate is oxidized to CO_2 by formate dehydrogenase (FDH), a NAD^+ dependent enzyme present in all methanotrophs (Serrano-Silva *et al.,* 2014). Thus, soils with a low redox potential will use CH_4 as a carbon source and convert it to CO_2. As both methanogenesis and methane oxidation can occur simultaneously, within a system, some of the CH_4 produced through organic matter decomposition can in turn be oxidized to CO_2 by methanotrophs in the soil. Latest studies have shown that anaerobic oxidation of methane in the soil is closely linked to nitrate availability (Zhu *et al.,* 2010). Indeed some of the methanotrophic activity in soils will come from nitrifying bacteria, that can use CH_4 as an alternative substrate to NH_4^+ (Schlesinger *et al.*, 2013). Atmospheric deposition of nitrate has also shown to reduce methane oxidation by forest soils (Schlesinger *et al.*, 2013). As such, irrigation and drainage systems may come to impact CH_4 consumption of soils, through the monitoring of soil nitrate and nitrite concentrations.

2.2.2.2 Effect of soil moisture and temperature

As previously mentioned, the largest controlling factor for methanogenesis in upland soils will be soil moisture and redox potential. Indeed, methanogens will need anaerobic soil conditions to remain active (Le Mer *et al.,* 2001). As such, in non-flooded soils, methanogenic activity is generally low and can even be negative.

A number of studies agree that upland soils are generally sinks for CH_4 (Robertson *et al.*, 2004; Ellert *et al.*, 2008). For maize and wheat cropping systems, the maximum rate of CH_4 oxidation was determined to be 2.19 kg CH_4-C/ha/season (Adviento-Borbe *et al.,* 2007). Methane oxidation will require proper soil aeration. In general, CH_4 oxidation will decrease with increasing soil water content. Nevertheless, CH_4 oxidation has been reported in soils with WFPS>60%, which could be attributed to remaining aerobic microsites (Serrano-Silva *et al.*, 2014). Adequate soil aeration will also improve CH_4 diffusion to the atmosphere. In a field study comparing effects of surface drip irrigation and subsurface drip irrigation on tomato productions,

Edwards reported methane flux values tended to be near zero and negative, indicating the soil was acting as a sink rather than a source of methane. However, fluxes were highly variable and could be positive, suggesting that methanogenic and methanotrophic processes were occurring at the same time within the soil (Edwards, 2014).

Methanotrophy seems to be less sensitive to temperature than methonogenesis and was found to be optimum at 20-30°C (Le Mer *et al.,* 2001). The uptake of CH_4 is suggested to be positively affected by soil temperature and has also shown diurnal patterns similarly to those of CO_2 fluxes (Sass *et al.,* 1994). However, these variations have not been reported in all studies. In the previous study by Edwards, soil temperature had little to no correlation with CH_4 fluxes in all treatments, for both years of the study (Edwards, 2014).

2.2.3 Nitrous oxide

2.2.3.1 Nitrification/Denitrification/Nitrification-Denitrification

The main pathway behind the production of nitrous oxide (N_2O) is *denitrification*, which occurs in anaerobic conditions. In this process, nitrate (NO_3^-) is reduced to nitrite (NO_2^-), which is then further reduced to nitric oxide (NO) followed by nitrous oxide (N_2O) and nitrogen gas (N_2). Within this reaction, there has been some debate as to whether NO is a true intermediate or a by-product in the process (Nieder *et al.,* 2008). If this reduction process is complete, nitrogen will be transferred to the atmosphere in the form of N_2, which is a benign gas. However, if the denitrification process is incomplete, nitrogen will be emitted as N_2O, which is of a potent GHG. In agricultural soil, N_2O may also be produced through a non-biological denitrification process, named *chemodenitrification*. The oxidative process of *nitrification* can also produce N_2O, yet to a much smaller extent. In this process, ammonium ions (NH_4^+) are oxidized to NO_3^- through NO_2^- under aerobic conditions. Nitrate and nitrite ions will then feed denitrification and nitrifier denitrification processes thus increasing the possibility for N_2O production. During the nitrification process, N_2O may be produced from the incomplete oxidation of NH_2OH.

When oxygen in the soil is limited but still present, both nitrification and denitrification processes can occur simultaneously. In these conditions, N_2O can be produced through a *nitrifier-denitrification* process (Wrage *et al.,* 2001)(Bouwman, 1990). However, the significance of this process in total N_2O contribution is uncertain and is considered small. Possible N_2O production pathways are expressed in **Figure 2.03**. Thus, within soil, both NH_4^+ and NO_3^- can be

sources for N_2O production and the increase of their respective concentrations may lead to greater N_2O emissions. It is estimated that 1 to 5% of the nitrogen added to agricultural soils is lost to the atmosphere in the form of N_2O (Scialabba *et al*., 2010).

Contrarily to CO_2 and CH_4, the two other major greenhouse gases, there are no significant biological sinks for atmospheric N_2O. The main process by which N_2O is removed is through its reaction in the stratosphere with excited oxygen atoms formed by photolysis of ozone (Nieder *et al*., 2008). In soils, microorganisms may reduce N_2O to N_2 under anaerobic conditions, but the significance of soil as a sink to N_2O is uncertain and considered to be negligible.

Figure 2.03 **Main N_2O production pathways: nitrification, denitrification, and nitrification-denitrification (Wrage *et al.,* 2001)**

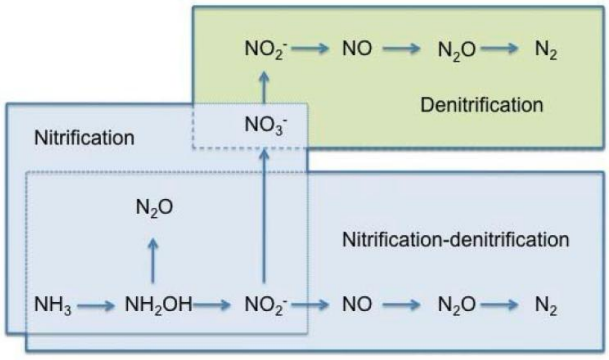

2.2.3.2 Effect of soil moisture

There exists a positive correlation between soil moisture and N_2O production. However, the importance of soil moisture influence on emissions will depend on predominant pathways responsible for N_2O production, as well as the rate of diffusion of the GHG in the soil (Nieder *et al*., 2008). Nitrification pathways will be the main source of emissions up to approximately 65% WFPS. Beyond this threshold, denitrification will be the predominant contributor to N_2O production. The production of N_2O from nitrification will increase with water content up to 55-65% WFPS and then decrease substantially. Maximum rates of nitrification at 60% WFPS were found to correspond to optimum conditions as neither the diffusion of substrates nor the diffusion of O_2 was restricted (Bateman and Baggs, 2005). From 65% WFPS, denitrification processes will be dominant and will increase considerably with increasing WFPS. At 70% WFPS, all N_2O will be produced through denitrification. **Figure 2.04** illustrates these interactions. As indicated in

this figure, denitrification and nitrification processes can occur simultaneously in certain soil condition. Indeed, anaerobic microzones within the soil may act as denitrification sites in otherwise aerobic soils (Knowles, 1982)(Bouwman *et al*., 1990)(Schlesinger, 2013). Nitrate and nitrite concentrations as well as soil temperature will enhance the response of nitrification and denitrification to increases in soil WFPS (Nieder *et al*., 2008).

The alternate drying and wetting of soil through punctual irrigation or precipitation events was found to enhance the release of N_2O due to the stimulation of N mineralization and the accumulation NO_2^- during the dry periods (Bouwman, 1990)(Scholes *et al*., 1997). Furthermore, cycles of wetting and drying will increase available carbon in soil. During soil wetting through irrigation and precipitation, more N_2O would be produced through anaerobic denitrification processes, and the subsequent drying of the soil would inhibit the reduction of N_2O to N_2. As such, N_2O could be found to be greater in irrigated fields rather than in waterlogged soils, which remain continuously water saturated. Correspondingly, a number of studies have indicated peaks in N_2O fluxes following irrigation events. Scheer *et al*. found that N_2O 'emission pulses' accounted for 50-60% of the total emissions in all treatments. The peaks occurred following irrigation events coupled with fertilizer application or following heavy rainfall events. Peaks occurred within 24h of the rainfall or irrigation events and emissions could remain elevated for up to 5 days (Scheer *et al*., 2013). Similarly, in a study by Liu *et al*. undertaken in a semiarid temperature steppe in China, results showed that precipitation distribution and the length of dry periods prior to rainfall impacted the magnitude of N_2O emission pulses. The input of water and N fertilizer had greater positive effect on emissions in a dry year rather than under normal precipitation conditions (Liu et *al*., 2014).

Furthermore, spring thaw also creates short-term N_2O emission bursts, due to its rapid alteration of soil water dynamics. Field research has indicated that considerable N release can occur during spring thaw in seasonally cold ecosystems (Gregorich *et al*., 2005; Almaraz *et al*., 2009; Elmi *et al*., 2009; Ullah *et al*., 2011). Gregorich *et al*. suggest that freeze-thaw cycles would lyse microbial cells, releasing C, N and other nutrients in the soil, which could then feed denitrification processes in the anaerobic soil during thaw events in the winter and spring (Gregorich *et al*., 2005). Other mechanisms which may underlie these emissions are: rapid nitrification-denitrification processes as the soil surface warms and drains with almost all N released as N_2O, and/or nitrification or denitrification processes occurring below the frozen soil,

accumulating N_2O, which is then released in the spring (Cates *et al.,* 1987). Annual N_2O emissions calculation based solely on growing season measures will be considerably underestimated, and should include spring-thaw emission events particularly in seasonally cold ecosystems. Thus, due to the high degree of spatial and temporal variability of N_2O emissions, the timing and frequency of sampling events will be particularly important to catch short-term 'emission pulses' of N_2O fluxes.

Figure 2.04 Influence of water-filled pore space (WFPS) on contributions of nitrification and denitrification to N_2O production from soils (Bateman and Baggs, 2005)

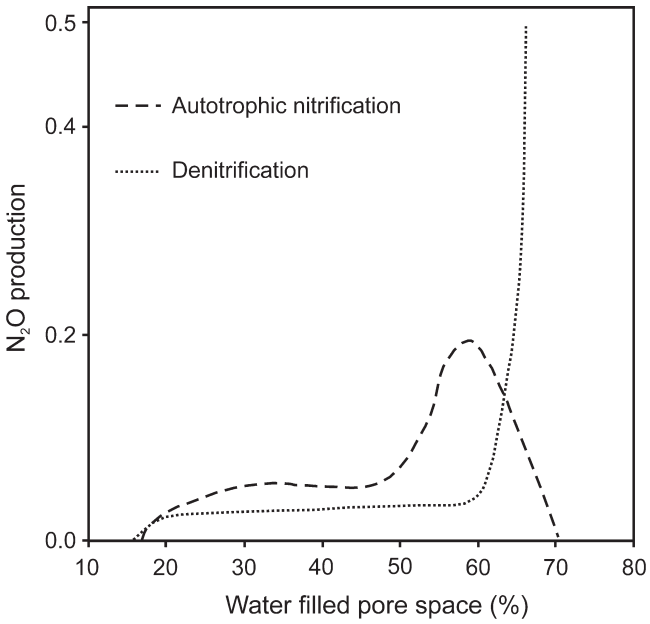

2.2.3.3 Effect of soil temperature

Soil temperature will influence rates of denitrification, rates of nitrification, and their associated terminal products, and will thus be a controlling factor in the production of N_2O. Denitrification rates were found to increase exponentially from 0 to 25°C and will continue to increase up to 60°C (Rochette *et al.,* 2004). However, at 37°C, N_2O/N_2 ratio declines with increasing temperature (Nieder *et al.,* 2008). Optimum denitrification rates occurred at temperatures above 25°C and lowest rates were at temperatures below 15°C (Bouwman, 1990). For nitrification, optimum rates were found in the range of 30-35°C. At temperatures below 5°C or above 40°C, nitrification rates were negligible (Bouwman, 1990).

There is no one N_2O flux driver, and many of the reported peaks in N_2O fluxes were attributed to the combined effects of controlling factors such as fertilizer application and rainfall events or fertilizer application and high temperatures (Bouwman, 1990)(Scheer *et al.,* 2013). Both soil moisture and temperature have shown to be two determining factors, with soil moisture having relatively stronger influence than soil temperature on N_2O fluxes. Consequentially, irrigation and drainage could be expected to alter N_2O emissions through three mechanisms: (1) nitrates will be retained within the soil matrix, (2) increased soil moisture will slow nitrification processes and (3) denitrification will be favoured through the presence of higher dissolved organic carbon and may occur before nitrates reach the groundwater.

2.3 Role of soil microbes in biogeochemical models

2.3.1 Identification

GHG production processes are catalyzed by soil microorganisms, which are dominant players in almost all global biogeochemical processes. These organisms will mediate individual reaction steps within soil nutrient cycles through the expression of functional marker genes, which encode enzymes catalyzing specific processes (Wall *et al.,* 2012). As the majority of microorganisms cannot be cultivated on standard laboratory media, soil microbial communities are presently identified through analysis of their microbial genes. Nucleic acid methods will identify functional marker genes presence. Studies have determined that C degrading or CH_4 oxidizing micro-organisms will have *mmoX* and *pmoA* functional marker genes, which will encode soluble methane mono-oxygenase and particulate methane mono-oxygenase, respectively (Wall *et al.,* 2012). All methanogens will belong to the domain *Archaea* and to the phylum *Euyarchaeota*. **Table 2.01** presents some representative soil archaea involved in methanogenesis reactions.

Table 2.01 Methanogenesis reactions catalyzed by some representative soil archaea (Whalen *et al.,* 2010)

Reaction	Representative genera
$4H_2 + CO_2 \rightarrow CH_4 + 2H_2O$	All soil methanogens
$4\ Formate \rightarrow CH_4 + 3CO_2 + 2H_2O$	*Methanobacterium*
$Acetate \rightarrow CH_4 + CO_2$	*Methanosaeta, Methanosarcina*
$4\ Methanol \rightarrow 3CH_4 + CO_2 + 2H_2O$	*Methanosarcina*
$4\ 2\text{-}Propanol + CO_2 \rightarrow CH_4 + 4\ Acetone + 2H_2O$	*Methanobacterium*
$4\ Methylamine + 2H_2O \rightarrow 3CH_4 + CO_2 + 4NH_4^+$	*Methanosarcina*
$2\ Dimethylamine + 2H_2O \rightarrow 3CH_4 + CO_2 + 2NH_4^+$	*Methanosarcina*
$4\ Methylamine + 6H_2O \rightarrow 9CH_4 + 3CO_2 + 4NH_4^+$	*Methanosarcina*
$4CO + 2H_2O \rightarrow CH_4 + 3CO_2$	*Methanobacterium, Methanosarcina*

In the denitrification cycle, the genes *narG* or *napA*, *Cu-nir* or *cd1-nir*, *norB*, and *nosZ* were found to code respectively for dissimilatory nitrate reductase (Nar), nitrite reductase (Nir), nitric oxide reductase (Nor) and nitrous oxide reductase (Nos). Denitrifying bacteria involved in the reduction of NO_2^- are recognized by the presence of two structurally different Nir enzymes found in their periplasm: the first contains copper (Cu-Nir) and the second contains cytochromes *heme* c and *heme* d1 (cd1-Nir)(Whalen *et al*., 2010). Both of these enzymes have identical functions. Copper-containing Nir was found in strains of bacteria in the genera *Pseudomonas* and *Alcaligenes*, *Bacillus, Rhizobium, Nitrosomas* and *Thiosphaera*. However, the majority of denitrifying bacteria will use the cd1-Nir gene, including most of the *Pseudomonas, Alcaligenes, Paracoccus, Thiobacillus* and *Azospirillum* (Whalen *et al*., 2010). Some studies suggested that microbes with Cu-Nir will be found primarily in carbon rich zones of the soil profile, such as the rhizosphere whereas microbes presenting cd1-Nir will rather be found in bulk soils (Wall *et al*., 2012). The characteristics and location of key reductases, as well as their representative microorganisms are presented in **Table 2.02**. Much of this published data remains to be confirmed. Current information is often based on single isolates, which may not accurately represent complex microbial communities in the soil. A large part of microbes involved in nutrient cycles remains to be identified. Furthermore, until recently, it was believed that denitrification processes were primarily driven by bacterial activity. However, recent findings indicated that fungi and archaea also possess enzymes, which catalyse denitrification transformation steps (Whalen *et al*., 2010).

Enzymes involved in Denitrification process:

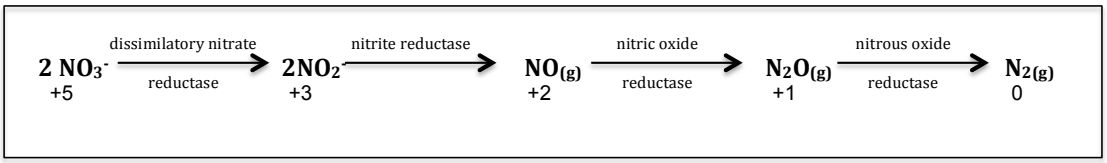

Table 2.02 Enzymes and representative microorganisms involved in respiratory denitrification under anaerobic soil conditions (Whalen *et al.*, 2010)

Enzyme	Enzyme location and characteristics	Representative organisms
Dissimilatory nitrate reductase (Nar)	Membrane-bound Periplasmic	Bacteria: *Paracoccus denitrificans* Fungi: *Fusarium oxysporum* Bacteria: *Pseudomonas* sp. and *Rhodobacter sphaeroides* f. sp. *denitrificans*
Nitrate reductase (Nir)	Periplasmic, containing copper (Cu-Nir) Periplasmic, containing cytochromes (cd1-Nir)	Bacteria: *Alcaligenes*, *Bacillus* and others Fungi: *Fusarium oxysporum, Leptosphaeria maculans* Bacteria: *Alcaligenes, Flavobacterium, Pseudomonas* and others
Nitric oxide reductase (Nor)	Membrane-bound, has cytochromes b c Membrane-bound, cytochrome P450 (P450-Nor)	Bacteria: all denitrifying bacteria Fungi: all denitrifying fungi
Nitrous oxide reductase (Nos)	Periplasmic	Bacteria: all denitrifying bacteria Fungi: all denitrifying fungi

2.3.2 Effects of soil moisture and temperature

2.3.2.1 Microbial population dynamics

Soil biogeochemical processes, through which GHG will be produced, will be mainly regulated by the microbial activity and particularly shifts in microbial gene expression, which in turn will be affected by a number of controlling factors. In response to changes in soil conditions, microbes adjust more rapidly though modifications in gene transcription than by shifting their community composition (Wall *et al*., 2012). Studies have proven an interaction between the

transcription rates and nutrient turnover rates within the soil. A study by Sharma *et al*. investigated microbial N_2O release during thawing of the soil and found a correlation between increased transcription levels of nitrite reductase Cu-Nir and N_2O release rates (Sharma *et al*., 2006). As microbial DNA remained constant at that time within in the soil, increased N_2O release could not be attributed to a growth in microbial population, but was rather linked to increased activity. It was found that regulators such as nitrate (NO_3^-) concentration, C availability, O_2 concentration, pH and temperature will influence the induction of gene transcription (Morales *et al*., 2015).

Understanding the effect of controlling factors such as WFPS and temperature on the activity and composition of microbes would provide a deeper knowledge of biogeochemical processes involved in GHG production. Water management practices can influence soil microbial activity by affecting redox reactions, the concentration of substrates, osmotic pressure, soil pH, and particularly, soil aeration. In denitrification processes, the activity and synthesis of Nar and Nir as well as that of Nor and Nos enzymes will be inhibited by oxygen (Whalen *et al*., 2010). It was found that Nar was activated within 40 minutes to 3 hours after wetting or re-wetting. Nir will be more strongly repressed by the presence of O_2 than Nar and will thus require a greater soil moisture increase to be activated (Knowles, 1982.) Further research is necessary to understand the influence of soil moisture and temperature on microbial community composition and their activity.

2.3.2.2 Fungal population dynamics

It must be noted that soil water content and temperature will also influence fungi activity, which also play an important role in soil biogeochemical processes. Fungal activity will be optimal from 20 to 37°C and will decline at higher temperatures. Soil bacteria have greater tolerance to flooded conditions than fungi, and will thus be the principal actors in decomposition in anaerobic soils whereas fungi will be the principal drivers of aerobic decomposition. In denitrification processes, a study found that fungi dominated bacteria in N_2O production, irrespective of the water-filled pore space (WFPS) (Chen *et al*., 2015). However, at WFPS greater than 90%, the degree of fungal dominance decreased significantly. In fungi, nitrate and nitrite reductases will be found in the mitochondria, and will be involved in the respiratory chain for ATP production and will thus require aerobic conditions. However, the fungal reductases

(P450-Nor) can obtain electrons directly from NAD(P)H, and can thus operate in oxygen-limited environments. For fungi, denitrification and oxygen respiration can occur simultaneously. Thus, contrarily to bacteria, fungal denitrification processes can occur in sub-anoxic conditions (Whalen *et al.,* 2012). However, the relative contribution of both bacteria and fungi in N_2O production across different soil water content gradients is still to be clarified.

2.3.2.3 Importance of microbiology application to biogeochemical processes

A study by Morales *et al*. suggested that 'proximal' regulators such as nitrate (NO_3^-) concentration, C availability, soil moisture, pH and temperature will influence the induction of gene transcription, but will only transiently affect microbial communities by 'expressing' a pre-defined genetic potential. Indeed, at larger time and space scales, 'distal' regulators such as soil type, microbial functional diversity and geography would determine the ability of soils to emit GHGs. Soil conditions created by 'distal' regulators would select for microbial populations, creating a genetic potential. Thus, these soils would be more prone to emit GHGs (Morales *et al.,* 2015). 'Proximal' regulators such as soil moisture and temperature would only have a short-term effect on soil GHG emissions, as they would only influence of expression of this accumulated genetic potential to emit GHGs.

Microbiology will need to be suitably integrated in biogeochemical models of ecosystem C and N cycling. Models originally used simple response functions for processes. Soil organic models would only include a pool labeled "microbial biomass", which was undifferentiated from pools of active forms of soil organic matter. The DeNitrification-DeComposition model (DNDC) has successfully integrated a microbiological component. This model incorporated two interacting components. The first relates three sub-models (soil climate, plant growth and decomposition) to predict soil environmental variables. The second presents nitrification, denitrification and fermentation sub-models to simulate microbial activity and predict associated gas fluxes and N leaching. This model reasonably reflects possible effects of soil temperature, moisture, redox potential and nutrient profiles on microbial activities in the soil. It will be important for models not to render microbiology implicit to reactions. To accurately depict possible changes in denitrification-decomposition processes, models must be able to depict possible variations in SOC as a result of changes in the activity or characteristics of soil organisms.

2.4 Conclusions

Many uncertainties remain in global biogeochemical predictions of the fluxes and intensity of GHG emissions. Current studies are still unclear due to the low frequency of seasonal sampling and due to the strong interference of climatic events. The complexity of soil and microbial factors, which present high spatial variability, creates another challenge for the modeling of GHG emissions from agricultural soil. Soil water content and the availability of substrates (nitrate and nitrite) are two important drivers of denitrification and decomposition processes. This study focused on two agronomic activities, drainage and irrigation practices and N-fertilizer amounts, which can considerably influence these two soil parameters.

Chapter 3 : Materials and Methods

3.1 Research site

3.1.1 Location

The study was conducted on a 4.2 ha experimental site located in Côteau-du-Lac, Quebec, Canada, approximately 30 km southwest of the Macdonald Campus of McGill University. The field surface was relatively level with a slope of about 0.5% (Tait *et al.,* 1995). The soil was a Soulanges sandy loam of the gleysol soil order. These soils are characterized by a very fine sandy loam alluvium parent material, underlain by marine clay at depths of 60 to 180 cm. Due to the flat topography of the field and the presence of clay, this field was imperfectly to poorly drained. Moderate mottling of yellowish brown and brownish gray was observed in the B horizon. This was attributed to the periodic saturation of these soils and altering between reduction and oxidation processes. At the surface, these soils had a dark horizon due to the enrichment of the soil in organic matter.

Gleysols have a good natural fertility. However, their poor natural drainage presents a considerable limitation to agricultural production. Field trafficability is particularly limited in the early spring and late autumn, at seeding and harvest. Machinery entering fields with saturated soil conditions will not only have reduced traction but will have detrimental effects on the soil structure. Machinery loads of 5 tons and more can create deep compaction in saturated soil, which is particularly difficult to correct. When poorly drained, gleysols may also be a source of environmental pollution to due nutrient losses through runoff, erosion, leaching and denitrification. Thus, surface modelling and the addition of subsurface drains are crucial for this soil order (Parent *et al.,* 2010).

A representation of the different horizons present in gleysols can be found in **Table 3.01**.

Table 3.01 Soulanges soil profile (Martin and Nolin, 1992)

Horizon	*Depth in cm*	*Description*
A_p	0-37	Humic fine sandy loam; very dark grey and dark greyish brown; granular structure; very friable consistence; moderately porous
B_{mgj1}	37-49	Fine sandy loam; brown; yellowish brown mottling; Numerous particulates
B_{mgj2}	49-62	Fine sandy loam; dark brown; dark yellowish brown mottling; lamellar structure
BC_g	62-71	Sandy loam; dark greyish brown; dark yellowish brown mottling; lamellar structure; moderately porous; coarse fragments of fine to medium gravel
Cg	≥ 71	Heavy marine clay; dark gray; dark yellowish brown mottling; polyhedral sub-angular structure

3.1.2 Experimental design

This study was conducted over four years. The site used had three blocks A, B and C with buffer separations of 30 m of width. Each block was subdivided into 8 plots of 15 by 75 m, separated by vertical plastic sheets of 1.5 m of depth. Subsurface pipes of 0.076 m diameter were laid at the center of each plot, at an average depth of 1.00 m. For this study, the delimitations of plots in the field were found using the north-eastern instrumented building as the benchmark and using the respective distances defined in the subsurface drainage construction plans, prepared by R. S. Broughton, P. Eng. in 1992. In seasons 2012 and 2013, the plot was freely drained. In 2014 and 2015, the experimental design of the field site was a split-plot design with two water treatment factors, free drainage (FD) and controlled drainage with sub-irrigation (CDSI). As can be seen in **Figure 3.01**, half of the plots in each block were dedicated to either of two treatments: free drainage (FD) and controlled drainage with sub-irrigation (CDSI). Two instrumented buildings on-site collected drainage outflow from each of the plots, before it was drained out of the field to a nearby ditch. These buildings also contained control mechanisms to stop outflow from pre-defined drains to obtain a controlled drainage configuration. Irrigation inlets were opened, so as to feed water back into these closed tile drains, thus creating the controlled

drainage with sub-irrigation configuration. A more detailed description of the instrumentation at the experimental site is presented by Tait *et al*. (1995).

Five different N-fertilizer treatments were applied. In 2012, the field received 70 kg N/ha. In 2013, a total of 170 kg N/ha was applied. In 2014, a total of 200 kg N/ha was applied. Finally, in 2015, the first half of the field received 230 kg N/ha with only one bulk application in the end of May. The second half of the field received the same total N-fertilizer amount, but divided in two equal applications in early June, at a one-week interval, as indicated in **Figure 3.04**.

Figure 3.01 Layout of free drainage (FD) and controlled-drainage with sub-irrigation (CDSI) treatments within the experimental site

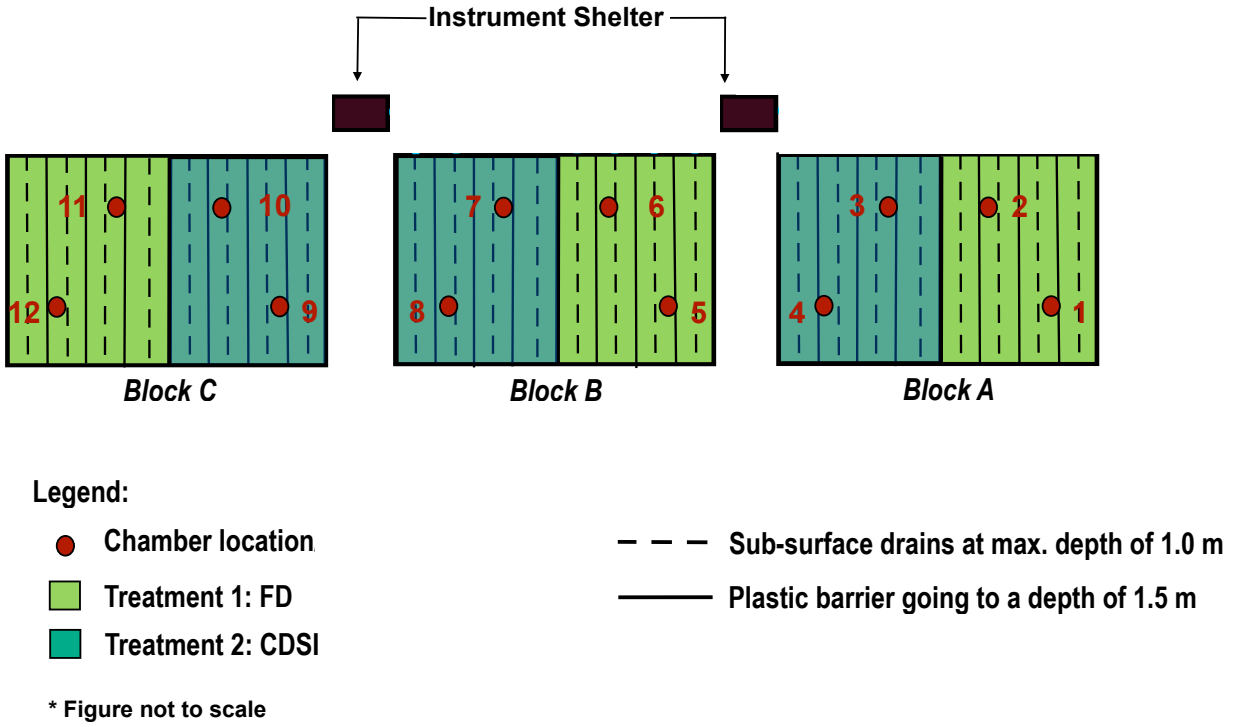

3.1.3 Soil physical properties

Soil samples were taken on May 10th, 2012 near each of the 12 GHG chamber locations, and analysed to obtain measurements of bulk density, porosity and particle density. For each location, samples were taken at three depths: 0-20 cm, 20-40 cm and 40-60 cm. Results reported in **Table 3.02** are the average of the values from each soil sample, respective to each depth.

Bulk density measurements were obtained using the core method, adapted from procedures by Culley (1993). The bulk density of a soil is the mass of the dry soil solids per unit

total volume of soil. Bulk density is indicative of compaction in a given soil. Three-inch diameter soil cores were hammered into the soil, and then dug out preserving the soil structure and porosity of the sample. Samples were brought back to a McGill laboratory and weighed without the soil core. Samples were oven dried at 105°C for 48 hours. Then, the oven-dried samples were weighed again. The bulk density (g/cm^3) was obtained by dividing the measured mass of dry soil per sample by the internal volume of a core.

Porosity was then obtained using the following equation:

$$\textbf{Porosity} = 1 - (\textbf{bulk density}/\rho_s) \qquad [3.1]$$

Where ρ_s is the particle density of each sample. A reference value for mineral soils of 2.65 Mg/m^3 was used (Hillel, 2003).

Particle size analysis was done by the hydrometer method, following procedures developed by Sheldrick *et al*. (1993). For each sample, 40.0 g of soil were placed in a beaker, to which 100 ml of Calgon were added (50 g/ml sodium metahexaphosphate and 4 g/ml sodium carbonate, pH ≈ 8). Hydrometer readings were taken at 30s, 40s, 60s and 7h. For each sample, a plot of percentage of particles by particle size was drawn, using a semi-log x-axis. The percent of clay (<2 μm diameter) per sample corresponded to the percentage of particles in suspension for the reading at 7h. The percent of sand (>53 μm diameter) was obtained by interpolating the percentage for a diameter of 53 μm and subtracting it from 100. The percent of silt (2 μm< diameter <53 μm) corresponded to the remaining percentage. Using these calculations, the textural class respective to each depth was determined using the soil textural triangle.

Saturated hydraulic conductivity (K_{sat}) was determined from soil samples taken on June 14th, 2013. Samples were taken at six locations, two in each of the three blocks and one per treatment. All samples were taken at three depths: 0-20 cm, 20-40 cm and 40-60 cm. Saturated hydraulic conductivity was obtained using the constant head permeability test methodology following procedures developed by Youngs (2001). The constant head method follows Darcy's law, which states that the discharge rate is proportional to the gradient in the hydraulic head and the hydraulic conductivity. By measuring the discharge volume of fluid flowing through the system during a defined period of time t, the saturated hydraulic conductivity K_{sat} of the soil is calculated from the following equation:

$$K_{sat} = QL/Aht \qquad [3.2]$$

Where Q is the discharge volume, calculated from the weight of discharged water, A is the cross sectional area, L is the length of the core, h is the head difference and t is the period of time elapsed.

3.1.4 Soil chemical properties

Soil samples were taken on September 8th, 2015 at approximately one meter from each GHG chamber location. At each of the 12 locations, samples were taken at depths of 0-20, 20-40 and 40-60 cm. For each depth, 3 replicates were taken and mixed in a bucket to have a more representative soil sample. Samples were taken back to a McGill laboratory. Results from all chemical tests are presented in **Table 3.02**.

Measurements of pH were taken following procedures developed by Hendershot *et al*. (1993). To obtain the soil pH, first, 7 g of soil were diluted in 14 ml of water to obtain a 1:2 ratio. These dilutions were mixed thoroughly for 30 minutes, and then left to decant for an hour. Readings of pH from the supernatant were taken using a pH meter.

Measurements of organic matter content and C content were obtained using the Weight Loss on Ignition (LOI) method as described by Skjemstad *et al*. (2009). A representative subsample of 2g was taken from each of the 36 soil samples (12 locations x 3 depths). Each subsample was first dried at 105°C for 24 hours, and then heated to 360°C for 5 hours. The difference in weight between the two steps corresponds to the amount of organic matter lost. The final organic matter percentage corresponds to the ratio of this difference to the weight of dried subsample at 105°C. Finally, an estimation of the soil carbon content was obtained as % organic matter/1.724 = %C.

Measurements of nitrate and exchangeable ammonium nitrogen NH_4^+, NO_3^- were obtained using the 2.0 M KCL extraction method described by Maynard *et al*. (2009). First, five grams of each sample were weighed and placed in 250 ml Erlenmeyer flasks. Two additional flasks were prepared with a sample duplicate and a reference soil. Then, 50 ml of 2 M KCl was added to each flask to obtain a 1:10 soil to solution ratio. All flasks were then shaken for 30 minutes on a rotary shaker. Mixed solutions were filtered using Fisherbrand Q5 filter paper. The filtrate was analyzed by colorimetry to obtain measurements of N as NH_4^+ and N as NO_3^- on a multi-channel Lachat auto analyser.

Measurements of extractable Ca, Mg, K, Mn, Al, and P were obtained following procedures by Ziadi *et al*. (2008). The Mehlich III solution was used, which is a mixture of acetic

acid, ammonium nitrate, ammonium fluoride, nitric acid and EDTA. For each sample, 2.5 g were placed in plastic cups to which 25 ml of Mehlich extractant were added. Samples were shaken and then filtered through Fisherbrand Q5 filter paper. Phosphorus content was then determined by a colorimetric technique using the Lachat Instrument flow injection analysis. An Atomic Absorption Spectrophotometer Perkin Elmer 2380 was used to determine the samples' contents in K, Ca, Al, Mg and Mn. Phosphorus and potassium were determined using undiluted samples. For calcium and magnesium determination, samples were diluted 20 times and received Lanthanum solution to improve the accuracy of measurements. Sodium was not recorded for any of the samples, because values were below the blank reference value of 8.8 mg Na/l.

Table 3.02 Soil physical and chemical properties at depths of 0-20 cm, 20-40 cm and 40-60 cm of the experimental site

	Depth		
Property	**0-20 cm**	**20-40 cm**	**40-60 cm**
Classification	Soulanges series; Gleysol type		
Physical			
Soil texture, %			
Sand	2	4	9
Silt	33	25	22
Clay	65	71	69
Textural class	Sandy loam	Sandy loam	Sandy loam
Bulk density, g cm^{-3}	1.36	1.60	1.46
Porosity, %	49	40	45
Saturated hydraulic conductivity K_{sat}, cm x 10^{-3} s^{-1}	3.00	1.55	1.70
Chemical			
Mean pH	7.0	7.2	7.3
Organic matter, %	3.51	4.51	1.32
Carbon, %	2.0	2.6	0.8
Available NO_3-N, mg kg^{-1}	5	2	1
Available NH_4-N, mg kg^{-1}	1	0	1
Available P, mg kg^{-1}	98	32	9
Available K, mg kg^{-1}	141	46	45
Available Al, mg kg^{-1}	482	512	634
Available Ca, mg kg^{-1}	1364	1120	1424
Available Mg, mg kg^{-1}	157	164	374
Available Mn, mg kg^{-1}	12	10	17

3.1.5 Agronomic management practices

The length of the growing season in the Vaudreuil-Soulanges region is approximately of 201-208 days. The time window without frost is of 140-155 days in the eastern part of the region. The growing season generally starts on the 10-14th of May and ends between mid-October and mid-November (Tabi *et al.,* 1990). In 2012, the cultivated crop was yellow bean, which was followed by three years of grain-corn. For grain-corn cultivation, tillage practices were identical. The fertilizer source and rate for each year was decided by the farmer, who based his calculations on yearly soil nutrient analysis. General recommendations for yellow beans in Quebec are of 45-60 kg N/ha side dressed or broadcast prior to seeding whereas, for grain-corn, they are of 120 to 170 kg N/ha, of which 30 to 50 kg/ha should be side dressed at seeding (Parent *et al*., 2010). Thus, it must be noted that nitrogen inputs for grain-corn can be more than twice the inputs for yellow beans. In May-June 2015, a first half of the site received one bulk application of N-fertilizer. The second half of the field received the same total amount but subdivided into two equal applications, spaced one week apart. This configuration is represented in **Figure 3.02.**

Figure 3.02 Season 2015: one application of 200 kg N/ha on the first half of experimental plot, and two applications of 100 kg N/ha spaced one week apart on the second half of the plot (based on Figure 3.01)

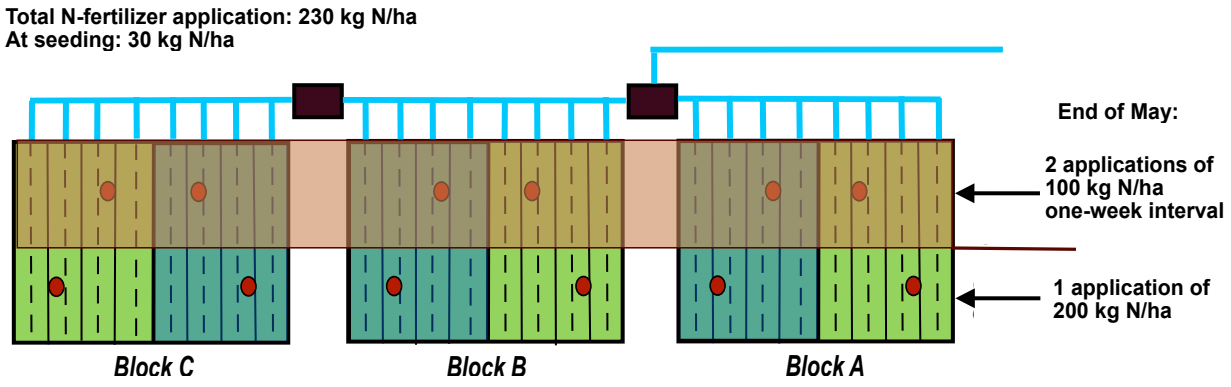

Table 3.03 Timing of agronomic management practices and fertilizer amounts (kg ha^{-1}) for each growing season

	2012	2013	2014	2015
GHG sampling	*May 18-Sep 7*	*Apr 26-Nov 7*	*May 15-Nov 4*	*Apr 27-Nov 3*
Soil sampling	*May 10th* Physical analysis	*Jun 14th* Physical analysis		*Sep 8th* Chemical analysis
Tillage	Chisel in the preceding Oct; Harrow with teeth 24h before seeding (2 passes)			
Liming	Dolomite 3 t/ha	-	-	-
Seeding date	*Jun 22*	*May 2*	*May 12*	*May 3*
Cultivated crop	Yellow beans; half-thin variety	Grain-corn; P9918 (2650 CHU); non-conventional	Grain-corn; P9855 (2900 CHU); P9411 (2800 CHU); conventional	Grain-corn; P9917AMX (2950 CHU); non-conventional
Starter fertilizer				
kg N/ha	60	44	44	28
kg P_2O_5/ha	60	81	81	27
kg K_2O/ha	70	50	50	21
kg Mg/ha	5.4	5.4	5.4	-
kg Ca/ha	5.0	5.0	5.0	-
kg Bo/ha	7.7	7.7	7.7	2.6
Second fertilization				
Date	*Aug 20*	*May 29*	*Jun 7*	*May 29*
Amount	10 kg N/ha †	115 kg N/ha ‡	160 kg N/ha ‡	200 kg N/ha§; 100 kg N/ha ‡ ††
Third fertilization				*Jun 3* 100 kg N/ha ‡ ††
Harvest date	*Oct 10*	*Oct 20*	*Oct 14*	*Oct 21*
Cover crop	*Oct 15* ¶			
Total N fertilizer	**70 kg N/ha**	**170 kg N/ha**	**200 kg N/ha**	**228 kg N/ha**
Yields	**6.9 tons/ha**	**11.6 tons/ha****	**10.6 tons/ha** **FD: 9.56 t/ha** **CDSI: 9.68 t/ha**	**12.7 tons/ha****

† Applied at flowering
‡ Urea: dry, granular; broadcast and then incorporated using a row crop cultivator; applied at the V6 stage of crop growth
§ Applied on first half of experimental plot (see Figure 3.02)
†† Applied on second half of experimental plot
¶ Seeding of green manure (oats); estimated 10 kg N/ha; 20 kg P_2O_5/ha; 8 kg K_2O/ha accountable for the next season; incorporated on Nov. 1 with rotary disk
** Average dry yields for the field (~0% moisture)

3.2 Drainage and irrigation

3.2.1 Growing seasons 2012 and 2013

For both 2012 and 2013, the experimental site was under free drainage throughout the season. Each pipe drained an area of 75 m length by 15 m width. Pipes of Block A discharged in the eastern instrumented building. Pipes of Block B and C discharged in the western building. Drainage outflow was then evacuated from each building to a large sump, from which it was then pumped into a collector pipe. The pipe then drained by gravity into an open ditch on the eastern side of the experimental plot. Tile drains remained open throughout the winter.

3.2.2 Growing season 2014

In the spring of 2014, drains were left open to improve the evacuation of melted ice and snow from the field. Tile drains were left open for seeding on the 12th of May, and for the second application of fertilizer on June 7th, so as to keep the field dry and avoid deep compaction from the traffic of machinery. Once field operations were done, for defined plots indicated in **Figure 3.01**, individual drains were closed, using ball-valve control systems installed in the instrumented buildings. Each control system also included a water table control chamber with a float valve, which allowed for the drainage of overflow water in CDSI plots. This system was designed to obtain a water table depth between 65-75 cm. Water table observation pipes were installed on June 19th.

For the 2014 season, the desired treatment differences were obtained for four sampling days over a 4-week period, in September and early October. This is due to a number of repairs to the sub-irrigation system, which had to be completed this season. Notably, the pump of the well was replaced, along with its pipeline network. The pump at the sump, which evacuated the drainage water from the instrumented buildings was changed. Irrigation inlets to the water table control chambers were changed due to leaks. Ideally, adequate water supply for grain-corn should be ensured at the tasseling and silking stages, which started at the end of July. However, for this year, the sub-irrigation system was effective starting at the end of August. A week prior to harvest, all drains were opened so as to evacuate water from the field to allow for machine traffic. Drains were left open throughout the winter. Recorded water table measurements for the season are presented in **Figure 4.02.**

3.2.3 Growing season 2015

Due to warmer conditions in the spring, the field was seeded earlier in 2015. Seeding was on May 3rd followed by fertilizer applications on May 29th and June 3rd. All tile drains remained opened during that time. Water table observation pipes were set on June 17th. The water table depth was first checked on June 17th, and then on June 25th. As the water table depth was below 1 m for all plots, it was appropriate to activate the drainage control systems for the defined plots, identical to those of 2014.

The sub-irrigation system was first activated on July 13th, due to high temperatures and dry conditions. Following the activation of the irrigation system, more than 60 mm of precipitation fell from July 19th to July 21st. Thus on July 20th, the sub-irrigation was deactivated. On July 22nd, there was a noticeable difference in the water table depth of control-drained plots, as a result of precipitation. For the next 3 weeks, the irrigation system was left deactivated and the water table retrieved to depths greater than 1 meter. A greater water table depth was expected to encourage a more rapid downward growth of roots as the grain-corn was reaching its later vegetative stages (V10-V14). The measured water table difference between free-drained and control-drained plots on August 14th was due to preceding heavy precipitation events. On August 17th, the water table had dropped below 1m for all plots. Moreover, the corn had reached its reproductive stage. At that time, adequate water supply was important to ensure proper filling of the grain. Thus, the sub-irrigation was reactivated. Effects of the sub-irrigation on the water table were observed on August 20th and in the following weeks. An additional two water table observation pipes were added at chambers 3 and 9 (as indicated in **Figure 3.01**) on September 4th, to obtain additional readings of the water table depth. For these chambers, the water table had not risen following the activation of sub-irrigation. It was later identified that these problems were due to clogging of the irrigation inlets from rust in the instrumented buildings. These inlets were fixed for the following sampling week of September 7th. On September 11th, the sub-irrigation was stopped due to 30 mm of rainfall expected over the following weekend. These precipitation events led to the shallow recorded water table on September 15th. In the following weeks, as there were lower temperatures and less consumption of water by the crop, the sub-irrigation remained deactivated. Heavy precipitation events led to the observed water table levels of October 1st. At that time, all drains were opened to allow the water table to retrieve and to allow the field to dry before harvest.

Overall, in 2015, there were 8 days in which the treatments were well differentiated from mid-August to the end of September. All records of the water table depth can be found in **Figure 4.02**. Challenges were encountered due to the difficulty to accurately predict the time and intensity of rainfall events. A heavy rainfall event can lead to a rapid rise of the water table level over just a few days of time. The water input rate from rainfall far exceeded the input rate from the sub-irrigation system. Thus, deactivating the irrigation was not sufficient. Opening all drains prior to heavy rainfall events could have helped prevent the excessive rise of the water table level, particularly towards the end of the season.

3.3 Data collection

3.3.1 GHG sampling method

3.3.1.1 Preparation of evacuated exetainers

Exetainers used for sampling were capped with a double septum: a Teflon/silicon septum (National Scientific, Rockwood, TN) inserted between the standard rubber septum so as to reduce leakage from the container. Exetainers were evacuated in batches of 10 Exetainers for 60 seconds using a single stage rotary vane mechanical vacuum pump (Welch Duoseal ® Vacuum Pump 1399, Gardner Denver Thomas, Inc.) with an ultimate pressure of 1×10^{-2} torr. With the double-wadded cap, it was estimated that 98% of the vacuum in exetainers could be preserved after 136 days of storage (Carter *et al.*, 2008).

3.3.1.2 Non-steady state vented chamber method

Samples were taken using a vented non-steady state chamber method adapted from Hutchinson and Livingston (Hutchinson *et al.*, 2000)(Hutchinson and Livingston, 2001)(Livingston *et al.*, 2006). Twelve acrylic chamber frames of 0.556 m x 0.556 m x 0.140 m (W x L x H) dimensions were inserted 10 cm in the soil, leaving 4 cm of height above the surface. Frames were installed in the field after seeding and after the early-season application of fertilizer and removed before harvest, so as not to disturb the passage of machinery in the field. For sampling events without chamber bases, shovels were brought to the field so as to cover chamber peripheries with soil and prevent the movement of air between the chamber headspace and the atmosphere. Headspace volume was adjusted when calculating GHG concentrations.

At the time of sampling, chamber covers of 0.53 x 0.53 x 0.14 m (W x L x H) dimensions were placed on top of the frames. A headspace volume of 51, 691.44 cm^3 was obtained. This volume was adjusted according to the base above-ground height set each year. In each chamber, two holes were drilled: one for the insertion of a tube with the septa of a 0.6 cm diameter for gas sampling and the other for the insertion of a vent tube of 1.6 cm of diameter. Each chamber bottom was lined with a 0.6 cm strip of acrylic plastic of dimensions 0.04 x 0.597 cm onto which a plastic gasket seal of closed cell foam was glued to improve the sealing of the chamber when set on the frames. **Figure 3.03** illustrates the non-steady state vented chamber design.

Figure 3.03 Non-steady state vented chamber design

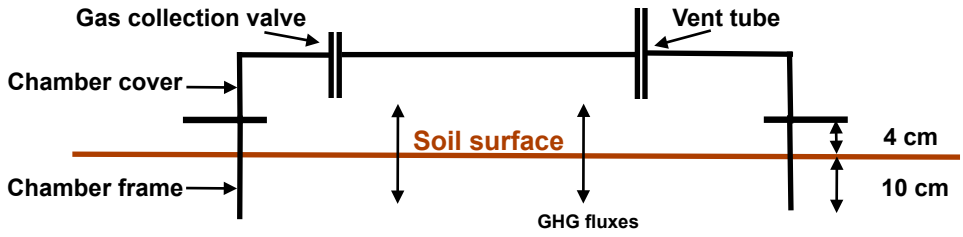

3.3.1.3 Sampling location

Chambers were set in identical geo-referenced locations for the entire season, in all four years. Two sampling locations were designated per water treatment per block. For each treatment, central plots were chosen for sampling leaving one buffer plot on each side as indicated in **Figure 3.01**. The chambers were not placed exactly above tile drain lines. The margin of error was of approximately 3 meters.

3.3.1.4 Gas sampling procedure

Immediately after a chamber was set onto a frame, a gas sample corresponding to time t=0 was taken using a 20 ml syringe with a needle tip (25 gauge, 1.6 cm, Benton and Dickson). Gas samples extracted from the chamber headspace were placed in evacuated 12 ml Exetainers containing 15 mg of magnesium perchlorate to absorb water vapour (Labco, High Wycombe, UK). Subsequent samples were taken at every 15 minutes, at times t=15, t=30, t=45 and t=60 minutes. For each of these sampling times, the syringe was inserted in the chamber septa and

flushed three times so as to homogenize air within the headspace. At sampling location 1 in **Figure 3.01**, three air samples outside the chamber were taken at times t=0, t=30 and t=45 minutes, as control.

3.3.2 Water table depth

Water table depth was monitored and recorded at every sampling event. PVC pipes of 0.04 m diameter were installed near each chamber location to an average depth of 1.32 m. Pipes were perforated with 2 mm holes along their length, with 5 cm spacing and covered with a geo-textile so as to prevent clogging with fine soil particles. Water table measurements were obtained by placing, within the PVC pipes, a measuring rod containing an open electric circuit wired to a sensor. The sensor set off an alarm once the end of the rod was submerged in water. The water table depth was obtained by subtracting the above-ground observation well length (offset) from the measuring rod reading, as indicated in **Figure 3.04**.

Figure 3.04 Water table depth monitoring

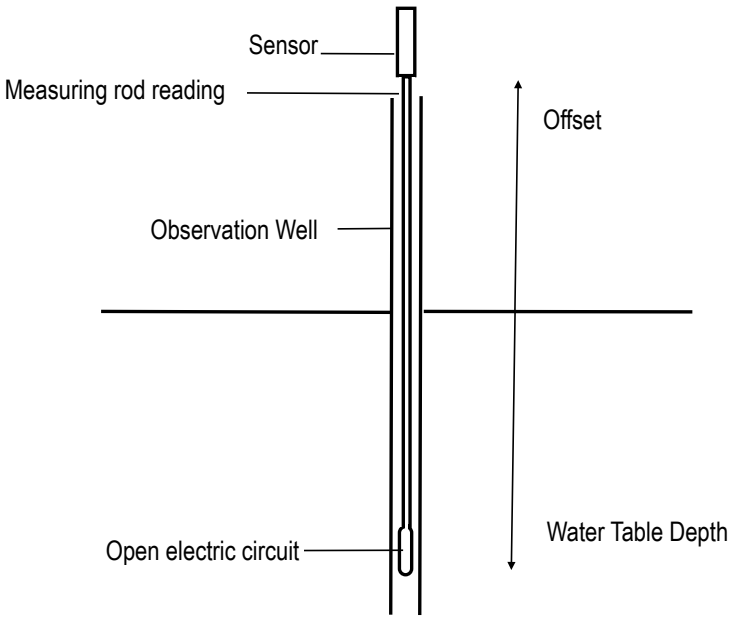

3.3.3 Meteorological data

An on-site weather station (Campbell Scientific Inc., Logen, UT, USA) equipped with a tipping bucket rain gauge (Model TE525MM, Texas Electronics, Dallas, TX, USA) provided daily, hourly readings of air temperature and precipitation during the year. Weather data was compared to data recorded for the Environment Canada weather station at Côteau-du-Lac (Station ID – 7011947; Lat 45.32, Long -74.17).

3.3.4 Ancillary measurements

At each sampling event and for each chamber location, soil temperature, air temperature and soil volumetric water content measurements were taken using hand-held probes. Soil temperature was taken using a hand-held thermometer of ±0.5°C accuracy, outside (Hanna® Instruments). Air temperatures were taken and then, compared to those obtained by the on-site weather station, located approximately 500 m from the experimental plots.

A ThetaProbe was used to obtain the topsoil volumetric soil water content (θ_v) for the top 6 cm of the soil (Model ML2x; Delta-T Devices Ltd., 1999, Cambridge, UK). Volumetric soil water content is the ratio between the volume of water present in the soil and the total volume of the sample. Readings of this parameter were expressed as a percentage (% volume). Three measurements were taken around each chamber at the time of sampling. The average soil moisture per chamber was recorded.

ThetaProbes measure volumetric soil water content by obtaining an apparent dielectric constant using the following equation:

$$\theta_v = (\sqrt{\varepsilon} - a_0)/a_1 \qquad [3.3]$$

where ε is the apparent dielectric constant. Constants a_0 and a_1 are soil-specific and were determined through laboratory calibration of the probe. Soil specific calibration will achieve a typical accuracy of at least ±0.02 m^3m^{-3}, whereas use of the generalised calibration parameters of the probe will have an accuracy of ±0.05 m^3m^{-3}.

3.3.5 Laboratory measurements

Samples were brought back to a laboratory of McGill University to be analysed through a Bruker 450-GC System (Bruker corp., Bremen, Germany). This system enabled the analysis of all three gases of interest (CO_2, CH_4, and N_2O). Samples were simultaneously injected onto two channels. The first channel was equipped with two detectors: a thermal conductivity detector (TCD) and a flame ionization detector (FID). The second channel was equipped with an electron

capture detector (ECD). CO_2 and CH_4 were analysed using the FID, set at 300°C. The ECD set at 350°C was used to detect N_2O. Helium was used as the carrier gas for the FID with a flow rate of 30 ml/min, and argon was used as the carrier gas for the ECD with the flow rate of 10 ml/min.

The gas chromatograph (GC) was equipped with two 30 m packed columns of 250 μm diameter. The first column of 2 m x 1/8" Stainless steel was installed with the ECD and packed with HayeSep D, 80/100 Mesh. The second column of 3.6 m x 1/8" Stainless steel was installed with the FID and packed with HayeSep A D, 80/100 Mesh (produced by Bruker corp., Bremen, Germany). The oven temperature was set constantly at 80°C for a run time of 4.5 min. The data was recorded and analysed using an integrated GC data system (Compass CDS, Version 3.0.0.68, Bruker). For every 20 samples, three gas standards (A, B and C) were run for quality control (Benslim, 2014). The composition of these standards are indicated in **Table 3.05** (Supplier: Linde):

Table 3.04 Air standards used for the analysis of greenhouse gas samples

Standards	*A*	*B*	*C*
CO2	350 ppm	1000 ppm	5000 ppm
CH4	2 ppm	3 ppm	5 ppm
N2O	0.3 ppm	1 ppm	10 ppm

3.3.6 Gas flux calculations

The GC analysis provided raw data in parts per million (ppm) units. A lower threshold was then applied for data filtering. The lower limits for N_2O, CH_4 and CO_2 were 0.15 ppm, 1.7 ppm and 300 ppm, respectively. The raw data was converted from ppm to mg of main constituent (C for CO_2 and for CH_4, and N for N_2O) per m^3 of air using the following equation **[3.4].**

$$\mathbf{C_m = C_v MP/RT} \qquad \mathbf{[3.4]}$$

Where:

C_m: Mass/volume concentration (mg/m^3)

C_v : Concentration (v/v) in ppm

M: Gram molecular weight (CO_2 = 12 mg/mol; CH_4 = 12 mg/mol; N_2O = 28 mg/mol)

P: Atmospheric pressure = 760 mmHg

R: Universal gas constant = 0.0624 $m^3.mmHg\ .K^{-1}.mol^{-1}$

T : Room temperature during lab work = 293.15 K

For each sampling event, the flux of each gas over the 1-hour sampling time was calculated from the 5 concentrations taken at 15-min intervals. For each two gas concentrations obtained, the slope of the linear regression was obtained. As such with 5 concentrations obtained per 1-hour sampling time, 10 possible slopes were calculated. The median of these fluxes was taken for each given chamber, using equation **[3.5].** Then, the slope was multiplied by the height of each chamber so as to obtain the final flux for each gas per each 1-hour sampling event, using equation **[3.6].**

$$Slope_{median} = \Delta C / \Delta t \qquad [3.5]$$

$$f_t = H\,(\Delta C / \Delta t)_{median} \qquad [3.6]$$

Where:
$Slope_{median}$: median slope ($mg/m^3.h$)
ΔC : Difference of gas concentration (mg/m^3)
Δt : Difference of time (hour)
f_t : flux ($mg.m^{-2}.h^{-1}$)
H : chamber height (m)

3.4 Yields

Crop yield samples were taken right before harvest, on October 14th, 2014. Sampling was done along three east-west lines, equally spaced, for each treatment (FD or CDSI), within each of the three blocks on the site. Along each line, corn plants were collected along a 2.5 m length in one row. Stalks were tied together. Cobs were placed in separate paper bags, labelled by sampling location.

The wet mass of bundles of stalks was measured. Stalks were then chopped and a sub-sample of each bundle was taken. Sub-samples were then dried at 170-200 °F in a propane dryer. The dried weight of the sub-samples were taken on October 17th, so as to calculate the water content and the total dry biomass of the stalks.

The wet mass of the cobs was measured. The cobs were dried in a propane dryer at 170-200 °F. On October 17th, the dried cobs were weighed again. The cobs were then shelled. The dry grain weight was obtained for each sampling location.

The dry biomass and the mass of dry grain were added to obtain a total dry yield in tons/ha.

Table 3.05 Growing season 2014 yields

Growing season 2014 grain-corn yields					
Block	Treatment	Dry grain (t/ha)	Dry grain with 15% moisture (t/ha)	Dry biomass (t/ha)	Total dry yields (t/ha)
A	FD	9.5	10.9	15.7	25.2
A	FD	9.3	10.7	17.3	26.7
A	WTM	10.0	11.4	14.8	24.8
A	WTM	9.2	10.6	12.4	21.6
B	FD	9.1	10.4	14.0	23.1
B	FD	9.8	11.2	18.0	27.8
B	WTM	10.6	12.2	17.8	28.5
B	WTM	9.4	10.8	15.7	25.2
C	WTM	9.6	11.1	16.0	25.6
C	WTM	9.3	10.7	17.5	26.8
C	FD	10.4	12.0	14.8	25.3
C	FD	9.3	10.7	16.2	25.5

3.5 Statistical analysis

All statistical results are presented in **Appendix B**.

A number of limitations were encountered, particularly in meeting the assumptions of statistical tests. It must be noticed that the days, on which samples for each year were taken, were different. Moreover, the total number of sampling days within each year were different: 9 in 2012, 14 in 2013, 21 in 2014 and 24 in 2015. The total number of flux values obtained for each day was different for some days. This is due to experimental errors noticed during the processing of exetainer GHG concentrations. Therefore, some of the flux values were not kept. The assumption of homogeneity of variances could not be met. Finally, GHG flux results follow trendlines throughout the season. As such the independence of responses to variables could not be met.

As was explained in a previous section, our experimental layout includes three blocks spaced 30 m apart. Their soil physical and chemical properties are similar. It is accepted that all three blocks undergo the same meteorological events over time. All three blocks contain each treatment studied in each year. For each year, and each greenhouse gas, the effect of block identity on fluxes were tested using a standard least square test of the JMP Statistical Visualization software (JMP® **11.2.0).** Blocking was found to have an effect on fluxes in year

2012 for CO_2, and in year 2014 for CO_2 and CH_4. However, in 2012 and 2014, blocking did not interact with the effect of the factors of interest, sampling day in 2012, and drainage/sub-irrigation treatment and sampling day in 2014. However, in 2014 for CH_4, blocking interacted with the effect of drainage/sub-irrigation treatment. This may have influenced the obtained results, which indicate that drainage/sub-irrigation treatment had an insignificant effect that year. For all other years and greenhouse gases, blocking effect was removed from the model.

For seasons 2012 and 2013, a one-way analysis of variance was run to compare the mean fluxes between each two sampling days, for CO_2, CH_4 and N_2O respectively, throughout the season. In 2014, a two-way analysis of variance (ANOVA) was run to compare the means from the 6 chambers of either free drainage or controlled drainage/sub-irrigation treatments, for CO_2, CH_4 and N_2O respectively, and on each sampling day. Factors of interest were days and drainage/irrigation treatment. The Tukey-Kramer method was used so as to compare all possible pairs of means. In 2015, a factorial model was set up to include the effects of sampling day, drainage/sub-irrigation treatment and fertilizer application. A standard least square test indicated that drainage/sub-irrigation treatment and fertilizer application effects did not interact amongst each other. As such, two-way ANOVA results respective to each test are presented separately in **Appendix B**. The Tukey-Kramer method was used so as to compare all possible pairs of means. A 95% confidence interval was used for all tests.

For each year, data was classified by each treatment combination. Mean fluxes of each gas by treatment, and their respective recorded soil volumetric water content were graphed on a scatter plot and fit to either 2nd order polynomial or exponential equations. Pearson correlation coefficients were obtained, to suggest the strength of the relationship between the two variables. The same was done to obtain correlation coefficients (R^2) respective to soil temperature. Correlations of each GHG with either soil temperature or soil volumetric water content are presented in **Appendix A**.

Chapter 4: Results and Discussion

4.1 Soil water dynamics

In this study, precipitation had a strong influence on soil water dynamics. The four cropping seasons of this study were marked by different climatic conditions. While in 2012, the cropping season precipitation (April-September) was nearly equal to the 40-year mean, 2013 could be considered a wet year with a cropping season precipitation that was 126 mm above the 40-year average. Seasons 2014 and 2015 were both dry with cropping season precipitations of 82 mm and 53 mm below the 40-year average, respectively. The monthly precipitation amounts for the four experimental years and the corresponding 40-year averages are shown in **Table 4.03**.

The distribution of precipitation events should also be observed. With the exception of 2012, June was by far the month with the most precipitation for all seasons. June 2014 and June 2015 represented 20% and 27% of their respective total seasonal rainfall amounts. The number of rainfall days within each month is also important. June 2014 was distinguished by three punctual events of daily precipitations of more than 20 mm followed by days without rain. In contrast, June 2015 had similar monthly rainfall quantities, but distributed in equal and more frequent events. Consequently, soil volumetric water content was much more stable in 2015 and did not show fluctuations of 15% as can be seen in 2014. The alternate drying and wetting of soil through punctual precipitation events was found to enhance the release of N_2O due to the stimulation of N mineralization and the accumulation NO_2^- during the dry periods (Zurbrigg, 2010). However, in this study, N_2O production does not consistently increase following punctual irrigation or precipitation events.

The experimental site was located in the Montérégie region of Quebec, which has a humid, temperature climate. As such, sub-irrigation was used to complement the relatively abundant precipitation and to avoid crop stress during the dry months of the season. With the equipment set up at this experimental site and considering average climatic conditions, a total of approximately 100 mm of irrigation water was added to the field. As such, the contribution of water input to the soil profile from sub-irrigation was relatively small compared to that of precipitation (~ 400 mm).

The average water table depth in CDSI plots was 83 cm in 2014 and 81 cm in 2015. This water table was obtained through the retention of precipitation water by controlled drainage and through the addition of sub-irrigation water. In free drainage plots for both seasons, the water

table depth could not always be reached through the observation wells, as the water table reached depths greater than 1.32 m. Values were brought back to 1.00 m in these cases. Thus, values for free drainage plots represented in **Figure 4.02** are adjusted values.

Comparatively to the effect of precipitation on soil water dynamics, controlled drainage/sub-irrigation only altered soil volumetric water content by 3.5% on average in 2014 and by 1.3% in 2015. At a one-week interval, the largest variations observed in FD and CDSI treatments were 8.2% in June 2014 and 4.4 % in 2015. These variations in soil moisture were relatively small compared to the fluctuations of 15% or more created by single daily precipitation events of more than 30 mm. Even at times of stable water table levels, large changes in the soil surface volumetric water content can be seen in **Figure 4.02**. Therefore, as compared to FD and CDSI treatments, precipitation had a much greater influence on the water content of the top 6 cm of the soil.

Soil water content can be expressed in a number of ways: water filled pore space, gravimetric water content, and volumetric water content. Volumetric water content in % (m^3/m^3) was used in this study. So as to compare results with publications using WFPS measurements, the following equation was used to convert values (Linn and Doran, 1984):

$$\% \ \mathbf{WFPS} = (\theta_v/\mathbf{TP})(100) \qquad [4.1]$$

Where:

WFPS = water filled pore space (%)

θ_v = percent volumetric water content

TP= percent total soil porosity

The calculated porosity of the soil in the top 20 cm of the soil was 49%. As such the range of soil volumetric water content per year and their equivalent water filled pored space were the following:

Table 4.01 Range of soil volumetric water content (%) and equivalent water-filled pore space (%)

	Soil water content values			
	Free drainage		Controlled drainage/Sub-irrigation	
	θv (%)	WFPS(%)	θv (%)	WFPS(%)
2012	7-36	14-73	-	-
2013	12-51	24-100	-	-
2014	15-40	31-82	17-44	35-90
2015	21-35	43-71	21-37	43-76

In 2013, the recorded soil volumetric water content of 51% could be inaccurate. For that year, we could question the accuracy of the probe calibration. At saturation, the soil volumetric water content should not exceed the calculated soil porosity of 49%.

The aim of controlled drainage/sub-irrigation is to maintain and replenish soil available water within the effective crop rooting depth. Soil available water will be the difference between the amount of water in the soil at field capacity and the amount at the permanent wilting point. As indicated in **Table 4.02** (Saxton and Rawls, 2006), in a sandy loam soil, water will be available in the range θ_v=8-18%, which should be the target range for irrigation schedules. The soil will be considered saturated at θ_v= 45%. As our soil had a slightly higher organic matter content of 3.51%, these values may alter slightly. Thus, in this study, we observed that for nearly all sampling dates, measured soil volumetric contents were above the permanent wilting point. With the exception of 7% obtained in 2012, soil volumetric water content was above 10%. At θ_v =10%, approximately 20% of the total soil available water capacity was present. Therefore, although controlled-drainage/sub-irrigation resulted in slightly higher WFPS values, all crops were sufficiently supplied with water even in free-drainage plots throughout the 4 years of the study.

Table 4.02 Estimates of field capacity and permanent wilting point by soil texture class at 2.5% organic matter (Saxton and Rawls, 2006)

Texture class†	Sand	Clay	Wilt pt.	Field cap	Saturation	Plant avail.	Saturated conductivity	Matric density
	%w		1500 kPa	33 kPa	0 kPa %v		mm h^{-1}	g cm^{-3}
Sa	88	5	5	10	46	5	108.1	1.43
LSa	80	5	5	12	46	7	96.7	1.43
SaL	65	10	8	18	45	10	50.3	1.46
L	40	20	14	28	46	14	15.5	1.43
SiL	20	15	11	31	48	20	16.1	1.38
Si	10	5	6	30	48	25	22.0	1.38
SaCL	60	25	17	27	43	10	11.3	1.50
CL	30	35	22	36	48	14	4.3	1.39
SiCL	10	35	22	38	51	17	5.7	1.30
SiC	10	45	27	41	52	14	3.7	1.26
SaC	50	40	25	36	44	11	1.4	1.47
C	25	50	30	42	50	12	1.1	1.33

† Sa, sand; L, loam; Si, silt; C, clay.

Saturated conditions were attained in 2013 and in 2014. These sampling dates are important for this study, to better understand greenhouse gas production under anaerobic conditions. As indicated in **Table 4.02,** a sandy loam has a good saturated hydraulic conductivity relatively to finer-textured soils. The measured saturated hydraulic conductivity for this study was 3.00 x 10^{-3} cm/s or 108 mm/h in the top 20 cm of the soil. This is a good conductivity, suggesting an efficient drainage rate. As such, prolonged periods of saturated soil conditions should not be expected.

Although higher soil water contents may increase greenhouse gas production, sufficient air-filled pore space will be important to the diffusion of these gases to the atmosphere. Greenhouse gas fluxes will follow Fick's Law of Diffusion, representing the time-dependent rate of gas exchange across the surface-atmosphere boundary:

$$\mathbf{F_d = \tau \theta_A D\ (dc/dz)} \qquad \mathbf{[4.2]}$$

Where:
F_d = flux of greenhouse gas (mg C or $N/m^2/h$)
τ = tortuosity
θ_A = air-filled porosity
D = diffusion coefficient
dc/dz = ratio of the change in the gas concentration (c) along the soil depth (z)

In air, the diffusion coefficient of CO_2 at 25°C is of $1.42.10^{-1}$ cm^2/s and decreases to $1.95.10^{-5}$ cm^2/s in water. Similarly, nitrous oxide will have a diffusion coefficient of 1.81 cm^2/s at

25°C in air and a coefficient of $1.92.10^{-5}$ cm^2/sec at 20°C in water (Thomas *et al*., 1964)(Healy *et al*., 1996). As such, greenhouse gases will escape the soil much more efficiently through air pathways within soil pores. Moreover, it is important to note that the slowed diffusion of N_2O to the atmosphere will increase chances of its reduction to N_2 in the soil. Therefore, large changes in soil volumetric water content as observed in this study may first, increase GHG production and then, allow GHG diffusion through increased air-filled pore space.

Table 4.03 Rainfall days and amount, and historical 40-year average

	2012		2013	
	Amount (mm)	**Rainfall Days**	**Amount (mm)**	**Rainfall Days**
April	87.2	15	35.4	12
May	136.4	16	84.6	13
June	82.6	15	207.4	18
July	88.4	8	141.2	8
August	63.4	10	72.2	13
September	89.5	8	132.6	11
Total	**547.5**	**72**	**673.4**	**75**

	2014		2015	
	Amount (mm)	**Rainfall Days**	**Amount (mm)**	**Rainfall Days**
April	91.7	21	64.4	9
May	85.3	15	56.8	9
June	132	14	135.1	17
July	61.9	10	87.9	10
August	51.4	18	74.5	15
September	42.6	11	75.3	12
Total	**464.9**	**89**	**494**	**72**

	Historical
	40 Year Average (mm)
April	73.0
May	86.5
June	98.7
July	100.7
August	93.4
September	94.8
Total	**547.1**

Figure 4.01 Daily rainfall (mm) from on-site weather station over the 2012 and 2013 seasons, and recorded soil volumetric water content (%) with respective standard deviation on each sampling event

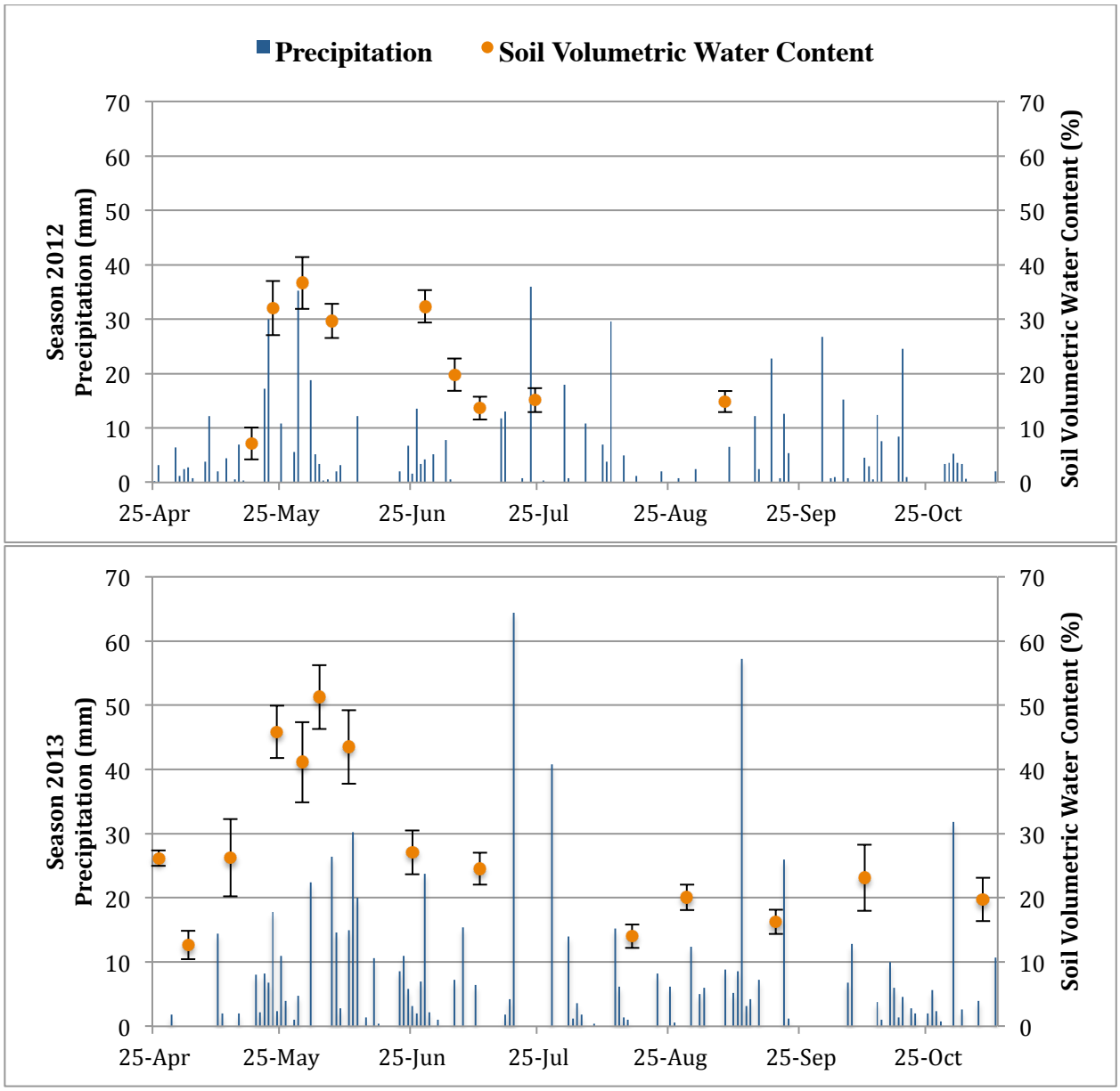

Figure 4.02 **Daily rainfall (mm) over the 2014 and 2015 seasons, recorded soil volumetric water content (%) and water table depth (cm) per water treatment**

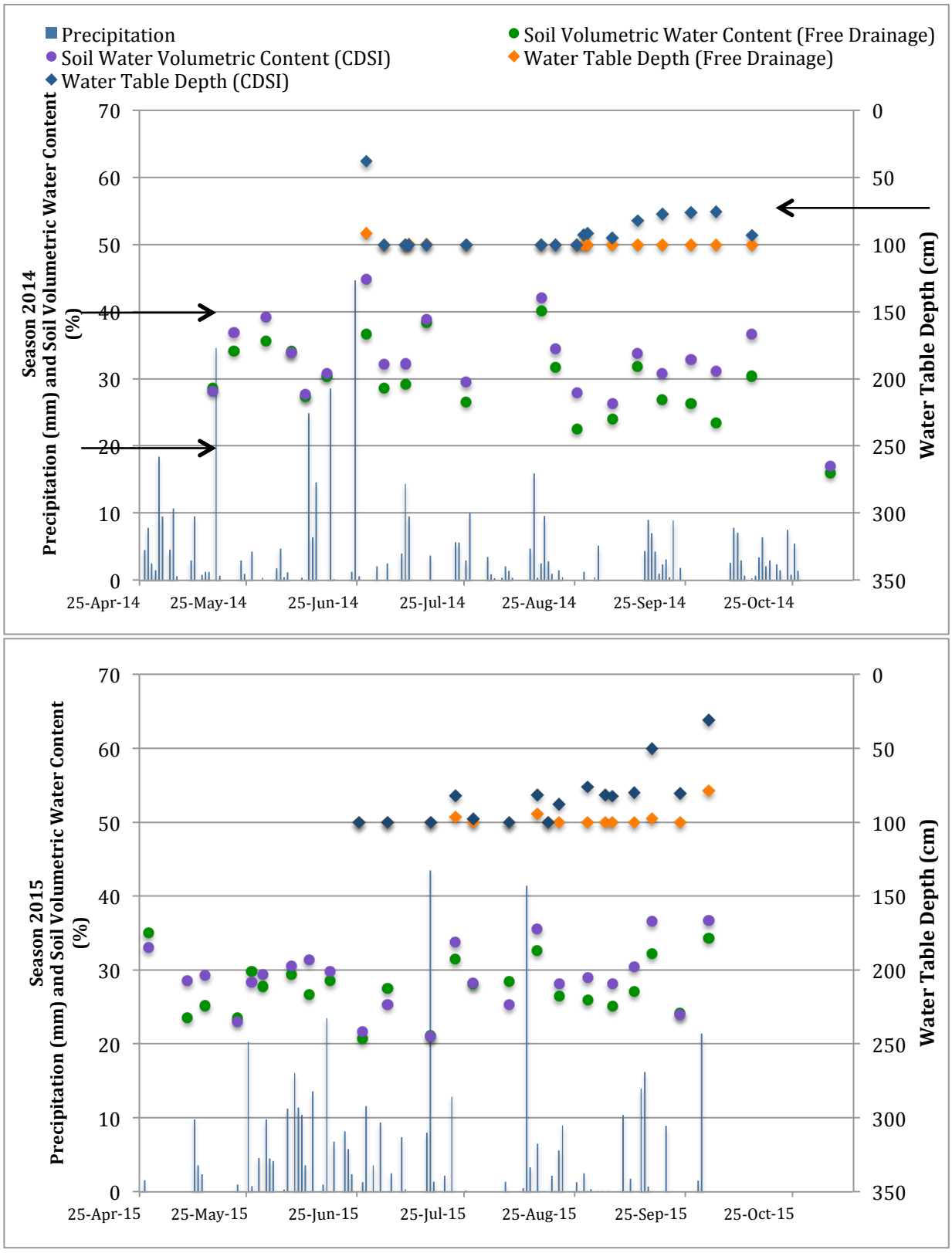

4.2 Temperature fluctuations

Air temperatures followed similar trend lines through all four seasons with maximum temperatures attained mid-season and temperatures dropping below zero in the winter. Maximum temperatures per season were: 27°C on June 20th 2012, 27°C on July 17th 2013, 25°C on June 30th 2014 and 25°C on September 7th 2015. For 2013, 2014, and 2015, June had the highest monthly precipitations, which were systematically followed by the highest seasonal temperatures in July. For 2012, 2013 and 2014, we notice a relatively linear increase of air temperatures from April to the first half of July. Temperatures then decrease at a slower rate over the next 2.5 months.

Table 4.04 Mean monthly temperatures and 40-year average for each month

	Mean monthly temperatures (°C)				
	2012	**2013**	**2014**	**2015**	**40-Year Average**
May	15.6	15.2	13.8	16.3	13.1
June	19.7	17.7	19.4	17.2	18.0
July	21.3	21.1	19.9	20.4	20.4
August	21.3	19.0	18.9	19.9	19.2
September	15.2	14.1	15.0	18.1	14.6
5-month average	**18.6**	**17.4**	**17.4**	**18.4**	**17.1**

Soil temperature in the top 9.5 cm of the soil was measured at each chamber location, on each sampling date. Temperatures ranged from 12-24°C in 2012, 5-23°C in 2013, 5-30°C in 2014 and 11-27°C in 2015. As was discussed in a previous section, temperatures of interest will be 30°C at which microbial respiration is expected to be optimum (Linn and Doran, 1984), and 20-30°C range for optimum methanotrophy (Le Mer *et al.,* 2001). Denitrification rates are expected to increase exponentially from 0-25°C (Rochette *et al.,* 2004).

This study did not prove that better aerated soils warm and cool faster, due to the much lower heat capacity of air compared to water. For 2014 and 2015, seasonal differences in measured soil temperature between the free drainage and controlled-drainage/sub-irrigation treatments are negligible. In 2014 and 2015, the seasonal average of differences were of 10^{-4}-10^{-2} °C.

Soil temperature readings in the field were taken outside the boundary of the chamber bases. It was assumed that readings would not be significantly different within the base area. To

avoid a significant rise in temperature (>5°C) in the chamber headspace during deployment, chambers were covered with reflective aluminum foil. Moreover, each chamber was fit with a vent tube of 5/8". Both of these chamber criteria were installed to avoid changes in temperature and resulting disturbances in pressure within the headspace (Ideal Gas Law). Temperature increases within chambers would not only increase headspace pressure but also increase the feedback effect of the chamber on the soil during deployment. The feedback effect of the chamber corresponds to the effect of the change in gas concentration in the headspace on the vertical and horizontal gradients involved in the diffusion of that gas in the underlying substrate (Hutchinson *et al*., 2000). This change in gas concentration, which can be altered by temperature changes can thus affect the flux of gases at the soil surface. Diffusion coefficients in air and in water involved in Fick's Law are also temperature-dependent. The effect of temperature on GHG production will be discussed in the following section.

Figures 4.03 Soil and air temperature records throughout each season

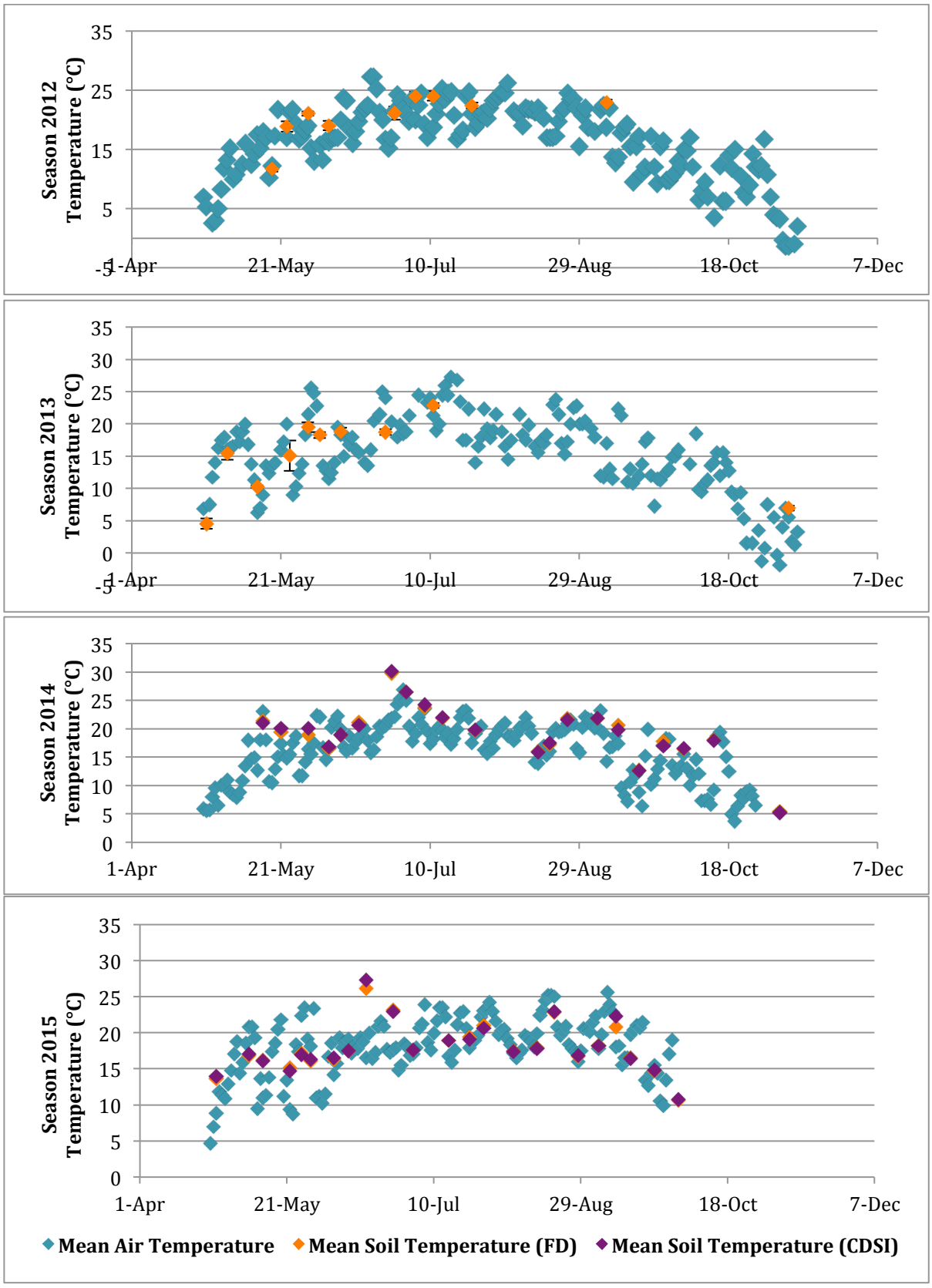

4.3 Carbon dioxide

Chamber bases were set in the 30-inch inter-rows of grain corn, and in between yellow bean crops for 2012. As such, fluxes reflect rhizosphere respiration, which includes both root respiration and CO_2 produced from microbial decomposition of soil organic matter in the root zone.

4.3.1 Effects of temperature

The four years of data indicate that soil temperature is an important regulator of CO_2 fluxes. In 2014 and 2015, CO_2 fluxes draw a 'M' shape as can be seen in **Figure 4.05**. A similar 'M' shape is present in recorded soil temperatures presented in **Figure 4.03**. For 2014, a clear depression is visible in both CO_2 flux values and soil temperatures between June 27th and August 25th. For 2015, a similar depression is present in both CO_2 flux values and soil temperatures between June 17th and September 10th. This depression is not visible in air temperature trends in either season. The drop in soil temperatures in mid-season could be attributed to the establishment of the corn canopy, creating a barrier to light radiation. As such, soil temperatures would decline as the crop canopy thickens and increase again when the crop leaves loose vigour towards the end of the season. Looking at results from the yellow-bean field in 2012, soil temperatures are more consistent with air temperatures. Accordingly, there is no depression in CO_2 flux values in mid-season. Therefore, yellow bean crops may not create a microclimate as is observed below the corn-canopy. This study shows that the canopy in cornfields creates slower soil temperature variations than in a yellow bean field.

Similarly, in 2013, maximum flux values were obtained on June 25th and August 19th, with lower fluxes between these two dates. In 2013, recorded soil temperatures did not exceed 19°C. The maximum flux value obtained that season was of 110 mg C-CO_2.m^{-2}.hr^{-1}, which could be explained by lower soil temperatures that season. In 2014 and 2015, soil temperatures reached 27°C and 30°C, resulting in maximum mean fluxes of 190 and 203 mg C-CO_2.m^{-2}.hr^{-1}.

Looking at **Figure A.1**, a linear increase of CO_2 fluxes is observed from 10-30°C. The best obtained Pearson R^2 coefficient for the correlation of soil temperature to CO_2 flux in the 4 years was of 0.72. The mean of all correlation coefficients obtained was of 0.53. Although this study indicated that soil temperature is an important regulator of CO_2 fluxes, its influence is limited.

There is a clear seasonality of CO_2 fluxes. For years 2013-2015, maximum values were obtained on June 26th. Looking at seasons 2014 and 2015 in **Figure 4.05**, for similar temperatures at the beginning and end of the season, resulting CO_2 fluxes are not the same. Comparing June 26th to September 10th 2015, both had soil temperatures near 23°C. However, measured fluxes on each day were quite different: 191 mg $C\text{-}CO_2.m^{-2}.hr^{-1}$ on June 26th and 107 mg $C\text{-}CO_2.m^{-2}.hr^{-1}$ on September 10th (looking only at free drainage plots). Although temperature is an important driver of CO_2 fluxes, other factors should be taken into consideration.

4.3.2 Effects of soil water content

In this field study on sandy-loam soil, soil respiration peaked following 27-45% soil volumetric content, which corresponded to 55-97% WFPS. For 2013-2015, CO_2 flux values increased exponentially in the month of June, which had highest seasonal precipitation amounts for each of these years. However, as root and soil microbial respiration increasingly consumed O_2 in June, they depleted the soil's oxygen reserve resulting in soil anaerobic conditions. Nitrous oxide production was present at the end of June in years 2013-2015. Moreover, in 2014, methane production was also present indicating highly reduced soil conditions.

Season 2012 had considerably higher rainfall amounts than years 2014 and 2015, which were both dry seasons. However, following June 2012, soil volumetric water contents fluctuated within 10-20%, whereas values fluctuated around 30% in 2014 and 2015. This may have been due to the canopy effect of grain-corn. This further supports the previously mentioned idea of a microclimate created by corn canopies. The corn canopy slowed soil temperature variations but also retained soil humidity in this study. Indeed, the canopy could not only act as a barrier to light exposure but also as a wind-shield.

Following the month of June, the effect of higher soil volumetric water content in 2014 and 2015 did not result in higher values of CO_2 fluxes, compared to 2012. Looking at Pearson's R^2 coefficients, the mean value was of 0.18 for the correlation between soil volumetric water content and CO_2 flux. Stronger correlations were not found, suggesting that volumetric water content only had a weak influence on CO_2 fluxes. In terms of drainage and irrigation treatments, results of a two-way ANOVA including sampling date and drainage/irrigation factors showed, a significant effect of drainage/irrigation treatments on fluxes. Looking at **Tables B.03** and **B.05**, statistically significant differences between free drainage (FD) and controlled-drainage/sub-

irrigation (CDSI) were found on the majority of sampling days in 2014 and 2015. However, for 2014, the fluxes were on average greater in CDSI plots while in 2015, they were greater in FD plots (differences for both years ranged from 15-18 mg C-CO_2.m^{-2}.hr^{-1}). For both years, soil water contents were greater in CDSI plots. Therefore, CO_2 fluxes in this study are neither intrinsically linked to soil water content nor to drainage/irrigation practices.

4.3.3 Plant and microbial biology

Season 2012 had the particularity of showing a low of 32 mg.m^{-2}.hr^{-1} on June 28th, followed by three seasonal peak flux values in July when fluxes usually dropped for all other seasons. For the three values of interest in June 2012, soil temperatures and volumetric water content were comparable to those measured in 2013 at that time. It should be noted that in 2012, yellow beans were seeded on the 22nd of June. As such, CO_2 fluxes could be due to agronomic fieldwork (tillage) and/or the application of starter fertilizer at that time.

The greatest CO_2 fluxes were not obtained at the tasseling stage, as could be expected. Indeed, at tasseling, root biomass is at its maximum (Amos *et al.,* 2006). In this study, CO_2 efflux from the soil was greatest in the early vegetative growth of the corn. On June 27th 2014, when a CO_2 peak flux occurred, the corn stage was V9. Although two corn hybrids were grown that year, each variety reached the same stages at the same time. The field reached the tasseling stage towards July 22nd. In terms of root biomass growth, from emergence to around V6, studies have shown very little variation in root biomass amongst different soil conditions (Amos *et al.,* 2006). It is during the much more rapid and linear phase of growth (V8 to VT) that environmental factors such as temperature, soil conditions and moisture levels will be expressed through variations in root biomass (Amos *et al.,* 2006). As such, exponential increase of CO_2 fluxes at the beginning of the season could be explained by the combined effects of increasing temperatures, high monthly precipitation and by high root activity in the soil, which could have in turn stimulated soil microbial respiration.

Yields were taken for each water management treatment in 2014. Respective dry biomass yields were of 25.57 tons/ha in FD and 25.40 tons/ha in CDSI plots. Yields of dry grain were also similar at 9.6 and 9.7 tons/ha for FD and CDSI, respectively (equivalent to 11.1 and 11.2 tons/ha at 15.5% moisture). From the measured aboveground corn biomass, the root biomass was calculated in the following manner (Amos *et al.*, 2006):

Total aboveground shoot biomass = 25.4 t/ha **[4.3]**

Using a population of 40 000 plants/ha,

Aboveground biomass/plant= 635 g/plant **[4.4]**

Using an average corn root/shoot ratio of 0.16, at physiological maturity,

Belowground biomass/plant= 101.6 g/plant for CDSI plots **[4.5]**

For FD plots a below ground biomass/plant value of **102.2 g/plant** was calculated. As such, considering that for our study, there were no substantial differences in root biomass at maturity, the use of controlled-drainage/sub-irrigation did not show additional C sequestration potential compared to free drainage. Moreover, similar root respiration rates could have been expected between the two treatments. Therefore, differences in CO_2 fluxes from drainage/sub-irrigation treatments in 2014 appeared to be due to microbial activity rather than root respiration.

This study cannot absolutely differentiate CO_2 fluxes attributed to root respiration and fluxes produced by microbial soil decomposition. It is estimated that root-derived respiration from corn is between 30 to 50% of total soil respiration (Sey *et al*., 2010). However, it is important to note that the two will be interlinked: roots will provide carbon to the soil in the form of root turnover, root cap mucigel and organic exudates. These carbohydrates will in turn feed microbial communities and will be oxidized as CO_2 (Sey *et al*., 2010). Considering the relatively low organic matter content of our site (OM = 3.5%), this process of rhizodeposition may play an important role in relation to microbial activity.

4.3.4 Effects of N-fertilizer applications on CO_2 fluxes

For all years, fertilizers were broadcast, as it was considered to promote better development of the root volume. Fertilizers were then incorporated to avoid immediate atmospheric losses of nitrogen. **Figure 4.04** presents CO_2 fluxes measured respective to five N-fertilizer applications: 70 kg N/ha, 170 kg N/ha, 200 kg N/ha, 230 kg N/ha in one application and 230 kg N/ha in two applications. From this figure, we observe that irrespective of the crop and corresponding biomass and root production, irrespective of seasonal precipitation and irrespective of N-fertilizer application, all fields reached mean fluxes of 110 mg $C\text{-}CO_2.m^{-2}.hr^{-1}$ in mid-season. Moreover, we notice that for corn, at rates of 200 kg N/ha and over, an additional

100 mg C-CO_2.m^{-2}.hr^{-1} is recorded for these treatments on June 26th. For these fields, N-fertilizer application was between May 29th and June 7th, when the corn was at stage V6. Peaks in CO_2 flux could be attributed to a high response of root growth and respiration to N-fertilizer application. For the rest of the season, all treatments obtain similar values of CO_2 flux.

Results from this study indicate higher soil efflux of CO_2 from plots receiving higher rates of N-fertilizer application. This short-term emission burst of CO_2 was met by the highest recorded N_2O fluxes as well as the lowest and highest CH_4 flux measurements, indicating accentuated soil microbial and root activity at that time of the season.

Figures 4.04 Carbon dioxide fluxes for the four growing seasons

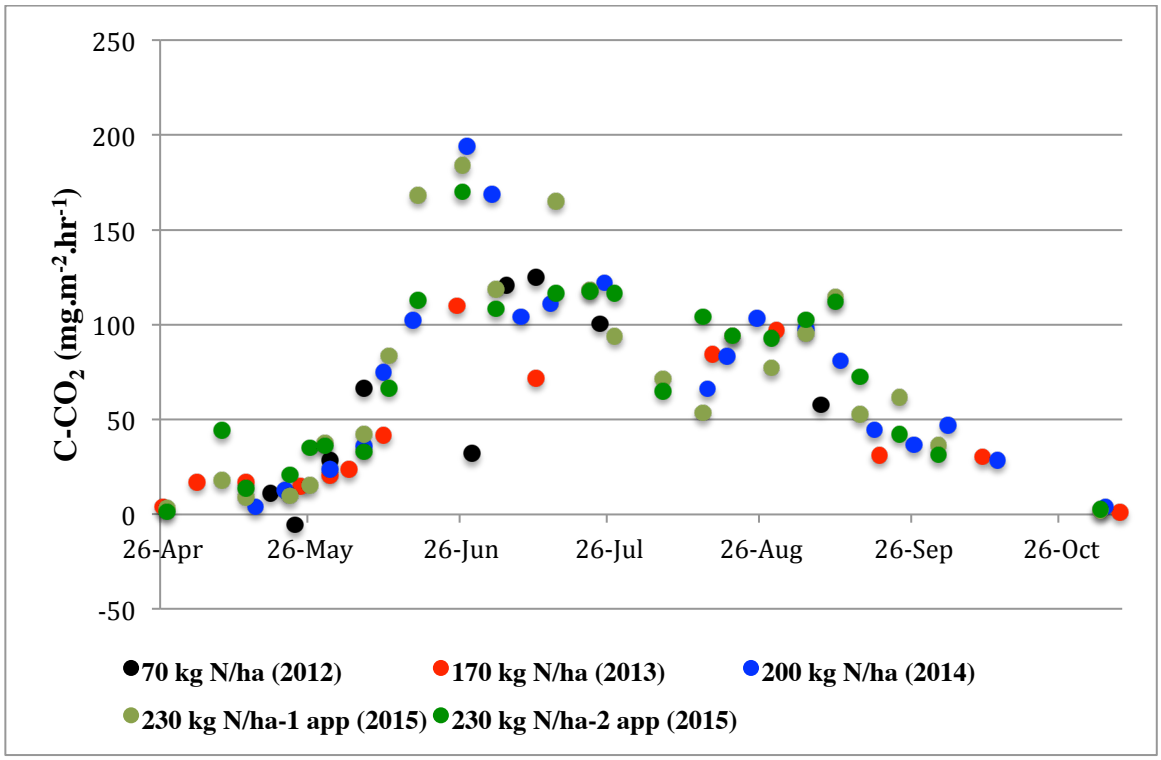

Figures 4.05 Carbon dioxide fluxes per season with standard deviation

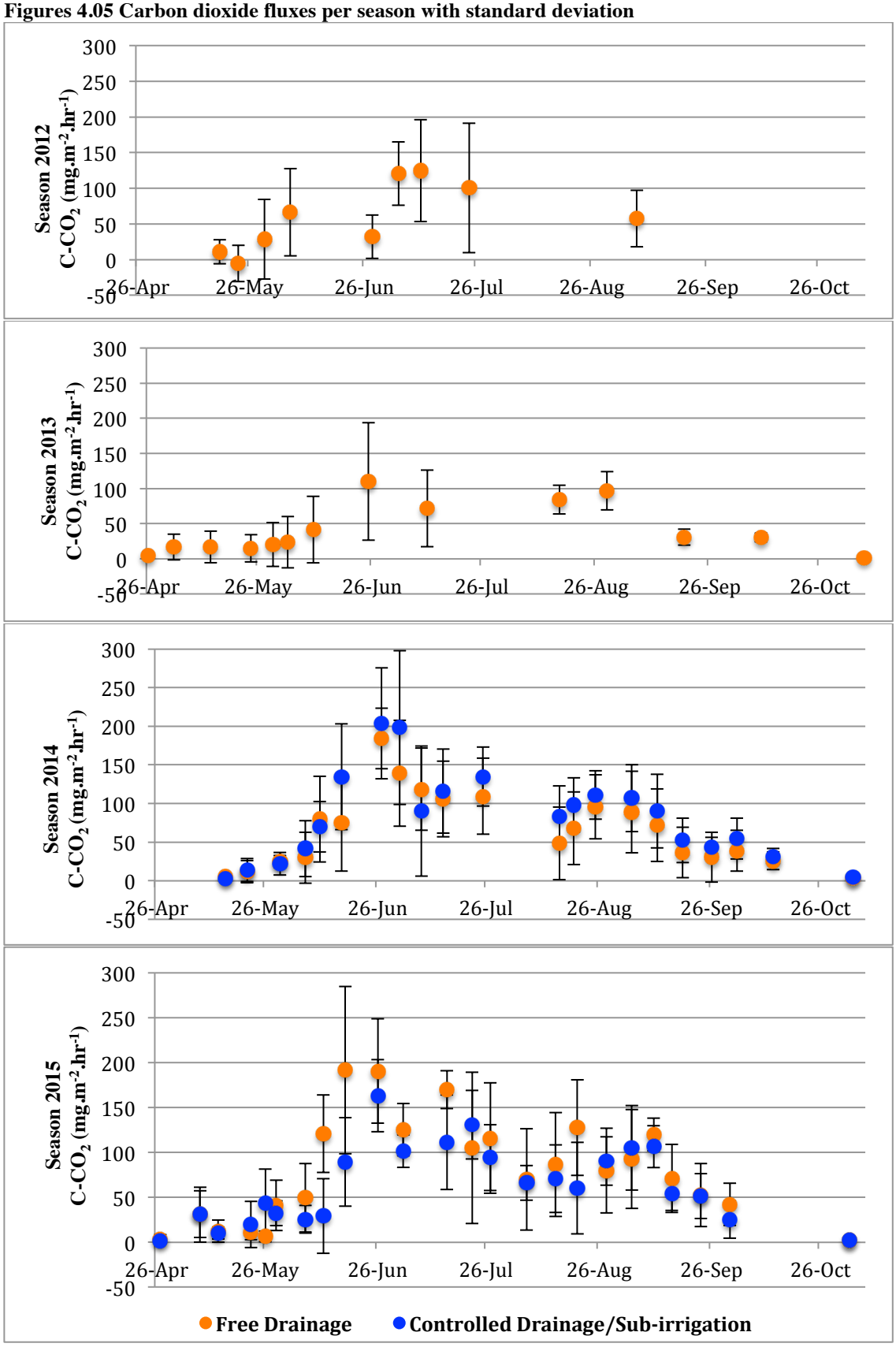

4.4 Methane

4.4.1 Seasonal fluctuations

For most sampling dates and for both FD and CDSI treatments, both positive and negative CH_4 flux values were obtained from GHG chambers. This indicated the simultaneous presence of methanogenic and methanotrophic processes throughout each season. As such, the measured methane fluxes were the difference between CH_4 oxidation and methanogenesis. Results showed that methane oxidation predominated over methanogenesis for most of the season.

4.4.2 Effects of temperature and soil water content

Neither soil temperature nor soil volumetric water content was found to be a strong regulator of methane fluxes. This field study presented a large range of soil conditions. Soil temperature ranges were 5-30°C. Volumetric water content ranged from 14-100% WFPS. However, very few significant flux events were measured. A low R^2 value of 0.23 was found for the correlation between soil temperature and CH_4 fluxes. A lower R^2 value of 0.18 was found for the correlation between soil volumetric water content and CH_4 fluxes. Due to the presence of two counterbalancing processes (methanogenesis and methane oxidation), it is possible that increasing soil temperatures may have equally accelerated both processes, each of which compensated the effects of the other. Optimum methane oxidation occurred at 20°C and 30% volumetric water content (61% WFPS).

4.4.3 Effects of drainage/irrigation treatments

Statistically significant differences in the effect of FD and CDSI on CH_4 fluxes were found only in 2014, on the two days when peak CO_2 emissions were measured: June 16th and June 27th. At that time of the season, tile drains were closed in CDSI plots but sub-irrigation was not activated. A large difference in the water table level was observed on June 27th, following a precipitation event of 45 mm. Comparing June 27th to August 15th 2014, similar water table levels were reached. However, a high water table was met by rising CH_4 fluxes only at the beginning of the season. Therefore, this study does not show a linear relationship between CH_4 fluxes and the water table level nor with soil volumetric water content. Moreover, other factors may largely influence in CH_4 fluxes other than soil water content.

Flooded soil conditions did not lead to methane production in this study. Our study was set on a sandy loam, with a relatively good saturated hydraulic conductivity of 3.00 x 10^{-3} cm/s in the top 20 cm of the soil. As such, following large precipitation events, the soil had a good capacity to evacuate water. Therefore, prolonged flooded conditions were not expected for this field. Furthermore, upon flooding, the rate of O_2 depletion from the soil solution and entrapped air pockets may take days, depending on soil temperatures and the activity of micro-organisms and plant roots (Colmer *et al*., 2005). In this study, neither free drainage nor controlled-drainage/sub-irrigation created required soil conditions for substantial CH_4 production.

4.4.4 Effects of N-fertilization

Results indicated larger methane production and oxidation rates prior to seeding and following harvest. In 2012, methane oxidation rates of -0.006 to -0.02 C-CH_4.m^{-2}.hr^{-1} were recorded at the end of May. In 2013 and 2014, methane production rates of 0.003 were recorded prior to seeding and after harvest. Previous studies have shown that cultivation decreased net CH_4 oxidation (Mosier *et al*., 1996; Kessavalou *et al*., 1998). This study indicated that cultivation may have interfered with both methane producing and oxidizing processes.

A common pattern was observed at times of fertilization. First, methane oxidation rates increased for up to 20 days. This was followed by a sharp presence of methanogenic processes. This inverse of negative to positive CH_4 fluxes was observed on June 28th 2012, May 3rd 2013, June 26th 2014 and June 26th 2015. These results contradict previous findings that nitrogen fertility dramatically decreases CH_4 consumption activity (Mosier *et al*., 1991; Castro *et al*., 1994). Application of N-fertilizer supports the growth of nitrifying bacteria populations, which can metabolize nitrate but also methane as a source of energy. Moreover, methanotrophic bacterial populations can oxidize both methane and nitrate. Results of this study indicated that application of N-fertilizer accelerated methane oxidation processes from either nitrifying bacteria or methanotrophs. After methane substrates were depleted, methane oxidation no longer counterbalanced methanogenic processes, resulting in positive CH_4 fluxes, approximately two weeks following fertilizer application. The presence of positive CH_4 fluxes did not systematically coincide with the highest soil volumetric water contents in this study. Methanogenesis could rather be explained by highly reduced soil conditions at that time.

These findings agreed with results of N_2O fluxes. Optimum methane oxidation rates in June coincided with optimum nitrous oxide production rates. Methane production occurred once N_2O production had considerably decreased, indicating that both nitrate and methane substrates had been depleted at that time. The presence of any of oxidants (nitrate, manganese dioxide, and Fe^{2+}) in the soil will delay the reduction of CO_2 to CH_4 (DeLaune *et al*., 2005). Results of this study agreed with latest findings, which showed that oxidation of methane in the soil was closely linked to nitrate availability (Zhu *et al*., 2010). Moreover, this study gave an indication of the residual time of N-fertilizer in the soil following its application.

Looking at **Figure 4.06**, for grain-corn, less methane oxidation was present at higher fertilizer application amounts for grain-corn. The highest methane oxidation and production was recorded for plots with 200 kg N/ha, which met the general recommendations for grain-corn in the region. Below 200 kg N/ha, it was possible that nitrifying bacteria populations were less developed. Above 200 kg N/ha, it was possible that with more nitrate substrates available, nitrifying bacteria did not need to metabolize methane. FD plots with 230 kg N/ha had available substrates for a week longer than plots with 200 kg N/ha. However, both reached identical optimum methane oxidation rates of -0.005 $C\text{-}CH_4.m^{-2}.hr^{-1}$ on June 16th. This indicated that at 230 kg N/ha, nitrates were probably leached in free drainage plots in 2015. Compared to FD plots, CDSI plots of 2015 had a longer period of methane oxidation, lasting until the 3rd of July. This indicated that substrates remained present much longer in the soil. CDSI plots of 2014 had higher rates of methane oxidation (-0.012 $C\text{-}CH_4.m^{-2}.hr^{-1}$) than in 2015 (-0.004 $C\text{-}CH_4.m^{-2}.hr^{-1}$). With less N-fertilizer amounts, nitrifying bacteria in these CDSI plots consumed more methane in 2013.

For the rest of the season, CH_4 fluxes remained close to zero, indicating a balance of methane production and oxidation processes. Measurements of soil volumetric water content did not explain CH_4 flux variations. This study supports the idea that methanogens occupy different niches in the soil than methane-consuming methanotrophs or nitrifiers, as suggested in previous studies (Sey *et al*., 2008). Methanogens may occupy flooded micropores in which anaerobic conditions are met. Methanotrophs may be active in the boundary between oxic and anoxic zones, within microaggregates or between microaggregate particles. As such, much of the CH_4 efflux was oxidized prior to reaching the surface (Sey *et al*., 2008).

Figure 4.06 Methane fluxes for the four growing seasons

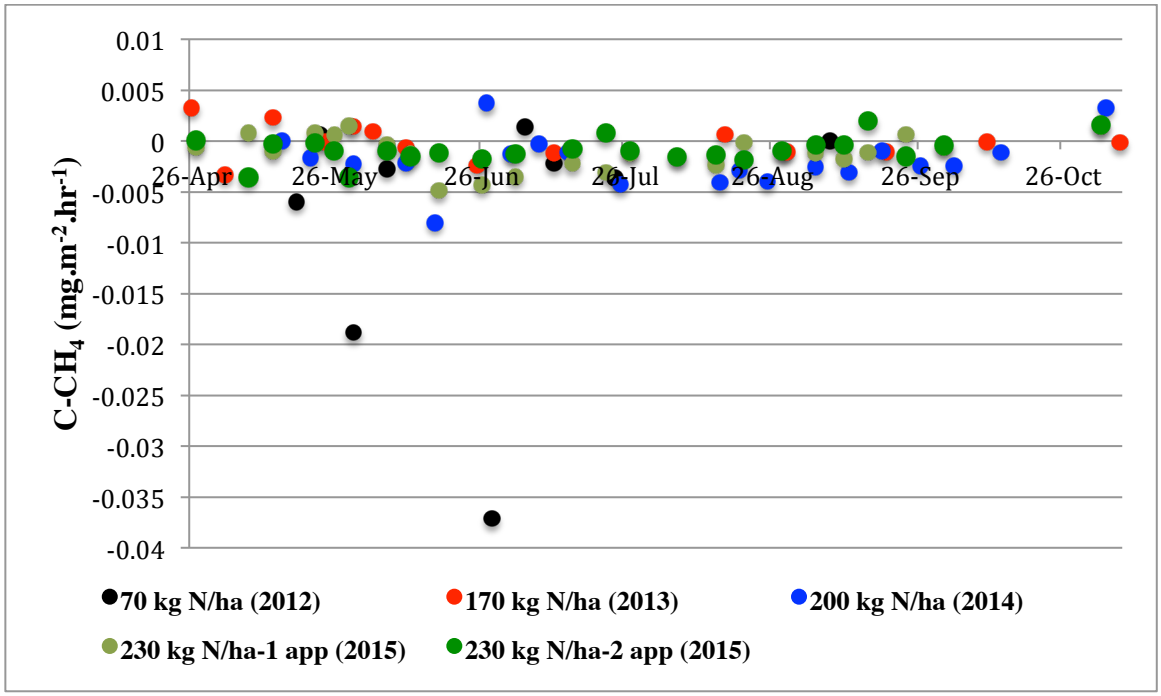

Figures 4.07 Methane fluxes per season with standard deviation

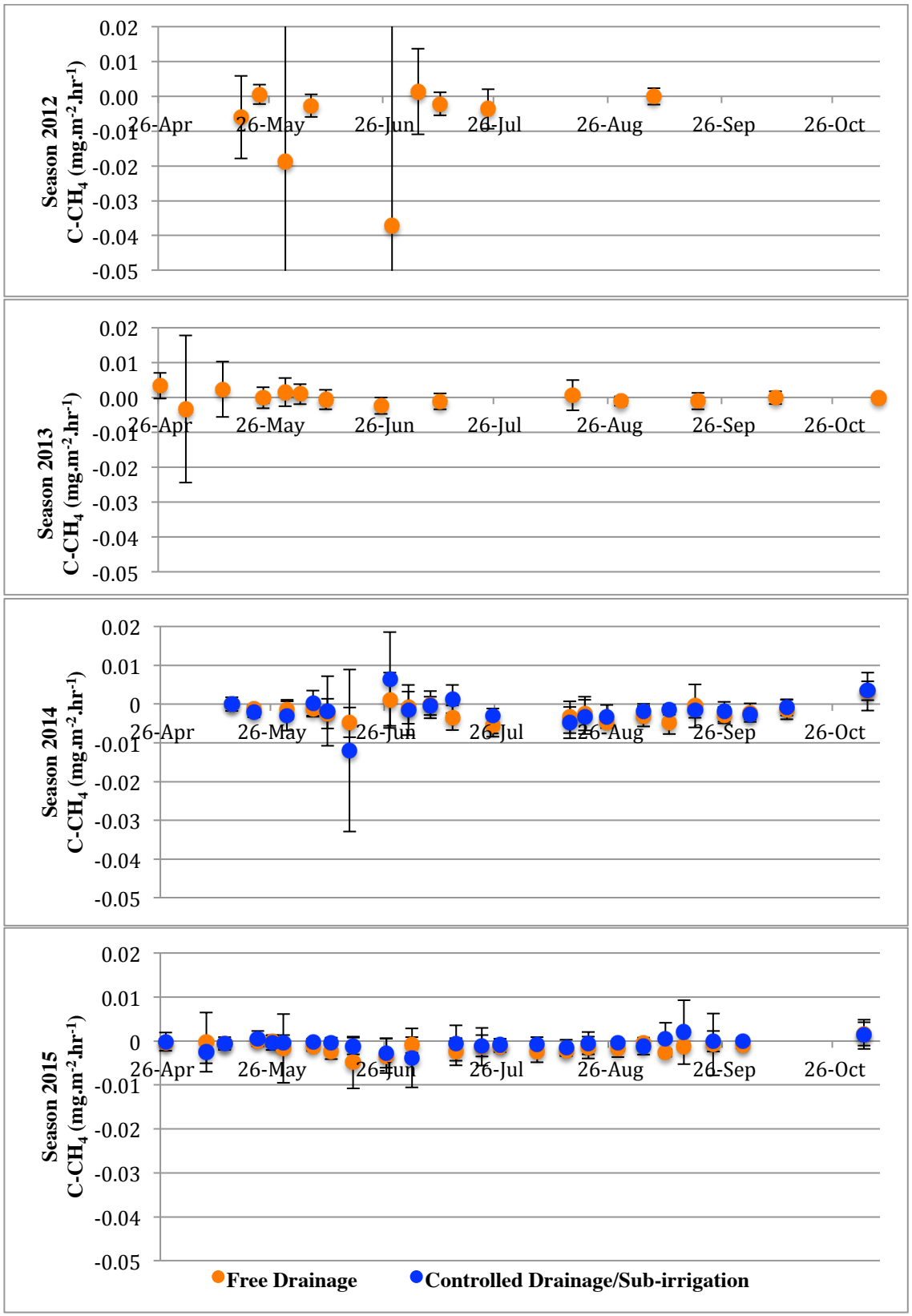

4.5 Nitrous oxide

4.1.1 Effects of N-fertilization

As can be seen in **Figure 4.08**, there was a clear seasonality of N_2O flux. Nitrous oxide production was mostly present in June of 2014 and 2015, following the application of N-fertilizer. In 2014 and 2015, optimum N_2O production rates were obtained on June 27th and June 17th, respectively, which coincided with optimum CO_2 production rates. As N_2O production rates increased in June, CH_4 oxidation rates also increased. Therefore, results indicated that, by increasing the amount of N available for microbial processes, fertilization accelerated organic matter decomposition, methane oxidation, nitrification and denitrification processes.

Large punctual bursts of N_2O production (≥ 0.5 mg $N\text{-}N_2O.m^{-2}.hr^{-1}$) were obtained for fertilizer treatments of ≥200 kg N/ha. These emissions were all approximately 15-20 days following fertilizer application. Plots with 230 kg N/ha in two applications had respectively a third and half of the N_2O fluxes of 230 kg N/ha plots in one application on June 11th and June 17th. Therefore, sub-dividing total N-fertilizer into two applications spaced one-week apart avoided excessive rates of N_2O efflux. Interestingly, highest emissions were found for 200 kg N/ha plots in 2014. Compared to plots with 230 kg N/ha, N_2O fluxes were 1.4 times greater in 200 kg N/ha plots. Therefore, although nitrogen availability was the main regulator of N_2O fluxes in this study, other factors should also be considered.

Positive N_2O fluxes were observed at the beginning of 2013 ranging from 0.06-0.2 mg $N\text{-}N_2O.m^{-2}.hr^{-1}$. The previous crop was yellow bean, a leguminous species, which has the ability to fix nitrogen in its roots. Moreover, a green manure crop (oats) was seeded in the autumn of 2012. Fluxes before harvest in 2013 could be attributed to the action of nitrifying and denitrifying bacteria consuming residual nitrogen from the previous year. Nitrous oxide production prior to harvest was not observed in subsequent years.

4.1.2 Effects of soil water content

Results support previous findings of peak emissions following important, short-term precipitation events (Scheer *et al.,* 2013; Liu et *al*., 2014). For both 2014 and 2015, maximum N_2O fluxes were measured 2-3 days following precipitation events of 45 and 24 mm, respectively. In 2014, optimum N_2O emissions were obtained at 45% and 37% volumetric water content (92% and 76% WFPS) in CDSI and FD plots respectively. In 2015, optimum emissions

were at 30% and 29% (61% and 60% WFPS) volumetric water content in CDSI and FD plots respectively. Therefore, the higher N_2O fluxes in both FD and CDSI plots in 2014 could be explained by higher soil volumetric water contents.

In 2015, lower N_2O fluxes in CDSI were accompanied by lower respiration rates compared to FD plots. Moreover, dominant methane oxidation processes occurred over a longer period in June than in FD plots. This may indicate lower O_2 concentrations in CDSI plots that year. It is possible that highly reducing conditions were met at some locations. Moreover, denitrification processes may have occurred more slowly in 2015, due to lower soil temperatures than in 2014. Therefore, it is possible that, in CDSI plots of 2015, denitrification processes were more complete. As such, a portion of N_2O production was completely converted to N_2. Further investigation would be necessary to confirm this point.

Soil water content was not found to be a determining factor for N_2O fluxes in this study. The average of R^2 correlation coefficients found between soil volumetric water content and N_2O fluxes was of 0.21. Sub-irrigation towards August-September did not show any significant production rates of N_2O in either 2014 or 2015. Significant differences amongst FD and CDSI treatments were only observed on June 27th 2014 and June 11th and 17th 2015, at a time when only controlled drainage was activated. In 2014, controlled drainage retained precipitation water leading to N_2O fluxes in CDSI plots of 4.2 times greater than in FD plots. However, in 2015, differences in FD and CDSI plots were not consistent with soil water measurements. Moreover, in 2015, the soil volumetric water content was nearly the same on June 11th and June 17th, which does not explain for the large increase in N_2O flux. Soil water content was not a strong regulator of N_2O fluxes in this study.

4.5.6 Effects of temperature

Higher R^2 correlation coefficients were found between soil temperature and N_2O flux. A mean value of 0.58 was found for the correlation between soil volumetric water content and N_2O fluxes. In previous studies, denitrification rates were found to increase exponentially from 0 to 25°C (Nieder *et al.,* 2008). Indeed, results of this study in **Figure A.1** show some exponential increase to a maximum value of 2.2 mg $N\text{-}N_2O.m^{-2}.hr^{-1}$ at 30°C. Peak N_2O fluxes in 2014 and 2015 occurred under the maximum recorded seasonal soil temperatures (T=30°C in 2014 and T=27°C in 2015). However, within the ranges of 15-25°C, many obtained flux values were near

zero. This indicates that temperature should not be considered as an independent controlling factor of N_2O fluxes.

Figure 4.08 Nitrous oxide fluxes for the four growing seasons

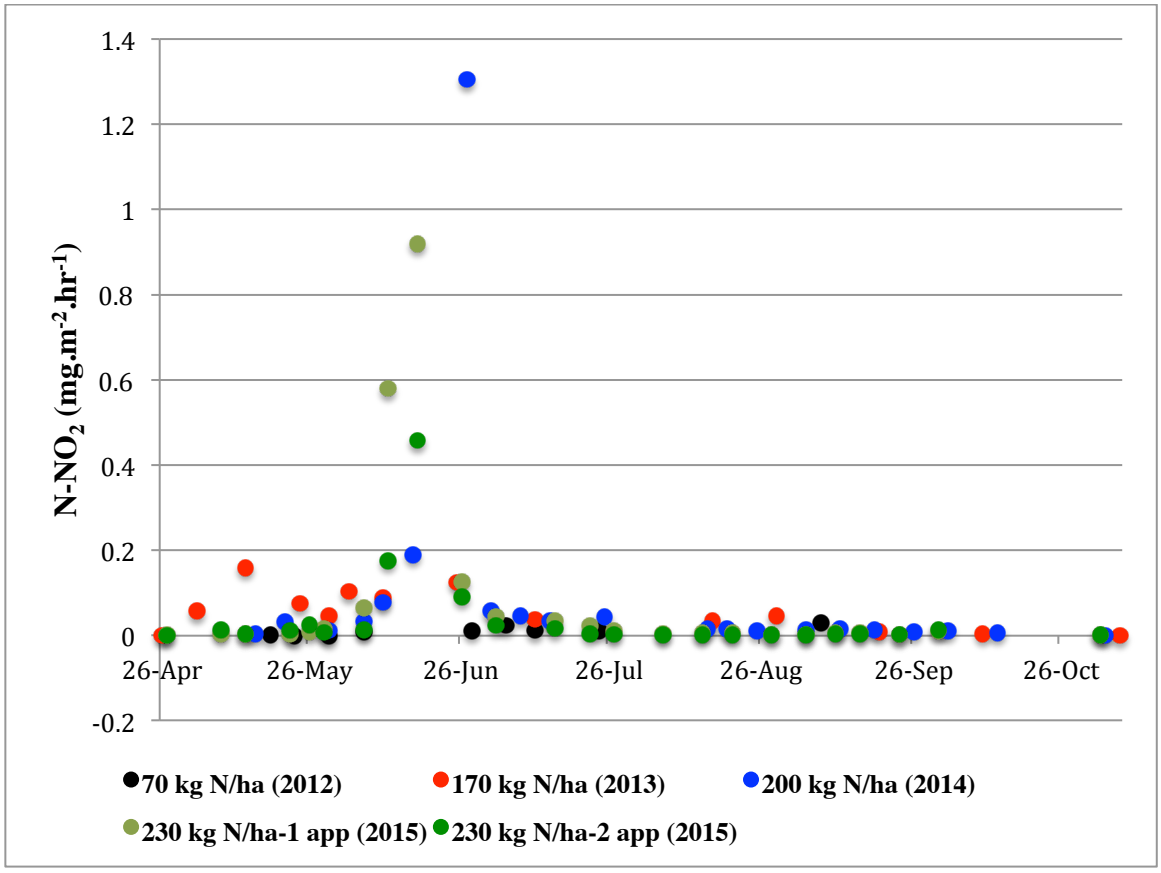

Figures 4.09 Nitrous oxide fluxes per season with standard deviation

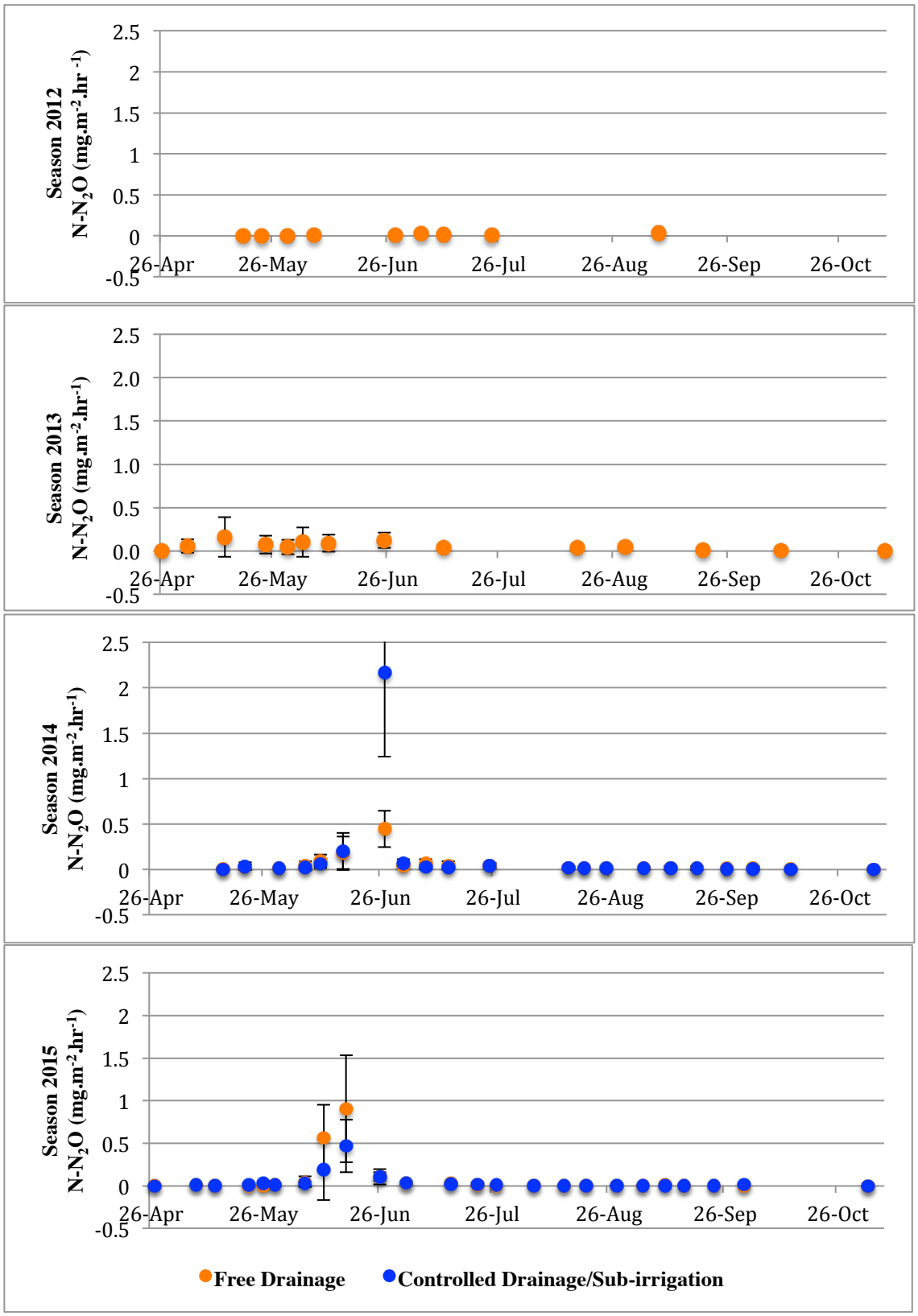

4.6 Limitations

It is important to notice that chamber frames were inserted 5-6 cm into the soil. Correspondingly, soil moisture probes read the volumetric water content in the top 6 cm of the soil. This characteristic of the non-steady state chamber was designed to avoid lateral diffusion driven by increasing gas concentration in soil beneath the chamber (Livingston *et al.,* 2006). Required depths of frame insertion are smaller for waterlogged or compacted soils rather than for other soils with great gas diffusivities. This model is also based on the assumption that greenhouse gases will be generated from a source with a magnitude that decreases exponentially from a maximum at the soil surface to zero at a hypothetical impermeable bottom 50 cm below the surface (Hutchinson and Livingston, 2001).

However, it must be noted that, when comparing controlled-drainage/sub-irrigated treatments to free drainage treatments, large rates of N_2O production were measured in the subsurface (0.15– 0.45 m) soil (Elmi *et al.,* 2005). Unlike the simulated domain of 0-50 cm, our chambers had no impermeable bottom boundary. We do not know with certainty the volume of soil air affected by the feedback effects of the chamber. This depth and volume is likely to vary with changes in soil type and soil water content (Hutchinson and Livingston, 2001). Thus, a significant portion of produced N_2O may be missed in this study, as gas flux and ancillary measurements were only made at the soil surface.

In evaluating contributions of sub-irrigation to final atmospheric emissions of greenhouse gases, the current non-steady state chamber method is well adapted to take into account the diffusivities of each gas from different soil depths to the surface. In this respect, a study using soil core methods found that although the denitrification rates under CDSI were greater than FD, the quantity of N_2O evolved to the atmosphere was similar for both treatments (Elmi *et al.,* 2005). This is attributed to a more complete reduction of N_2O to N_2 by denitrification but also to the longer diffusion time of N_2O at deeper depths to the atmosphere. In fact, surface emission of a gas can lag behind its subsurface production by several hours, and even days (Hutchinson and Livingston, 2001 citing Jury *et al.,* 1982). Thus, surface irrigation systems (drip irrigation, sprinkler irrigation) may have a more significant effect on greenhouse gas emissions by increasing the volumetric water content directly at the soil surface.

Chapter 5 : Summary and Conclusions

5.1 Summary

This study was conducted on a 4.2-ha sandy loam field over four years. The crop rotation was yellow beans followed by three years of grain-corn. Two water management treatments were studied: free drainage (FD) and controlled-drainage with sub-irrigation. Five different N-fertilizer applications were compared: 70 kg N/ha, 170 kg N/ha, 200 kg N/ha, 230 kg N/ha in one application and 230 kg N/ha in two applications with a one-week interval. GHG fluxes (CO_2, CH_4 and N_2O) were obtained using a vented non-steady state closed chamber method, with measurements taken at 15-minute intervals over a one-hour period, for 9 days throughout the growing season in 2012, for 14 days in 2013, for 21 days in 2014 and for 24 days in 2015. Rainfall amounts, daily air temperatures, soil temperatures and soil water contents were measured. The timing of agronomic practices were recorded. Increasing N-fertilizer application amounts accelerated soil respiration, methane oxidation and the production of nitrous oxide. Soil temperature was a stronger regulator of GHG fluxes compared to soil water content. Neither FD nor CDSI were found to have significant effects on any of the GHG fluxes.

5.2 Conclusions

GHG measurements were taken over a wide range of soil volumetric water conditions. Soil volumetric water content ranged from 14-100% WFPS. However, the effects of drainage/sub-irrigation in this study are obstructed by the strong interference of climatic events. Precipitation not only largely contributed to total water input volumes, but also created large changes in the soil water content due to the distribution and intensity of rainfall events. Precipitation accounted for fluctuations in soil volumetric water contents of up to 15% within a week. Therefore, precipitation had an important influence on soil water content in this study.

The corn canopy created a microclimate within the field and regulated both soil temperatures and soil volumetric water contents in this study. As such, a depression of soil temperatures was observed in mid-season. Moreover, humidity was retained by the canopy resulting in higher soil water contents in mid-season.

Although high-yielding corn-fields have been considered as means of C sequestration, this study shows that agricultural corn-fields also emit CO_2. This study focused primarily on the

effect of rhizosphere respiration on gas production. As such, CO_2 fluxes were the combination of root respiration and CO_2 produced from microbial decomposition of organic matter. Controlled-drainage/sub-irrigation did not lead to higher yields nor did it increase CO_2 fluxes as compared to free drainage in this study. Application of fertilizer of 200 kg N/ha and more created additional CO_2 emissions in June. Overall, soil temperature was the main regulator of CO_2 production. Carbon dioxide fluxes decreased at the end of June as the corn canopy was established and as soil temperatures dropped. The greatest CO_2 fluxes were not obtained at the tasseling stage as could be expected.

This study indicated the simultaneous presence of methanogenic and methanotrophic processes. As such, CH_4 fluxes were the difference between methane producing and oxidizing processes. Results indicated that methane oxidation predominated over methanogenesis in this study. Results showed that application of N-fertilizer accelerated methane oxidation processes from either nitrifying bacteria or methanotrophs. Increasing methane oxidation was followed by a peak of methanogenesis. This suggested that after methane substrates were depleted, methane oxidation no longer counterbalanced methanogenic processes, resulting in positive CH_4 fluxes, approximately two weeks following fertilizer application. Maximum CH_4 flux measured was of 0.006 mg $C\text{-}CH_4.m^{-2}.hr^{-1}$. The minimum flux was of -0.04 mg $C\text{-}CH_4.m^{-2}.hr^{-1}$. A strong relationship was not found between CH_4 fluxes and water table level or with surface soil water contents. At 100% WFPS, substantial methane production was not found in this study. For most of the study, CH_4 fluxes remained close to zero, indicating a balance of methane production and oxidation processes.

Nitrous oxide production was sparked by the application of N-fertilizer. Optimum N_2O production rates coincided with seasonal maximum CO_2 production rates and maximum CH_4 oxidation rates. For fertilizer amounts of ≥200 kg N/ha, large punctual bursts of N_2O production (≥ 0.5 mg $N\text{-}N_2O.m^{-2}.hr^{-1}$) were measured approximately 15-20 days following fertilizer application. Sub-dividing total N-fertilizer into two applications spaced one-week apart reduced the bursts of N_2O production. In 2013, N_2O production was present prior to harvest, which was attributed to bacterial consumption of fixed nitrogen from the green manure and yellow bean residues of the previous year. The highest N_2O fluxes were measured 2-3 days following precipitation events of 24-45 mm. In 2014, controlled drainage retained precipitation water

leading to N_2O fluxes in CDSI plots of 4.2 times greater than FD plots. However, overall, soil water content was not found to be a determining factor of N_2O fluxes. FD and CDSI treatments did not significantly effect N_2O production. Soil temperature was found to be a stronger regulator of N_2O fluxes than soil water content.

Recommendations for Best Management Practices must take into account constraints on agricultural management, including meteorological variability and inaccessibility of fields due to plant growth. Globally the following indications can be drawn from this study:

1. Within 15-20 days following fertilizer application, closing tile drains at times of high seasonal precipitation amounts and rainfall days could lead to greater losses due to increased denitrification and production of N_2O. Moreover, if the water table is close to the root zone, closing of tile drains is not recommended. Measurement of the water table depth will be necessary. Alternatively, leaving free drainage systems open could lead to nitrate losses through leaching of substrates.
2. The timing of fertilizer application should avoid high seasonal soil temperatures (≥27°C) and high soil volumetric water contents (≥30%). In this study, considering the high seasonal precipitation amounts and rainfall days in June and the high seasonal soil temperatures in July, fertilizer application at the V6 stage at the end of May is preferable compared to at the V8 stage.
3. Fertilizer application should not be applied near precipitation events of more than 20 mm. The timeframe of 2-3 days should be respected. If climatic conditions permit it, the splitting of fertilizer application at a one-week interval may lessen N_2O emissions.
4. Finally, this study did not show an increase of yields in controlled-drained/sub-irrigated plots as compared to freely drained plots due to sufficiently wet growing seasons in 2014 and 2015 and the absence of water stress.

Chapter 6 : Recommendations for future research

1. Concerning the non-steady state chamber method, the depth of insertion of chamber bases can be a considerable source of error. In its original design, the recommendation was to insert bases at a depth of 5 cm. This was considered adequate to limit soil lateral diffusion of gases and to catch accurate measurements of gas efflux at the soil surface. However, we notice that, as individuals must approach the chamber to take repetitive samples within one hour, considerable soil disturbance can be created from each footstep, effecting gas diffusion in the soil. For the soil type in this study, with a bulk density of 1.36 g/cm^3 and organic matter content of 3.51%, soil compression by footsteps was considered to be well attenuated. However, in cases of more friable soils of higher organic matter content and of higher field capacity, each footstep force exerted on the soil would be magnified and travel longer distances. For such soils, a deeper base insertion should be recommended. Moreover, setting a 30 cm wide platform around the base area as a frame would help in avoiding footstep disturbances effecting final chamber GHG measurements.
2. In this study, all samples were taken during the day. It may be interesting to obtain values at night, during which temperatures drop. By doing so, GHG samples over a wider range of temperature readings would have been obtained, which would have strengthened our understanding of the correlations between temperature and GHG fluxes. Carbon dioxide diurnal patterns have been previously documented (Scheer *et al*., 2013; Parkin and Kaspar, 2003; Wang, 2010). Less extensive research has been made on N_2O, and CH_4 24-h fluctuations.
3. Future research should perhaps focus on sampling within critical periods defined in this study, particularly mid-June to mid-July at which peak emissions of N_2O and CO_2 were recorded and some CH_4 consumption was observed. Increasing the sampling frequency within that period would perhaps help catch further 'emission bursts' not detected in this study. Indeed, this study found that particularly for N_2O, production rates increased 10-20 fold in the period of mid-June to the end of June.
4. Obtaining CO_2 atmospheric emissions from the corn canopy would be interesting. Carbon dioxide emitted from the soil can be consumed through photosynthesis by the

crop above-ground biomass. Indeed, corn is a high yielding crop with biomass that can reach heights of 2.5 meters. Considering the close spacing (30") of the corn-rows and the thick canopy of the field, it could be expected that a portion of CO_2 emitted from the soil was consumed by the plant. Higher yields obtained through irrigation may increase photosynthetic potential. As compared to yellow beans, one could expect corn to uptake higher amounts of CO_2 as it will produce more biomass. As such, final CO_2 released from the canopy to the atmosphere may differ from flux values measured in this study.

5. The economic trade-off between the benefits of controlling GHG emissions and the loss of NO_3-N through drainage outflow should be assessed.

Chapter 7 : References

Adviento-Borbe, M.A.A. Haddix, M.L. Binder D.L. Walters, D. T. Dobermann, A. 2007. Soil greenhouse gas fluxes and global warming potential in four high-yielding maize systems. *Global Change Biology 13*: 1972-1988.

Almagro, M. Lopez, J. Querejeta, J. I. Martinez-Mena, M. 2009. Temperature dependence of soil CO_2 efflux is strongly modulated by seasonal patterns of moisture availability in a Mediterranean ecosystem. *Soil Biology and Biochemistry 41*: 594– 605.

Almaraz, J.J. Mabood, F. Zhou, X. Madramootoo, C. Rochette, P. Ma, B-L. Smith, D. L. 2009. Carbon Dioxide and Nitrous Oxide Fluxes in Corn Grown under Two tillage systems in Southwestern Quebec. *Soil Science Society of America Journal 73:* 113-119.

Amos, B. Walters, D. T. 2006. Maize Root Biomass and Net Rhizodeposited Carbon: An Analysis of the Literature. *Soil Science Society of America Journal 70*: 1489-1503.

Bateman, E.J. Baggs, E.M. 2005. Contributions of nitrification and denitrification to N_2O emissions from soils at different water-filled pore space. *Biology and Fertility of Soils 41*: 379-388.

Benslim, H. 2014. Personal Communication.

Bootsma, Andy. 2013. Decadal Trends in Crop Heat Units for Ontario and Quebec from 1951 to 2010. Ottawa, Ontario: Agriculture and Agri-Food Canada (AAFC) Publication.

Broughton, R. S. 1992. Projet de Drainage et Irrigation Souterrains. Québec: Robert S. Broughton Consultants Inc.

Brouke, S. 2011. Measured and simulated water balances for agricultural fields under water table management [thesis]. [Montreal (Qc)]: McGill University.

Bouwman, A. F. 1990. Exchange of greenhouse gases between terrestrial ecosystems and the atmosphere. *In:* Soils and the greenhouse effect: the present status and future trends concerning the effect of soils and their cover on the fluxes of greenhouse gases, the surface energy balance, and the water balance. England: Wiley Publishing.

Brown, C. *et al*. 2009. Agronomy Guide for Field Crops: Publication 811. Toronto: Ontario Ministry of Agriculture, Food and Rural Affairs Publication.

Butterbach-Bahl, K. Dannenmann, M. 2012. Soil Carbon and Nitrogen Interactions and Biosphere-Atmosphere Exchange of Nitrous Oxide and Methane. *In*: Recarbonization of the Biosphere: Ecosystems and the Global Carbon Cycle. Switzerland: Springer Publication. p. 429-442.

Carter, M. R. Gregorich, E. G. 2008. Denitrification Techniques for Soils. *In:* Soil Sampling and Methods of Analysis. Second Edition. United States: Taylor and Francis Group Publication. p. 471- 490.

Castro, M. S. Peterjohn, W. T. Melillo, J. M. Steudler, P.A. 1994. Effects of nitrogen on the fluxes of N_2O, CH_4, and CO_2 from soils in a Florida slash pine plantation. *Canadian Journal of Forestry Research 24*: 9-13.

Cates, R.L. Keeney, D.R. 1987. Nitrous Oxide Production throughout the year from fertilized and manured Maize fields. *Journal of Environmental Quality 16*: 443-447.

Chen, H. Mothapo, N. V. Shi, W. 2015. Soil moisture and pH control relative contributions of Fungi and Bacteria to N_2O Production. *Microbial Ecology 69:* 180-191.

Colmer, T. D. Greenway, H. 2005. Oxygen Transport, respiration and anaerobic carbohydrate catabolism in roots in flooded soils. *In:* Plant Respiration. The Netherlands: Springer Publication. p.137-158.

CRAAQ. 2002. Ré-évaluation des unités thermiques disponibles au Québec pour le maïs et le soya. *In:* Bulletin technique VV026: 20.

Culley, J. L. B. 1993. Density and compressibility. *In:* Soil sampling and methods of Analysis. United States: Lewis Publishers. p. 529-540.

Davidson, E. A. 2000. Sources of nitric oxide and nitrous oxide following wetting of dry soil. *Soil Science Society of America Journa*l: 95-102.

DeLaune, R. D. Reddy, K. R. 2005. Redox potential. *In:* Encyclopedia of Soils in the Environment. United States: Elsevier Publication. p. 366-371.

Delta-T Devices Ltd. 1999. ThetaProbe Soil Moisture Sensor Type ML2x User Manual. United Kingdom: Delta-T Devices Ltd. p. 9-12.

Edwards, K. P. 2014. Greenhouse Gas Emissions from Drip Irrigated Tomato Fields [thesis]. [Montreal (Qc)]: McGill University.

Ellert, B.H. Janzen, H.H. 2008. Nitrous oxide, carbon dioxide and methane emissions from irrigated cropping systems as influenced by legumes, manure and fertilizer. *Canadian Journal of Soil Science 88*: 207–217.

Elmi, A. A. Madramootoo, C. Egeh, M. Dodds, G. Hamel, C. 2002. Water table management as a natural bio-remediation technique of nitrate pollution. *Water Quality Research Journal of Canada 37*: 563-576.

Elmi, A. Astatkie, T. Madramootoo, C. Gordon, R. Burton, D. 2005. Assessment of Denitrification Gaseous End-Products in the Soil Profile under Two Water Table Management Practices Using Repeated Measures Analysis. *Journal of Environmental Quality 34*: 446-454.

Elmi, A. Burton, D. Gordon, R. Madramootoo, C. 2005. Impacts of water table management on N_2O and N_2 from a sand loam soil in southwestern Quebec, Canada. *Nutrient Cycling in Agroecosystems 72*: 229-240.

Elmi, A. A. Mehdi, B. Madramootoo, C. Dam, R. Smith, D. 2009. Long-term Effect of Conventional and No-Tillage Production Systems on Nitrous Oxide Fluxes from Corn (*Zea mays* L.) Field in Southwestern Quebec. *American Journal of Environmental Sciences 5:* 238-246.

Grant, A. 2014. Greenhouse Gas Emissions from Cranberry Fields under Irrigation and Drainage in Quebec [thesis]. [Montreal (Qc)]: McGill University.

Gregorich, E. G. Rochette, P. VandenBygaart, A. J. Angers, D. A. 2005. Greenhouse gas contributions of agricultural soils and potential mitigation practices in Eastern Canada. *Soil and Tillage Research 83:* 53-72.

Han, G. Zhou, G. Xu, Z. Yang, Y. Liu, J. Shi, K. 2007. Biotic and abiotic factors controlling the spatial and temporal variation of soil respiration in an agricultural ecosystem. *Soil Biology and Biochemistry 39*: 418–425.

Healy, R.W. Striegl, R.G. Russell, T.F. Hutchinson, G.L. Livingston, G.P. 1996. Numerical evaluation of static-chamber measurements of soil atmosphere gas exchange: identification of physical processes. *Soil Science Society of America Journal 60:* 740-747.

Hendershot, W. H. Lalande, H. Duquette, M. 1993. Soil Reaction and Exchangeable Acidity. *In*: Soil sampling and methods of analysis. United States: Canadian Society of Soil Science, Lewis Publishers. P. 499-557.

Hillel, D. 2003. Introduction to Environmental Soil Physics. United States: Elsevier Publication.

Hutchinson, G. L. Livingston, G. P. Healy, R. W. Striegl, R. G. 2000. Chamber measurement of surface-atmosphere trace gas exchange: Numerical evaluation of dependence on soil, interfacial layer, and source/sink properties. *In*: Journal of Geophysical Research. United States: American Geophysical Union Publication. p. 8865-8875.

Hutchinson, G. L. Livingston, G. P. 2001. Vents and seals in non-steady-state chambers used for measuring gas exchange between soil and the atmosphere. *European Journal of Soil Science:* 675-682.

IPCC, 2013: Summary for Policymakers. *In: Climate Change 2013: The Physical Science Basis. Contribution of Working Group I to the Fifth Assessment Report of the Intergovernmental Panel on Climate Change* [Stocker, T.F., D. Qin, G.-K. Plattner, M. Tignor, S.K. Allen, J. Boschung, A. Nauels, Y. Xia, V. Bex and P.M. Midgley (eds.)]. Cambridge University Press, Cambridge, United Kingdom and New York, NY, USA.

Jury, W. A. Letey, J. Collins, T. 1982. Analysis of chamber methods used for measuring nitrous oxide production in the field. *Soil Science Society of America Journal 46:* 250-256.

Kessavalou, A. Mosier, A. R. Doran J. W. Drijber, R. A. Lyon, D. J. Heinemeyer, O. 1998. Fluxes of carbon dioxide, nitrous oxide, and methane in grass sod and winter wheat-fallow tillage management. *Journal of Environmental Quality 27*: 1094-1104.

Knowles, R. 1982. Denitrification. *Microbiological Reviews 46:*43-70.

Le Mer, J. Roger, P. 2001. Production, oxidization, emission and consumption of methane by soils: a review. *European Journal of Soil Biology 37:* 25-50.

Linn, D.M., and J.W. Doran. 1984. Effect of water-filled pore space on carbon dioxide and nitrous oxide production in tilled and non-tilled soils. *Soil Science Society of America Journal 48*: 1267–1272.

Linquist, B. Van Groenigen, K. J. Adviento-Borbe, M. A. Pittelkow, C. Ven Kessel, C. 2012. An agronomic assessment of greenhouse gas emissions from major cereal crops. *Global Change Biology 18:* 194-209.

Liu, X., Qi, Y. Dong, Y. Peng, Q. He, Y. Sun, L. Jia, J. Cao, C. 2014. Response of soil N_2O emissions to precipitation pulses under different nitrogen availabilities in a semi-arid temperature steppe of Inner Mongolia, China. *Journal of Arid Land 6:* 410-422.

Livingston, G. P. Hutchinson, G. L. Spartalian, K. 2006. Trace Gas Emission in Chambers: A Non-Steady-State Diffusion Model. *Soil Science Society of America Journal:* 1459-1469.

Lorenz, K. Lal, R. 2012. Cropland Soil Carbon Dynamics. *In:* Recarbonization of the Biosphere: Ecosystems and the Global Carbon Cycle. Switzerland: Springer Publication. p. 303-344.

Martin, A. Nolin, M. C. 1992. Etude pédologique du comté de Chambly (Québec): Description et classification des séries de sols. Ontario: Agriculture Canada Research Branch. p. 130.

Maynard, D. G. Kalra, Y. P. Crumbaugh, J. A. 2009. Nitrate and Exchangeable Ammonium Nitrogen. *In:* Soil sampling and methods of analysis. United States: Canadian Society of Soil Science, CRC Press. p. 81-88.

Ministère du Développement Durable, de l'Environnement et de la Lutte contre les Changements Climatiques (MDDELCC). 2014. Inventaire québécois des émissions de gaz à effet de serre en 2011 et leur évolution depuis 1990. Quebec (Canada): Publication du Gouvernement du Québec.

Morales, S. E. Jha, N. Saggar, S. 2015. Biogeography and biophysicochemical traits link N_2O emissions, N_2O emission potential and microbial communities across New Zealand pasture soils. *Soil Biology and Biochemistry 82:* 87-98.

Morisset, M. *et al*. 2006. Profil Bioalimentaire de la Montérégie. Québec: Publication du Ministère de l'Agriculture, des Pêcheries et de l'Alimentation du Québec.

Mosier, A. Parton, W. J. Valentine, D. W. Ojima, D. S. Schimel, D. S. Delgado, J. A. 1996. CH_4 and N_2O fluxes in the Colorado shortgrass steppe. I. Impact of landscape and nitrogen addition. *Global Biogeochemical Cycles 10*: 387-399.

Mosier, A. Schimel, D. Valentine, D. Bronson, K. Parton, W. 1991. Methane and nitrous oxide fluxes in native, fertilized and cultivated grasslands. *Nature 350*: 330-332.

Nieder, R. Benbi, D.K. 2008. Carbon and Nitrogen in the Terrestrial Environment. Germany: Springer Science Publication. p. 45-80; p. 137-159; p. 235-305.

Parent, L. E. Gagné, G. G. 2010. Guide de Référence en Fertilisation. 2nd Edition. Québec (Québec): Centre de reference en agriculture et agroalimentaire du Québec (CRAAQ).

Parkin, T.B. Kaspar, T.C. 2003. Temperature controls on diurnal carbon dioxide flux: implications for estimating soil carbon loss. *Soil Science Society of America Journal 67*:1762–1772.

Radford, B.J. *et al*. 2001. Crop responses to applied soil compaction and to compaction repair treatments. *Soil Tillage Research 61*: 157-166.

Reicosky, D. C. *et al*. 2000. Agricultural Contributions to Greenhouse Gas Emissions. *In:* Climate Change and Global Crop Productivity. England: Imperial College Press. p. 37-55.

Refsgaard, J. C. Knudsen, J. 1996. Operational validation and intercomparison of different types of hydrological models. *Water Resources Research 32*: 2189-2202.

Robertson, G.P. Grace, P.R. 2004. Greenhouse gas fluxes in tropical and temperate agriculture: the need for a full-cost accounting of global warming potentials. *Environment, Development and Sustainability 6:* 51–63.

Rochette, P. Simard, R. R. Ziadi, N. Nolin, M. C. Cambouris, A. N. 2004. Atmosphere composition and N2O emissions in soils of contrasting textures fertilized with anhydrous ammonia. *Canadian Journal of Soil Science 84:* 339-352.

Sass, R.L. Fisher, F.M. Lewis, S.T. Jund, M.F. Turner, F.T. 1994. Methane emissions from ricefields - effect of soil properties. *Global Biogeochemical Cycles 8:* 135–140.

Saxton, K. E. Rawls, W. J. 2006. Soil Water Characteristic Estimates by Texture and Organic Matter for Hydrologic Solutions. *Soil Science Society of America Journal 70*: 1569-1578.

Schaufler, G. Kitzler, B. Schindlbacher, A. Skiba, U. Sutton. M.A. Zechmeister-Boltenstern, S. 2010. Greenhouse gas emissions from European soils under different land use: effects of soil moisture and temperature. *European Journal of Soil Science 61*: 683-696.

Scheer, C. Grace, P.R. Rowlings, D. W. Payero, J. 2013. Soil N_2O and CO_2 emissions from cotton in Australia under varying irrigation management. *Nutrient Cycling in Agroecosystems 95:* 43-56.

Schlesinger, W. H. Bernhardt, E.S. 2013. Biogeochemistry: An analysis of Global Change. United States: Elsevier Publication. p. 419-443.

Scialabba, N. E. Müller-Lindenlauf, M. 2010. Organic agriculture and climate change. *Renewable Agriculture and Food Systems 25(2):* 158-169.

Serrano-Silva, N. Sarria-Guzman, Y., Dendooven, L. Luna-Guido, M. 2014. Methanogenesis and Methanotrophy in Soil. *Pedosphere 24*: 291-307.

Sey, D. K. Manceur, A. M. Whalen, J.K. Gregorich, E. G. Rochette, P. 2010. Root-derived respiration and nitrous oxide production as affected by crop phenology and nitrogen fertilization. *Plant Soil Journal 326:* 369-379.

Sey, B. K. Manceur, A. M. Whalen, J .K. Gregorich, E. G. Rochette, P. 2008. Small-scale heterogeneity in carbon dioxide, nitrous oxide and methane production from aggregates of a cultivated sandy-loam soil. *Soil Biology and Biochemistry 40: 2468-2473*.

Sharma, S. Szele, Z. Schilling, R. Munch, J.C. Schloter, M. 2006. Influence of Freeze-Thaw Stress on the Structure and Function of Microbial Communities and Denitrifying Populations in Soil. *Applied and Environmental Microbiology*: 2148-2154.

Sheldrick, B. H. Wang, C. 1993. Particle Size Distribution. *In:* Soil Sampling and Methods of Analysis. United States: Lewis Publishers. p. 499-511.

Scholes, M. Martin, R. Scholes, R. Parsons, D. Winstead, E. 1997. NO and N_2O emissions from savannah soils following the first simulated rains of the season. *Nutrient Cycling in Agroecosystems 48:* 115-122.

Singh, A. K. 2013. Water and nitrogen use efficiency of corn (*Zea mays L.*) under water table management [thesis]. [Montreal (Qc)]: McGill University.

Skaggs, R. W. Youssef, M. A. Chescheir, G. M. 2012. DRAINMOD: Model Use, Calibration, and Validation. *In:* Transactions of the ASABE. United States: American Society of Agricultural and Biological Engineers. p. 1509-1522.

Skjemstad, J. O. Baldock, J.A. 2009. Total and Organic Carbon. *In:* Soil sampling and methods of analysis. United States: Canadian Society of Soil Science, CRC Press. p. 225-238.

Tabi, M. *et al*. 1990. Inventaire des Problèmes de Dégradation des Sols Agricoles du Québec: Région Agricole 7 Sud-Ouest de Montréal. Ontario: MAPAQ Publication.

Tait, R. Madramootoo, C. A. Enright P. 1995. An instrumented, field-scale research facility for drainage and water quality studies. *Computer and Electronic in Agriculture 12:* 131-145.

Thomas, W. J. Adams, M. J. 1964. Measurement of the Diffusion Coefficients of Carbon Dioxide and Nitrous Oxide in Water and Aqueous Solutions of Glycerol. *In:* Transactions of the Faraday Society. United Kingdom: Royal Society of Chemistry. p.668-673.

Ullah, S. Moore, T. R. 2011. Biogeochemical controls on methane, nitrous oxide, and carbon dioxide fluxes from deciduous forest soils in eastern Canada. *Journal of Geophysical research 116*: G03010.

Wall, D. H. Bardgett, R. D. Behan-Pelletier, V. Herrick, J.E., Jones, T.H. Ritz, K. Six, J. Strong, D.R. and van der Putten, W. H. 2012. Soil Ecology and Ecosystem Services. United Kingdom: Oxford University Press.

Wang, H. McConkey, B. Curtin, D. Cutforth, H. 2010. Estimation of daily soil CO_2 flux using a single-time-point measurement. *Canadian Journal of Soil Science 90*: 517–522.

Whalen, J. K. Sampedro, L. 2010. Soil Ecology and Management. United Kingdom: CABI International.

Wolfe, D. W. 2013. Contributions to Climate Change Solutions from the Agronomy Perspective. *In*: Handbook of Climate Change and Agroecosystems. England: Imperial College Press. p. 11-29.

Wrage, N. Velthof, G. L. Van Beusichem, M.L. and Oenema, O. 2001. Role of nitrifier denitrification in the production of nitrous oxide. *Soil Biology and Biochemistry 33*: 1723-1732.

Youngs, G.E. 2001. Hydraulic Conductivity of Saturated Soils. *In:* Soil and Environmental Analysis. United States: Marcel Dekker, Inc. p. 141-181.

Zhu, G. Jetten, M.S.M. Kuschk, P. Ettwig, K.F. and Yin, C. 2010. Potential roles of anaerobic ammonium and methane oxidation in the nitrogen cycle of wetland ecosystems. *Applied Microbiology and Biotechnology 86*: 1043–1055.

Ziadi, N. Sen Tran, T. 2008. Mehlich 3-Extractable Elements. *In:* Soil sampling and methods of analysis. United States: Canadian Society of Soil Science, CRC Press. p. 81-88.

Appendix A

Table A.1 **Pearson's R^2 correlation coefficients between soil temperature (°C) and soil volumetric water content (%), and GHG fluxes, using all mean values sorted per year, per water treatment, and per fertilizer treatment**

			Pearson's Correlation Coefficients					
			Soil Temperature			Soil Volumetric Water Content		
	WTM	Fertilizer (kg N/ha)	N_2O	CO_2	CH_4	N_2O	CO_2	CH_4
2012	FD	70	0.73	0.28	0.00	0.58	0.58	0.37
2013	FD	170	0.57	0.72	0.32	0.18	0.07	0.18
2014	FD	200	0.54	0.69	0.53	0.26	0.08	0.14
	CDSI	200	0.63	0.54	0.40	0.46	0.13	0.30
2015	FD	230-1 app	0.38	0.63	0.46	0.05	0.27	0.05
	FD	230-2 app	0.53	0.60	0.01	0.09	0.02	0.05
	CDSI	230-1 app	0.61	0.38	0.07	0.00	0.22	0.01
	CDSI	230-2 app	0.64	0.45	0.02	0.04	0.06	0.31
		Average	**0.58**	**0.53**	**0.23**	**0.21**	**0.18**	**0.18**

* All data sets were fit either to an exponential or to a polynomial equation (order 2).

** FD: Free Drainage; CDSI: Controlled Drainage/Sub-irrigation

Figures A.1 **Correlation between soil temperature (°C) and N_2O, CO_2 and CH_4 fluxes, grouped by water and fertilizer treatments**

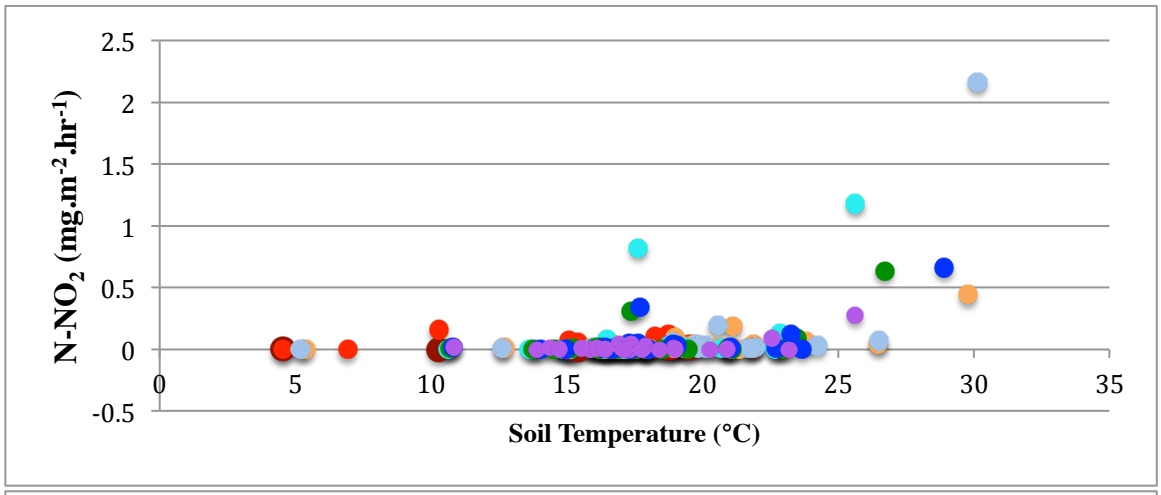

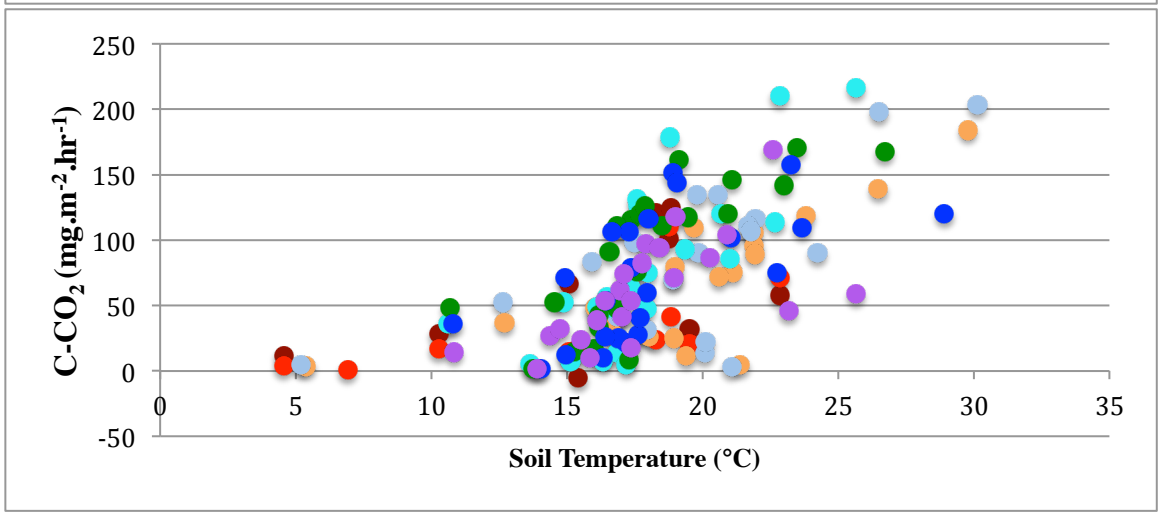

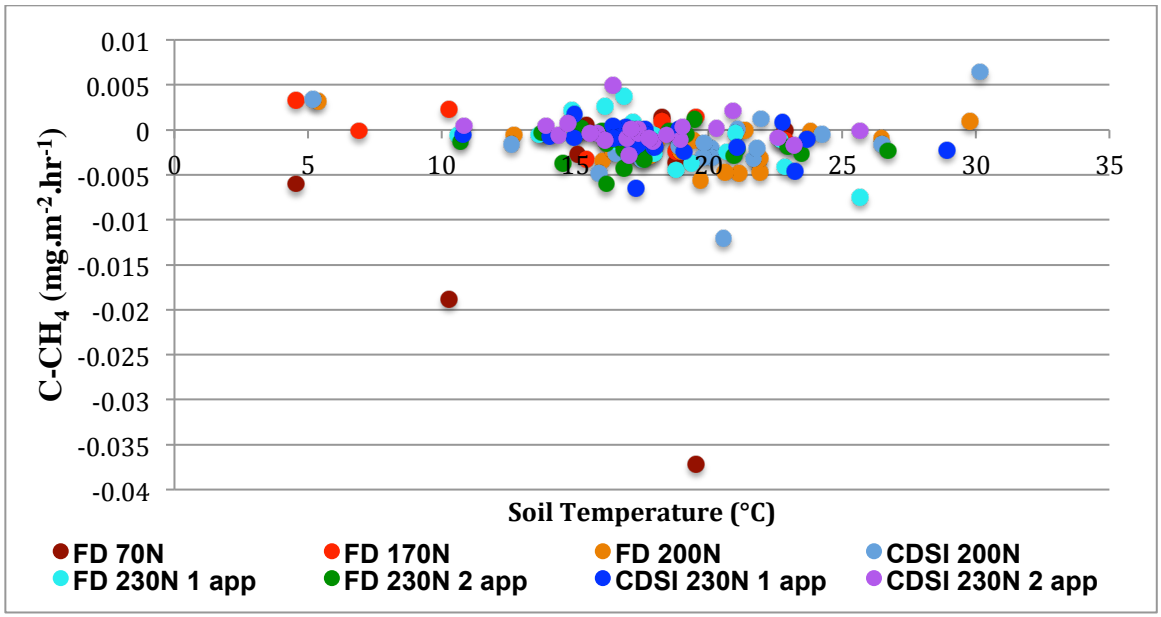

Figures A.2 **Correlation between soil volumetric water content (%) and N_2O, CO_2 and CH_4 fluxes, grouped by water and fertilizer treatments**

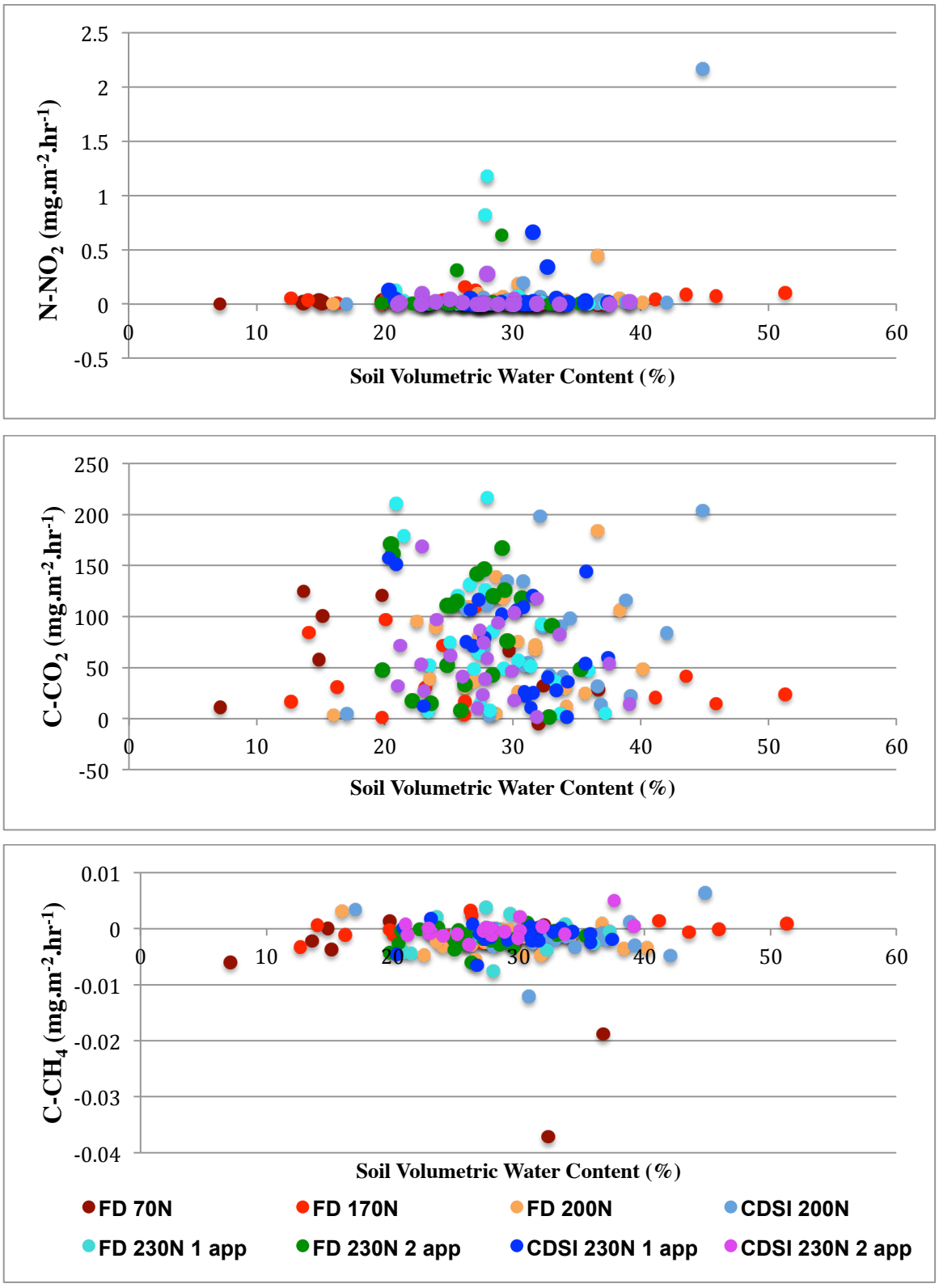

Appendix B

Table B.1 **Statistical results of effects tests for each season, each greenhouse gas and each treatment combination**

		Effect Test					
		N2O		CO2		CH4	
	Factors	Prob>F	Significance	Prob>F	Significance	Prob>F	Significance
2012	Block	N.S.S.		0.0036	S.S.	N.S.S.	
	Sampling Date	0.001	S.S.	<0.0001	S.S.	0.203	N.S.S.
	Block x Sampling Date	-	-	0.3508	N.S.S.	-	-
2013	Block	N.S.S.		N.S.S.		N.S.S.	
	Sampling Date	0.0004	S.S.	<0.0001	S.S.	0.7222	N.S.S.
2014	Block	N.S.S.		<0.0001	S.S.	<0.0001	S.S.
	Sampling Date	<0.0001	S.S.	<0.0001	S.S.	<0.0001	S.S.
	WTM	0.0001	S.S.	0.0067	S.S.	0.8339	N.S.S.
	Sampling Date x WTM	<0.0001	S.S.	0.832	N.S.S.	-	-
	Block x Sampling Date	-	-	0.8772	N.S.S.	0.0011	S.S.
	Block x WTM	-	-	0.2404	N.S.S.	-	-
2015	Block	N.S.S		N.S.S.		N.S.S.	
	Sampling Date	<0.0001	S.S.	<0.0001	S.S.	0.2273	N.S.S.
	WTM	0.0228	S.S.	0.0004	S.S.	0.0310	S.S.
	Fertilizer treatment	0.0031	S.S.	0.9014	N.S.S.	0.7903	N.S.S.
	Date x WTM	<0.0001	S.S.	0.0020	S.S.	-	-
	Date x Fertilizer	<0.0001	S.S.	-	-	-	-
	WTM x Fertilizer	0.6392	N.S.S.	-	-	-	-
	Date x WTM x Fert	1	N.S.S.	-	-	-	-

* For all years, if the blocking effect was found insignificant, it was removed from the model.

** The block effect had an interaction with one factor, sampling date in 2014 for CH4 fluxes.

*** In 2015, no interaction was found between WTM and Fertilizer. Results from both factors are presented separetly in the following tables.

Table B.2 **Season 2012 and 2013 mean flux values and standard error for N_2O, CO_2 and CH_4, respectively, outliers, minimum and maximum flux measured and statistical difference amongst sampling days for each gas**

Season 2012		N_2O					CO_2					CH_4				
Yellow Beans		Mean Flux (± S.E.)	Outliers #	Min Flux	Max Flux	Diff.	Mean Flux (± S.E.)	Outliers #	Min Flux	Max Flux	Diff.	Mean Flux (± S.E.)	Outliers #	Min Flux	Max Flux	Diff.
1	18-May-12	0.002 (±0.001)				BC	11.2 (±4.9)	2			CD	-0.006 (±0.003)	2			A
2	23-May-12	-0.002 (± 0.005)	1			C	-5.2 (± 7.3)		47.4		D	0.001 (± 0.001)	1			A
3	30-May-12	-0.000 (±0.010)	1	-0.102		BC	28.7 (±16.1)	1			CD	-0.019 (±0.016)	2			A
4	06-Jun-12	0.009 (±0.002)				ABC	66.7 (±17.7)				ABC	-0.003 (±0.001)	1			A
5	28-Jun-12	0.011 (±0.004)				ABC	32.1 (±8.8)				BCD	-0.037 (±0.030)	1	-0.358		A
6	05-Jul-12	0.024 (±0.005)				AB	120.8 (±12.8)				A	0.002 (±0.004)	1		0.039	A
7	11-Jul-12	0.013 (±0.003)				ABC	124.7 (±20.6)				A	-0.002 (±0.001)				A
8	24-Jul-12	0.010 (±0.009)	1		0.099	ABC	100.7 (±27.4)			243	AB	-0.004 (±0.002)				A
9	07-Sep-12	0.031 (±0.007)				A	57.7 (±11.5)				ABCD	0.000 (±0.001)				A

* All pairs compared with Tukey-Kramer HSD (p>0.05) ** Levels not connected by the same letter are significantly different *** Sampling day 8 only had 11 observations

Season 2013		N_2O					CO_2					CH_4				
Grain-Corn		Mean Flux (± S.E.)	Outliers #	Min Flux	Max Flux	Diff.	Mean Flux (± S.E.)	Outliers #	Min Flux	Max Flux	Diff.	Mean Flux (± S.E.)	Outliers #	Min Flux	Max Flux	Diff.
1	26-Apr-2013	0.000 (±0.001)	2			B	4.2 (±0.8)				D	0.003 (±0.001)	3			A
2	3-May-2013	0.057 (± 0.022)	2	-0.019		AB	17.0 (± 5.3)	1	-9		D	-0.003 (± 0.006)		-0.051	0.28	A
3	13-May-2013	0.160 (±0.066)				A	16.9 (±6.5)	1			D	0.002 (±0.002)				A
4	24-May-2013	0.075 (±0.030)				AB	14.8 (±5.6)				D	-0.000 (±0.001)				A
5	30-May-2013	0.047 (±0.025)	2			AB	20.6 (±9.0)	1			D	0.002 (±0.001)				A
6	3-Jun-2013	0.104 (±0.049)	1		0.571	AB	23.7 (±10.5)				CD	0.001 (±0.001)				A
7	10-Jun-2013	0.089 (±0.028)				AB	41.8 (±13.7)				BCD	-0.001 (±0.001)				A
8	25-Jun-2013	0.125 (±0.025)				AB	110.2 (±24.1)			235	A	-0.002 (±0.001)	1			A
9	11-Jul-2013	0.039 (±0.009)				AB	71.7 (±15.7)				ABC	-0.001 (±0.001)				A
10	16-Aug-2013	0.036 (±0.005)	1			AB	84.3 (±5.9)				AB	0.001 (±0.001)	1			A
11	29-Aug-2013	0.047 (±0.006)				AB	97.2 (±7.9)				A	-0.001 (±0.000)				A
12	19-Sep-2013	0.010 (±0.001)				B	31.1 (±3.3)				CD	-0.001 (±0.001)				A
13	10-Oct-2013	0.005 (±0.002)	1			B	30.5 (±2.1)				CD	0.000 (±0.001)				A
14	7-Nov-2013	0.001 (±0.000)				B	1.2 (±0.2)				D	0.000 (±0.000)				A

* All pairs compared with Tukey-Kramer HSD (p>0.05) ** Levels not connected by the same letter are significantly different *** Sampling day 13 only had 9 observations

Tables B.3 **Season 2014 mean flux values and standard error for N_2O and CO_2 by water treatment, outliers, minimum and maximum flux measured and statistical difference amongst sampling days for each greenhouse gas**

Season 2014		N_2O									
		Free Drainage					Controlled Drainage/Sub-irrigation				
Grain-Corn		Mean Flux (± S.E.)	Outliers #	Min Flux	Max Flux	Diff.	Mean Flux (± S.E.)	Outliers #	Min Flux	Max Flux	Diff.
1	15-May-14	0.006 (±0.002)				C	0.004 (±0.001)				C
2	21-May-14	0.027 (± 0.013)				C	0.038 (±0.018)				C
3	30-May-14	0.015 (±0.003)				C	0.012 (±0.004)				C
4	6-Jun-14	0.041 (±0.020)				C	0.024 (±0.008)				C
5	10-Jun-14	0.097 (±0.029)				BC	0.061 (±0.017)				C
6	16-Jun-14	0.185 (±0.073)		-0.012		BC	0.198 (±0.102)				BC
7	27-Jun-14	0.446 (±0.081)			0.694	B	2.166 (±0.377)			3.893	A
8	2-Jul-14	0.043 (±0.011)				C	0.071 (±0.018)				C
9	8-Jul-14	0.066 (±0.019)				C	0.028 (±0.012)				C
10	14-Jul-14	0.048 (±0.018)				C	0.022 (±0.009)				C
11	25-Jul-14	0.044 (±0.013)				C	0.423 (±0.008)				C
12	15-Aug-14	0.016 (±0.006)				C	0.016 (±0.005)				C
13	19-Aug-14	0.016 (±0.004)				C	0.015 (±0.004)				C
14	25-Aug-14	0.012 (±0.004)				C	0.093 (±0.002)				C
15	4-Sep-14	0.017 (±0.005)				C	0.012 (±0.004)	1			C
16	11-Sep-14	0.017 (±0.007)				C	0.015 (±0.008)	1			C
17	18-Sep-14	0.017 (±0.008)				C	0.010 (±0.006)	1			C
18	26-Sep-14	0.014 (±0.007)				C	0.005 (±0.002)				C
19	3-Oct-14	0.015 (±0.008)				C	0.005 (±0.002)				C
20	13-Oct-14	0.009 (±0.005)				C	0.004 (±0.001)	1			C
21	4-Nov-14	0.001 (±0.000)				C	-0.001 (±0.001)		-0.006		C

* All pairs compared with Tukey-Kramer HSD (p>0.05) ** Levels not connected by the same letter are significantly different

Season 2014		CO_2									
		Free Drainage					Controlled Drainage/Sub-irrigation				
Grain-Corn		Mean Flux (± S.E.)	Outliers #	Min Flux	Max Flux	Diff.	Mean Flux (± S.E.)	Outliers #	Min Flux	Max Flux	Diff.
1	15-May-14	5.5 (±0.4)				H	3.1 (±1.4)		-0.4		H
2	21-May-14	12.0 (±5.9)				GH	14.0 (±6.1)				GH
3	30-May-14	25.0 (±3.2)				FGH	22.2(±6.0)				FGH
4	6-Jun-14	29.9 (±13.6)				EFGH	41.6 (±14.8)				CDEFGH
5	10-Jun-14	79.9 (±22.7)				CDEFGH	69.8 (±13.3)				CDEFGH
6	16-Jun-14	75.5 (±25.8)				CDEFGH	134.6 (±30.6)				ABCDE
7	27-Jun-14	184.2 (±16.0)			220.3	AB	203.8 (±29.3)				A
8	2-Jul-14	139.0 (±28.0)				AB	198.3 (±40.7)			330.1	A
9	8-Jul-14	118.5 (±21.7)				ABCDEF	90.0 (±34.4)				BCDEFGH
10	14-Jul-14	105.9 (±20.0)				ABCDEFG	116.1 (±22.2)				ABCDEF
11	25-Jul-14	109.4 (±20.0)				ABCDEFG	134.8 (±15.6)				ABCD
12	15-Aug-14	48.6 (±19.2)		-33.3		CDEFGH	83.8 (±15.9)				CDEFGH
13	19-Aug-14	68.2 (±19.3)				CDEFGH	98.3 (±14.4)				BCDEFGH
14	25-Aug-14	95.7 (±16.9)				BCDEFGH	111.1 (±12.8)				ABCDEFG
15	4-Sep-14	89.2 (±21.6)				BCDEFGH	106.9 (±17.7)	1			ABCDEFG
16	11-Sep-14	72.0 (±19.2)				CDEFGH	90.2 (±19.5)				BCDEFGH
17	18-Sep-14	36.6 (±13.4)				DEFGH	52.3 (±11.7)				CDEFGH
18	26-Sep-14	30.6 (±13.2)				EFGH	43.2 (±5.3)				CDEFGH
19	3-Oct-14	38.8 (±10.8)				DEFGH	54.8 (±10.8)				EFGH
20	13-Oct-14	25.9 (±4.6)				FHG	31.6 (±4.2)				EFGH
21	4-Nov-14	3.6 (±1.0)				H	4.9 (±1.3)				H

Table B.4 **Season 2014 mean flux values and standard error for CH_4 by water treatment, outliers, minimum and maximum flux measured and statistical difference amongst sampling days**

Season 2014		CH_4									
		Free Drainage					Controlled Drainage/Sub-irrigation				
Grain-Corn		Mean Flux (± S.E.)	Outliers #	Min Flux	Max Flux	Diff.	Mean Flux (± S.E.)	Outliers #	Min Flux	Max Flux	Diff.
1	**15-May-14**	0.000 (±0.000)				ABC	0.00 (±0.001)				ABC
2	**21-May-14**	-0.001 (±0.000)				ABC	-0.002 (±0.001)				ABC
3	**30-May-14**	-0.002 (±0.001)				ABC	-0.003 (±0.002)				ABC
4	**6-Jun-14**	-0.001 (±0.001)				ABC	0.000 (±0.001)				AB
5	**10-Jun-14**	-0.002 (±0.002)				ABC	-0.002 (±0.004)				ABC
6	**16-Jun-14**	-0.005 (±0.002)				BC	-0.012 (±0.009)		-0.049		C
7	**27-Jun-14**	0.001 (±0.003)		-0.01	0.014	AB	0.007 (±0.005)			0.029	A
8	**2-Jul-14**	-0.001 (±0.002)				ABC	-0.002 (±0.003)				ABC
9	**8-Jul-14**	-0.000 (±0.001)				ABC	-0.001 (±0.001)				ABC
10	**14-Jul-14**	-0.004 (±0.001)				ABC	0.001 (±0.001)				AB
11	**25-Jul-14**	-0.006 (±0.001)				BC	-0.003 (±0.001)				ABC
12	**15-Aug-14**	-0.003 (±0.002)				ABC	-0.005 (±0.002)				BC
13	**19-Aug-14**	-0.002 (±0.002)				ABC	-0.004 (±0.002)				ABC
14	**25-Aug-14**	-0.005 (±0.000)				BC	0.003 (±0.001)				ABC
15	**4-Sep-14**	-0.003 (±0.001)				ABC	-0.002 (±0.001)				ABC
16	**11-Sep-14**	-0.005 (±0.001)				ABC	-0.002 (±0.001)				ABC
17	**18-Sep-14**	-0.001 (±0.002)	1			ABC	-0.002 (±0.001)	1			ABC
18	**26-Sep-14**	-0.003 (±0.001)				ABC	-0.002 (±0.001)				ABC
19	**3-Oct-14**	-0.002 (±0.001)				ABC	-0.003 (±0.001)				ABC
20	**13-Oct-14**	-0.001 (±0.001)				ABC	-0.001 (±0.001)				ABC
21	**4-Nov-14**	0.003 (±0.002)				AB	0.003 (±0.001)				AB

Table B.5 Season 2015 mean flux values and standard error for N_2O and CO_2 by water treatment, outliers, minimum and maximum flux measured and statistical differences amongst sampling days

Season 2015		N_2O									
		Free Drainage					Controlled Drainage/Sub-irrigation				
Grain-Corn		Mean Flux (± S.E.)	Outliers #	Min Flux	Max Flux	Diff.	Mean Flux (± S.E.)	Outliers #	Min Flux	Max Flux	Diff.
1	27-Apr-15	0.002 (±0.001)	1			D	0.001 (±0.000)				D
2	8-May-15	0.008 (±0.003)				D	0.011 (±0.004)				D
3	13-May-15	0.005 (±0.002)				D	0.006 (±0.002)	1			D
4	22-May-15	0.005 (±0.003)	1			D	0.011 (±0.007)	1			D
5	26-May-15	0.003 (±0.002)		-0.004		D	0.031 (±0.012)				D
6	29-May-15	0.013 (±0.006)	1			D	0.011 (±0.003)				D
7	6-Jun-15	0.049 (±0.027)	1			D	0.029 (±0.009)				D
8	11-Jun-15	0.566 (±0.158)				B	0.190 (±0.145)	1	-0.010	0.908	CD
9	17-Jun-15	0.907 (±0.257)			1.51	A	0.471 (±0.127)				BC
10	26-Jun-15	0.108 (±0.036)				D	0.109 (±0.022)				D
11	3-Jul-15	0.034 (±0.006)	1			D	0.036 (±0.016)				D
12	15-Jul-15	0.027 (±0.004)				D	0.245 (±0.007)				D
13	22-Jul-15	0.010 (±0.005)				D	0.018 (±0.010)	1			D
14	27-Jul-15	0.006 (±0.002)				D	0.008 (±0.005)				D
15	6-Aug-15	0.002 (±0.001)				D	0.004 (±0.002)				D
16	14-Aug-15	0.003 (±0.001)				D	0.005 (±0.004)	1			D
17	20-Aug-15	0.005 (±0.002)				D	0.005 (±0.004)	1			D
18	28-Aug-15	0.003 (±0.001)				D	0.003 (±0.001)				D
19	4-Sep-15	0.004 (±0.002)				D	0.002 (±0.000)				D
20	10-Sep-15	0.008 (±0.001)				D	0.004 (±0.001)				D
21	15-Sep-15	0.006 (±0.001)				D	0.007 (±0.004)	1			D
22	23-Sep-15	0.004 (±0.001)				D	0.003 (±0.001)				D
23	1-Oct-15	0.006 (±0.001)				D	0.019 (±0.007)				D
24	3-Nov-15	0.001 (±0.000)				D	0.000 (±0.001)				D

* All pairs compared with Tukey-Kramer HSD (p>0.05) ** Levels not connected by the same letter are significantly different

Season 2015		CO_2									
		Free Drainage					Controlled Drainage/Sub-irrigation				
Grain-Corn		Mean Flux (± S.E.)	Outliers #	Min Flux	Max Flux	Diff.	Mean Flux (± S.E.)	Outliers #	Min Flux	Max Flux	Diff.
1	27-Apr-15	3.3 (±2.1)	1			KL	1.6 (±0.5)				L
2	8-May-15	30.9 (±12.5)				EFGHIJKL	31.4 (±10.6)				EFGHIJKL
3	13-May-15	12.6 (±5.1)				IJKL	10.5 (±2.8)				JKL
4	22-May-15	11.1 (±3.3)				JKL	19.8 (±10.5)				HIJKL
5	26-May-15	6.7 (±2.5)				JKL	43.6 (±15.5)				DEFGHIJKL
6	29-May-15	41.3 (±11.5)	1			DEFGHIJKL	32.4 (±5.6)				EFGHIJKL
7	6-Jun-15	49.8 (±15.6)				DEFGHIJKL	25.7 (±6.3)				GHIJKL
8	11-Jun-15	120.9 (±17.6)				ABCDE	29.4 (±17.1)				FGHIJKL
9	17-Jun-15	191.9 (±38.1)				A	89.7 (±20.2)	-6.9			BCDEFGHIJKL
10	26-Jun-15	190.7 (±23.8)			274.6	A	163.3 (±16.4)			211.2	ABC
11	3-Jul-15	125.7 (±11.9)				ABCD	101.8 (±7.4)				ABCDEFG
12	15-Jul-15	179.1 (±8.6)				AB	111.6 (±21.5)				ABCDEFG
13	22-Jul-15	105.2 (±34.4)				ABCDEFGH	131.0 (±15.6)				ABCD
14	27-Jul-15	116.1 (±25.1)				ABCDEF	94.4 (±15.0)				BCDEFGHIJ
15	6-Aug-15	69.9 (±23.0)				DEFGHIJKL	66.2 (±7.9)				DEFGHIJKL
16	14-Aug-15	86.7 (±23.7)				BCDEFGHIJKL	71.1 (±15.4)				DEFGHIJKL
17	20-Aug-15	127.8 (±21.7)				ABCD	60.5 (±20.9)				DEFGHIJKL
18	28-Aug-15	79.9 (±19.3)				CDEFGHIJKL	90.5 (±11.0)				BCDEFGHIJKL
19	4-Sep-15	92.5 (±22.5)		-6.1		BCDEFGHIJK	105.4 (±19.3)				ABCDEFGH
20	10-Sep-15	120.2 (±7.4)				ABCDE	106.7 (±9.6)				ABCDEFGH
21	15-Sep-15	71.1 (±15.5)				DEFGHIJKL	54.0 (±7.5)				DEFGHIJKL
22	23-Sep-15	52.5 (±14.3)				DEFGHIJKL	51.5 (±10.3)				DEFGHIJKL
23	1-Oct-15	42.5 (±9.6)				DEFGHIJKL	25.3 (±8.5)				GHIJKL
24	3-Nov-15	2.3 (±1.1)				L	2.6 (±1.1)				L

Table B.6 **Season 2015 mean flux values and standard error for CH_4 by water treatment, outliers, minimum and maximum flux measured and statistical differences amongst sampling days**

Season 2015		CH_4									
		Free Drainage					Controlled Drainage/Sub-irrigation				
Grain-Corn		Mean Flux (± S.E.)	Outliers #	Min Flux	Max Flux	Diff.	Mean Flux (± S.E.)	Outliers #	Min Flux	Max Flux	Diff.
1	27-Apr-15	-0.001 (±0.000)				A	-0.000 (±0.001)				A
2	8-May-15	-0.000 (±0.003)				A	-0.002 (±0.000)				A
3	13-May-15	-0.000 (±0.001)	1			A	-0.001 (±0.000)				A
4	22-May-15	0.000 (±0.000)				A	0.001 (±0.001)				A
5	26-May-15	-0.000 (±0.000)				A	0.000 (±0.001)	1			A
6	29-May-15	-0.002 (±0.003)				A	-0.000 (±0.001)				A
7	6-Jun-15	-0.001 (±0.000)				A	-0.000 (±0.000)				A
8	11-Jun-15	-0.002 (±0.001)				A	-0.001 (±0.001)				A
9	17-Jun-15	-0.005 (±0.002)	1	-0.016		A	-0.001 (±0.001)				A
10	26-Jun-15	-0.003 (±0.002)				A	-0.003 (±0.001)				A
11	3-Jul-15	-0.001 (±0.001)				A	-0.004 (±0.003)	1	-0.017		A
12	15-Jul-15	-0.003 (±0.001)				A	-0.000 (±0.002)				A
13	22-Jul-15	-0.001 (±0.002)				A	-0.001 (±0.001)				A
14	27-Jul-15	-0.001 (±0.001)				A	-0.001 (±0.001)				A
15	6-Aug-15	-0.003 (±0.001)				A	-0.001 (±0.001)				A
16	14-Aug-15	-0.002 (±0.001)				A	-0.001 (±0.001)				A
17	20-Aug-15	-0.002 (±0.001)				A	-0.001 (±0.001)				A
18	28-Aug-15	-0.002 (±0.001)				A	-0.000 (±0.000)				A
19	4-Sep-15	-0.001 (±0.000)				A	-0.001 (±0.001)				A
20	10-Sep-15	-0.003 (±0.000)				A	0.001 (±0.002)	1			A
21	15-Sep-15	-0.001 (±0.000)				A	0.002 (±0.003)	1		0.017	A
22	23-Sep-15	-0.001 (±0.003)			0.012	A	-0.000 (±0.001)				A
23	1-Oct-15	-0.001 (±0.000)				A	-0.000 (±0.000)				A
24	3-Nov-15	0.002 (±0.001)	1			A	0.001 (±0.001)				A

Table B.7 **Season 2015 mean flux values and standard error for N_2O by fertilizer treatment, outliers, minimum and maximum flux measured and statistical differences amongst sampling days**

Season 2015		N_2O									
		Fertilizer 230 kg N/ha-1 application					Fertilizer 230 kg N/ha-2 applications				
Grain-Corn		Mean Flux (± S.E.)	Outliers #	Min Flux	Max Flux	Diff.	Mean Flux (± S.E.)	Outliers #	Min Flux	Max Flux	Diff.
1	27-Apr-15	0.002 (±0.003)	1			D	0.001 (±0.000)				D
2	8-May-15	0.005 (±0.002)	1			D	0.014 (±0.004)				D
3	13-May-15	0.006 (±0.003)	1			D	0.005 (±0.002)				D
4	22-May-15	0.003 (±0.001)				D	0.012 (±0.007)				D
5	26-May-15	0.009 (±0.008)		-0.004		D	0.026 (±0.012)				D
6	29-May-15	0.017 (±0.006)				D	0.007 (±0.002)				D
7	6-Jun-15	0.064 (±0.024)	1			D	0.014 (±0.004)				D
8	11-Jun-15	0.580 (±0.199)				B	0.177 (±0.066)		-0.010		CD
9	17-Jun-15	0.919 (±0.173)			1.51	A	0.459 (±0.224)			1.497	BC
10	26-Jun-15	0.126 (±0.034)				D	0.091 (±0.022)				D
11	3-Jul-15	0.046 (±0.005)				D	0.025 (±0.003)				D
12	15-Jul-15	0.035 (±0.004)				D	0.017 (±0.003)				D
13	22-Jul-15	0.023 (±0.010)				D	0.005 (±0.002)				D
14	27-Jul-15	0.011 (±0.005)				D	0.003 (±0.001)				D
15	6-Aug-15	0.005 (±0.002)				D	0.002 (±0.001)				D
16	14-Aug-15	0.006 (±0.004)	1			D	0.002 (±0.001)				D
17	20-Aug-15	0.007 (±0.004)				D	0.003 (±0.001)				D
18	28-Aug-15	0.004 (±0.001)				D	0.002 (±0.008)				D
19	4-Sep-15	0.004 (±0.001)				D	0.002 (±0.002)				D
20	10-Sep-15	0.007 (±0.001)				D	0.005 (±0.001)				D
21	15-Sep-15	0.008 (±0.004)				D	0.005 (±0.001)				D
22	23-Sep-15	0.004 (±0.001)				D	0.003 (±0.001)				D
23	1-Oct-15	0.011 (±0.004)				D	0.013 (±0.007)	1			D
24	3-Nov-15	0.000 (±0.000)				D	0.001 (±0.001)				D